ISSN 8755-6839

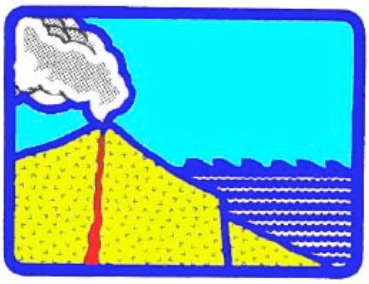

SCIENCE OF TSUNAMI HAZARDS

The International Journal of The Tsunami Society
Volume 28 Number 1 Published Electronically 2009

TSUNAMI SOCIETY, 1741 Ala Moana Blvd. #70, Honolulu, HI 96815, USA.

WWW.TSUNAMISOCIETY.ORG

OBJECTIVE: The Tsunami Society publishes this journal to increase and disseminate knowledge about tsunamis and their hazards.

DISCLAIMER: Although these articles have been technically reviewed by peers, the Tsunami Society is not responsible for the veracity of any statement, opinion or consequences.

Submit manuscripts of articles, notes or letters to the Editor. If an article is accepted for publication the author(s) must submit a scan ready manuscript, a Doc, TeX or a PDF file in the journal format. Issues of the journal are published electronically in PDF format. Recent journal issues are available at:
http://www.TsunamiSociety.org
http://www.sthjournal.org

Tsunami Society members will be advised by e-mail when a new issue is available. There are no page charges for one paper per calendar year for authors who are members of the Tsunami Society. Permission to use figures, tables and brief excerpts from this journal in scientific and educational works is hereby granted provided that the source is acknowledged.

Issues of the journal from 1982 thru 2005 are available in PDF format at
http://epubs.lanl.gov/tsunami/ and on a CD-ROM from the Society to Tsunami Society members. ISSN 8755-6839 http://www.sthjournal.org

EXPERIMENTAL AND COMPUTATIONAL ACTIVITIES AT THE OREGON STATE UNIVERSITY NEES TSUNAMI RESEARCH FACILITY

S.C. Yim[1], D.T. Cox[2] and M.M. Park[3]
[1] *Professor,* [2] *Associate Professor,*
[3]
NEES Site Operations Manager
School of Civil and Construction Engineering, Oregon State University, Corvallis, OR 97331 USA
Email: solomon.yim@oregonstate.edu, dan.cox@oregonstate.edu, melora.park@oregonstate.edu

ABSTRACT

A diverse series of research projects have taken place or are underway at the NEES Tsunami Research Facility at Oregon State University. Projects range from the simulation of the processes and effects of tsunamis generated by sub-aerial and submarine landslides (NEESR, Georgia Tech.), model comparisons of tsunami wave effects on bottom profiles and scouring (NEESR, Princeton University), model comparisons of wave induced motions on rigid and free bodies (Shared-Use, Cornell), numerical model simulations and testing of breaking waves and inundation over topography (NEESR, TAMU), structural testing and development of standards for tsunami engineering and design (NEESR, University of Hawaii), and wave loads on coastal bridge structures (non-NEES), to upgrading the two-dimensional wave generator of the Large Wave Flume. A NEESR payload project (Colorado State University) was undertaken that seeks to improve the understanding of the stresses from wave loading and run-up on residential structures. Advanced computational tools for coupling fluid-structure interaction including turbulence, contact and impact are being developed to assist with the design of experiments and complement parametric studies. These projects will contribute towards understanding the physical processes that occur during earthquake generated tsunamis including structural stress, debris flow and scour, inundation and overland flow, and landslide generated tsunamis. Analytical and numerical model development and comparisons with the experimental results give engineers additional predictive tools to assist in the development of robust structures as well as identification of hazard zones and formulation of hazard plans.

KEYWORDS: Tsunami, structure, sediment, experiment, computation, research

1. INTRODUCTION

Oregon State University (OSU) is home to the George E. Brown, Jr. Network for Earthquake Engineering Simulation (NEES) Tsunami Research Facility (TRF), one of the world's largest facilities for studying the effects of large waves. Of the 15 experimental sites supported by NEES, OSU is the only facility that supports the study of the hydrological effects of earthquakes, specifically tsunamis. The OSU experimental site is housed at the O.H. Hinsdale Wave Research Laboratory (HWRL), which was established in 1972 with the construction of a large wave flume (LWF) designed to study the stability of coastal structures. In 1989, the Office of Naval Research funded the construction of a wave basin to study complex, 3-dimensional fluid flow. In 2000, the HWRL was designated by the National Science Foundation (NSF) as a site for tsunami research as part of its NEES Program. Under the NEES support, the HWRL expanded the original wave basin, significantly increasing the physical dimensions of the basin, and at the same time, installed a state-of-the-art wave maker capable of 3-dimensional tsunami wave generation. This new expanded basin and wave maker are collectively known as the Tsunami Wave Basin (TWB), which together with the existing 2-dimensional Large Wave Flume (LWF), constitute the majority of experimental components utilized at the Tsunami Research Facility. In 2004, the operations and maintenance phase of the NEES facility began. By summer of 2008 (year 4 of operations), the facility has a full schedule of activities and has been fully occupied supporting six NEES research (NEESR) projects most of which are multi-year and multi-phase. In 2009, a new piston wave maker will be installed in the LWF funded by NSF under the MRI initiative.

2. OVERVIEW

The NEES mission is to improve the research and practice communities' understanding of earthquakes and their effects on structures and human safety by, in part, providing the most advanced experimental facilities for performing earthquake-engineering experiments. The United States has experienced major tsunamis that caused significant damage in Hawaii, Alaska and the West Coast, and research at the NEES OSU TRF is focused on improving the communities' understanding of earthquake generated tsunamis as they affect people's lives. The Indonesian earthquake and resulting tsunami in December 2004 increased awareness and concern about the possibility of a large magnitude event of this type occurring in the US. The US Office of Science and Technology Policy released a report in December 2005 entitled "Tsunami Risk Reduction for the United States: A Framework for Action (National Science and Technology Council, 2005)", which called for scientists to review the existing state of tsunami research and also to develop a strategic plan for tsunami research in the US. An organizing committee developed a framework which was then refined at a workshop that took place in July 2006. Experts from academic institutions, governmental agencies and the private sector contributed to a report that was released in December of 2006 entitled "National Tsunami Research Plan: Report of a Workshop Sponsored by NSF/NOAA" (Bernard et al., 2006).

A summary of the report recommendations that included all areas of tsunami risk assessment and mitigation identified three major areas of research:

- Hazard Assessment

  How and where tsunamis are created, how often tsunamis reoccur, an estimation of the

impact of tsunamis on community infrastructure and natural environment using field, laboratory and model data, and how lives are threatened.

- Warning Guidance Research and Recommendations
  Monitoring systems for detection, real-time forecasting, information dissemination and warning systems.

- Preparedness, Response and Mitigation
  Program development, education of communities, and legislative and incentive policies designed to reduce risk to human life and property based on hazard assessment.

Research at NEES OSU TRF coincides with the framework identified in the National Tsunami Research Plan (described above). Research projects at the site include experiments aimed at furthering our understanding of these scientific objectives and will be described in more detail below. Much of the work is concentrated in the "hazard assessment" area as the facility is uniquely constructed to specifically support many of these objectives. However, as pointed out in the National Tsunami Research Plan, there is inherent overlap in the three areas described above and some aspects of research and activities at the site also address "Warning Guidance" and "Mitigation".

3. ACTIVITIES

The research activities described below have been organized around the framework established by the National Tsunami Research Plan as described in the overview.

3.1 Hazard Assessment

The coupling between landslide motion and generated tsunami waves in three dimensions is of critical importance given the local source mechanism with a strong directionality and the characteristic trans-critical landslide versus tsunami velocity Froude numbers. Nearly a half-century after the Lituya Bay mega-event, Hermann Fritz from the Georgia Institute of Technology has successfully replicated a fully three dimensional scale model of a tsunami created by a deformable landslide. Using a unique landslide-generated tsunami simulator that was installed at the OSU NEES TWB, the researchers simulated the impact of landslides that occur both above and below the water's surface, generating simulated tsunamis in a three-dimensional environment. Fritz and a team of researchers have constructed the landslide tsunami generator—"an open box" that is mounted on a steel slide and filled with up to 1,350 kg of gravel (Figure 1a). The box accelerates down the slide by means of four pneumatic pistons. The granular mass is accelerated inside the box, and released while the sled is slowed down pneumatically. The box is 2.1 by 1.2 by 0.3 m with subdivisions to adjust initial slide length and thickness and is placed on a slide that can vary in length. The box itself is able to travel approximately 2 m before the gravel is released down the 2H: 1V slope at initial velocities of up to 5 m/sec. The researchers tested two types of landslides: those that fall into the water and those that occur beneath the surface. Sensors were placed on the simulator to measure the velocity of the gravel. Using cameras placed above and within the water, the researchers measured the shape, length,

and thickness of the gravel masses while they were in motion. The granular landslide deposits were scanned with an acoustic multi-transducer array (Figure 1b). Wave gauges were placed to measure the size and shape of the waves that were generated including the lateral onshore run-up. The recorded wave profiles were extremely directional, unsteady, non-linear and located mostly in the intermediate water depth wave regime. Among the principal differences between a tectonic-generated tsunami and a landslide-generated tsunami is that the latter has a strong directional component that can be devastating to the immediate area. However, because it has a shorter wavelength, it dissipates quickly over a short distance. Landslide tsunamis exhibit a more dispersive and strongly directional propagation than tectonic tsunamis. Planar PIV was applied to the tsunami surface and revealed the fully 3D tsunami generation. Currently more than 60 successful runs are completed and the main tsunamigenic parameters determined which would serve as a key benchmark for the numerical models.

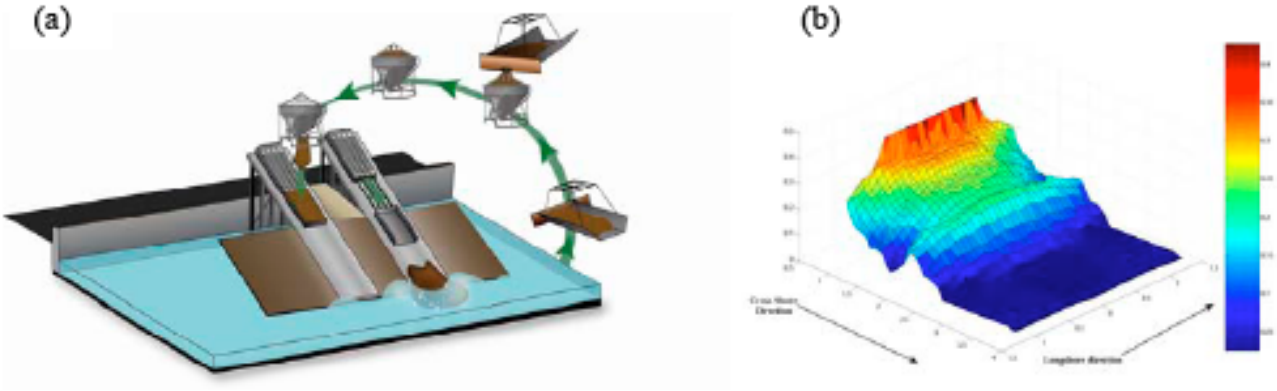

Figure 1. 3-Dimensional landslide tsunami experiments: (a) Landslide tsunami generator deployed in the NEES Tsunami Wave Basin at OSU in the winter 2006/2007; (b) granular landslide deposit scanned with an acoustic multi-transducer array.

Pre-NEES shared-use principle investigator Philip Liu of Cornell University and his research group conducted two sets of experiments on wave impact on cylinders. The scientific objectives were to understand the dynamic interactions among tsunamis, rigid and flexible structures and to develop benchmark problems with high quality experimental data for validating numerical simulation models. Figure 2 shows a focused wave impacting a single cylinder with design wave breaking right at the cylinder. A variety of wave conditions and water depths were used to collect benchmark data of wave force run-up on structures. Experimental results are used to calibrate the predictive capability of numerical models including a nonlinear-coupled fluid-structure interaction code, LS-DYNA (see description below for details), which specializes in accurate contact and impact modeling. A typical comparison of the numerical prediction and experiment results is shown in Figure 3. Figure 3a shows good agreement between measured and predicted results, while Figure 3b shows consistent estimates

of the time history of the free-surface elevation at the front of the cylinder, which was obtained, using the numerical model at variable depth below the mean water level.

Figure 2. Tsunami wave impact on cylinders.

3.2 Warning Guidance Research and Recommendations

NEESR principal investigator Patrick Lynett of Texas A & M University conducted phase I of a multi-year project in the TWB for 25 days in the spring of 2007, and phase II is beginning in July 2008. The proposed scientific objectives are to: (1) improve understanding of near shore, 3 dimensional tsunami evolution through an extensive set of physical experiments; (2) create an extensible framework to provide a systematic structure for validating computational models with experimental and field data; (3) refine modeling capabilities and couple the various components together to create a multi-scale simulation tool; and (4) develop a sustainable education and outreach program that educates the general public about tsunamis and appropriate responses to them. Concurrent to the experimental effort, a comprehensive tsunami simulator, TSUNAMOS (Tsunami Open Source Community Model), will be developed (Lynett et al., 2006).

Phase I included dense measurements of free surface and velocity measurements for 3-dimensional wave breaking under five different wave conditions including solitary and N-waves. For each wave, ADVs provided 3D velocity data at 120 different x, y, z combinations clustered near the onset of breaking. Wave height was measured with wave gauges and the breaking envelope was tracked using overhead video. In all, 225 trials were conducted.

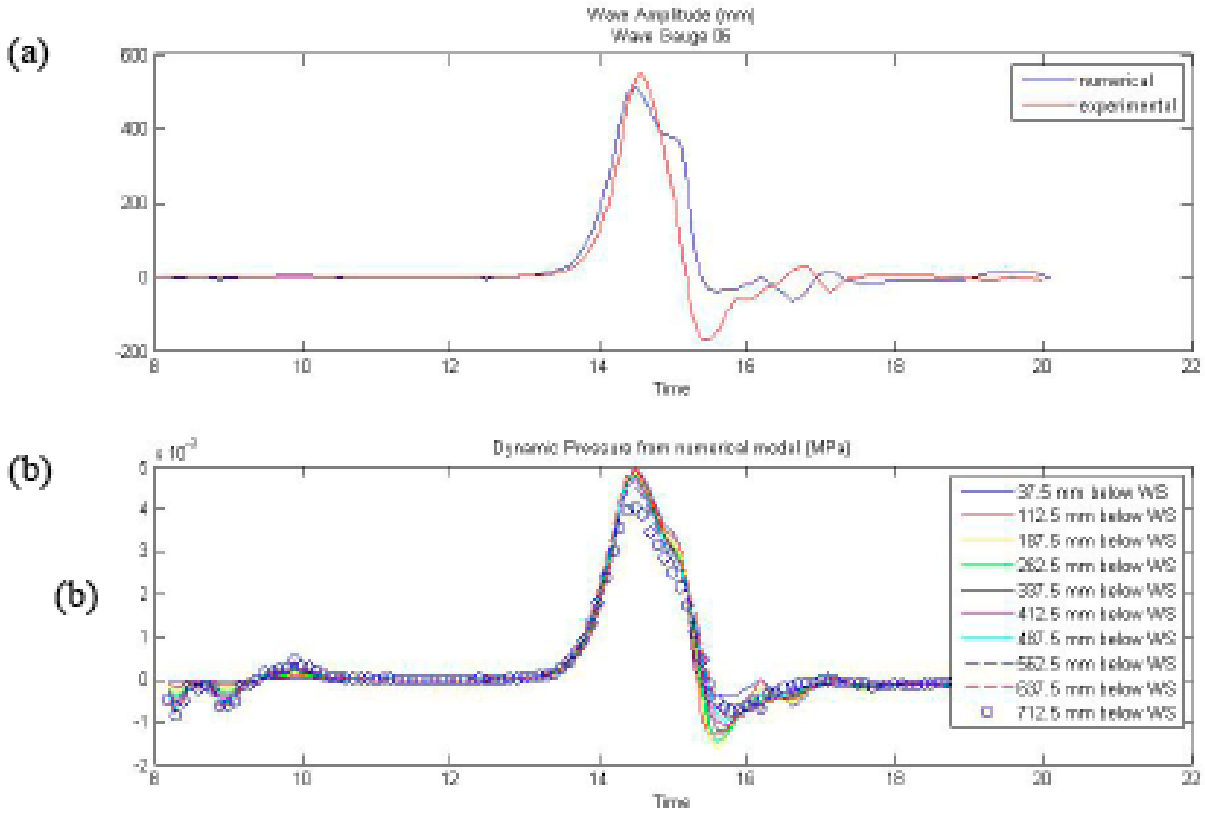

Figure 3. (a) Comparison of LS-DYNA numerical prediction and measured data; (b) Free-surface elevation predictions obtained from LS-DYNA at varying water depth.

Phase II of TSUNAMOS will make use of a longshore-variable sloping beach. This beach can be described as a triangular reef, where the largest shallow water extent (shelf) exists along the centerline of the tank, and linearly tapers to zero at the basin side wall (Figure 4). The purpose of this beach is to create a 3D, bathymetry-forced breaking pattern. A single solitary wave and depth condition will be investigated. Numerous ADV's will be used, with the goal of extracting turbulence (stress) information; many realizations with ADV's in the same location are needed. The free surface elevation will be mapped with approximately 170 resistance wave gage locations. Run-up will be recorded with video cameras. Additionally, dye studies will provide information on the mixing and transport by the solitary wave. Roughness studies will include both fixed and movable sand and gravel, stripes and wires (simulating bushes and trees), and small blocks (simulating small structures

in the path of tsunami inundation). 2HD run-up time series will be digitized from overhead cameras, and the inundation limit will be manually traced after each experimental trial. These experimental settings will simulate situations closer to what tsunamis encounter on natural beaches. With this data, accurate bottom dissipation models will be developed for transient tsunami flow, improving significantly upon the traditional approach. The data collected in these two phases address the run-up and drawdown research identified as needed for hazard assessment. Development of TSUNAMOS will provide officials and communities with an important warning guidance tool.

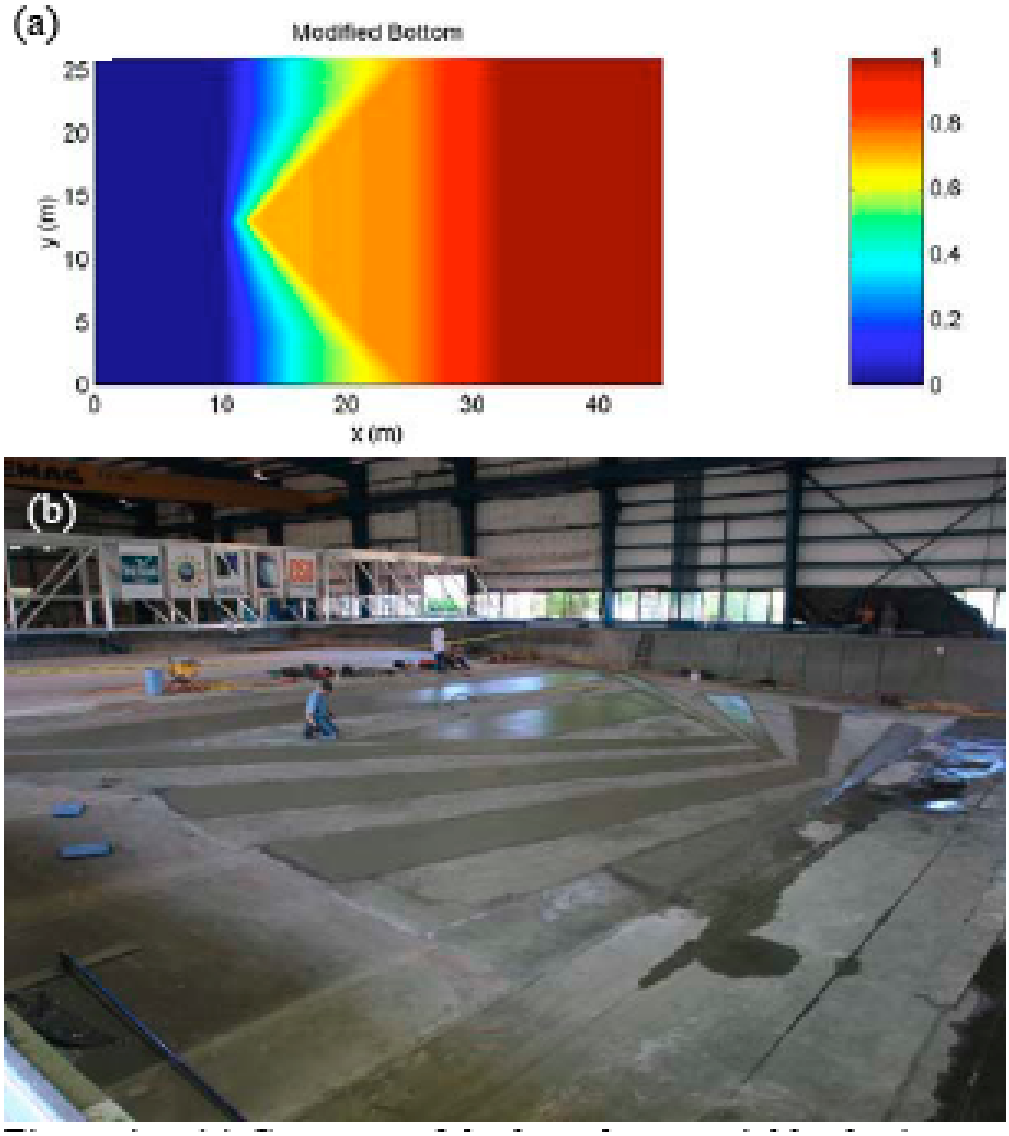

Figure 4. (a) Contours of the longshore-variable sloping beach in the TWB. Contour scale is vertical elevation in meters, and (b) Construction of the bathymetry.

3.3 Preparedness, Response and Mitigation

NEESR principal investigator Ron Riggs of the University of Hawaii and his research group conducted a multi-phase, multi-investigator research project that utilized the TWB through late 2007, and will utilize the new wave maker installed in the LWF in 2009. The proposed research will develop a methodology and validated simulation tools for implementation of site specific Performance Based Tsunami Engineering (PBTE) for use in the analysis, evaluation, design and retrofit of coastal structures and facilities, and code-compatible provisions for tsunami resistant structural design. Coastal inundation modeling will be developed to redraft the inundation mapping for the Hawaiian Islands. The analytical simulation tools will be validated through extensive experimentation at the TRF at OSU. The project is separated into two distinct types of experiments; 1) sediment transport and scour; 2) run-up/inundation and structural loading. Phase I in the TWB began with the sediment transport and scour testing June and July 2007. In August 2007 the testing transitioned to run-up/inundation and structural loading tests (Figure 5). By the end of fiscal year 2007, this project had run seven separate experiments involving ~350 trails and collected ~400GB of data. Work in the LWF in 2009 will provide data at a significantly different scale, which will allow further comparison and verification of models and further refinement of PBTE. The TWB and LWF data will be used to develop and validate coastal inundation codes including the influence of coastal plane and bathymetric variations, and 3-D RANS (Reynolds-Averaged Navier Stokes) simulations of fluid-structure interaction. Design code for development of tsunami resistant structures directly addresses the need for research in how best to prepare communities for tsunami waves and how to mitigate damage and save lives.

Figure 5. A solitary breaking wave in one of two flume channels instrumented to measure run-up.

A NEESR payload project, led by John van de Lindt at Colorado State University, was funded to utilize the University of Hawaii experimental setup. Waves generated by tsunamis and hurricanes have cost hundreds of thousands of lives and millions of dollars in loss of infrastructure and property damage. Currently there are few guidelines for engineers to utilize when designing structures in wave prone areas. The research objective is to test typical residential structural models in order to investigate impact due to wave loading and run-up, and wind/pressure driven surge. A 1/6th scale two story wood framed structure was tested in the north side of the TWB opposite of the UH testing area, utilizing water and wave conditions being generated for the UH experiments. Several aspects of building configuration were analyzed to determine how loading properties were affected. Forces were measured at each corner and deflection was measured at the second story roofline. The experimental setup was determined to be effective at capturing the wave-induced loads. Significant uplift forces were generated when water was allowed to pass beneath the structure, while overturning moments were generated when the front face of the structure was impacted. Structural irregularities, an overhanging roof and a reentrant corner, were found to have impact on how loading was distributed throughout the structure. Pushover tests are planned to verify the results of our analysis. One of the 1/6th scale residential structures was tested to failure (Figure 6).

Figure 6. 1/6th scale residential structure that was tested to failure by wave impact.

3.4 Education and Outreach

The OSU Tsunami Research Facility conducts an extensive education and outreach program including tours and open houses, K-12 educational tours and programs, undergraduate education (Research Experience for Undergraduates site in 2003-2005, 2007, 2008), Research Experience for Teachers (RET) in 2008, and graduate research and teaching opportunities. In all, the site hosts over 3000 visitors a year. Improving the understanding of the public about the science of tsunamis and at the same time disseminating information about warnings and proper hazard response is crucial in saving lives. The site has educational posters, guided tours and hands-on activities all designed to address preparedness and response. The site also utilizes its telepresence cyberinfrastructure to provide public access to on-going research, off-site researcher participation in experiments, and as a teaching tool. A Tsunami Structures activity was developed and implemented with 200 local middle school students, and 40 UH civil engineering fluid dynamics undergraduate students (who participated remotely utilizing the telepresence system). The students studied, designed and constructed shelters scaled at 1:50 (Figure 7) that were bolted to the floor of the TWB, and tsunami waves were generated impacting the structures. A Tsunami Shelter Challenge project funded by NSF was undertaken in the TWB involving 40 middle school teachers and included supplied computers, modeling and visualization design and testing of constructed shelters (http://shelter.nacse.org/).

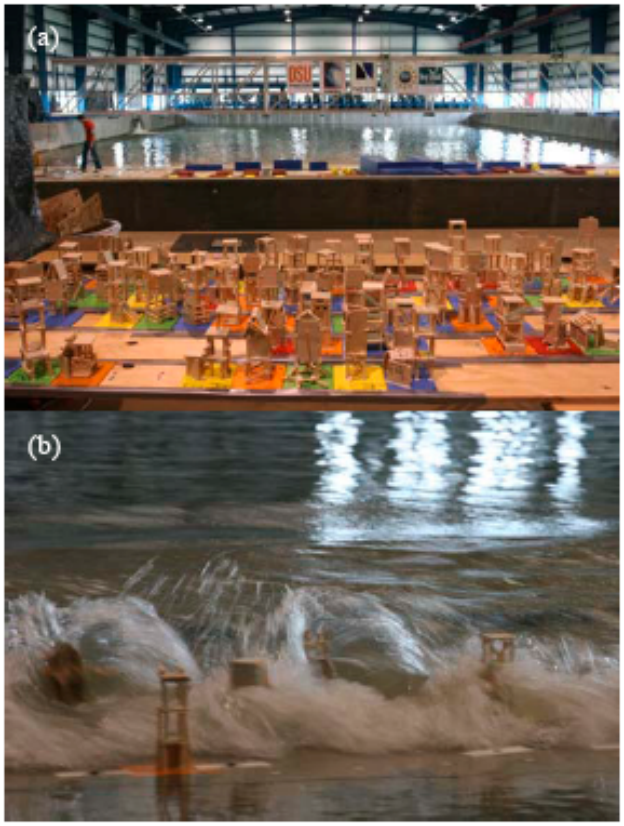

Figure 7. (a) Tsunami structures designed by middle school students waiting to be tested, (b) structures subjected to tsunami wave impacts.

4. NEW PISTON WAVEMER IN THE LARGE WAVE FLUME

The National Science Foundation Major Research Instrumentation program (CMMI-0723277) awarded OSU $1.1M to install a new 2- dimensional piston wave maker in the 342ft LWF in late 2008 (Figure 8). The new piston wave maker will replace the existing hinged-flap style wave maker currently installed. The large-stroke high performance piston wave maker will provide researchers with complementary capabilities due to the significantly wider range of scales available for testing.
The new wave maker will be able to produce tsunami type waves generated by earthquakes as well as extreme hurricane storms (Figure 9), an important step in understanding the impact these waves have on coastal infrastructure, and providing a national asset for precision, large-scale studies enabling safer and more cost effective design of offshore as well as coastal infrastructure including platforms, bridges, levees, buildings and lifelines. Outcomes include better practices for the repair and retrofit of existing structures and improved design codes for new construction.

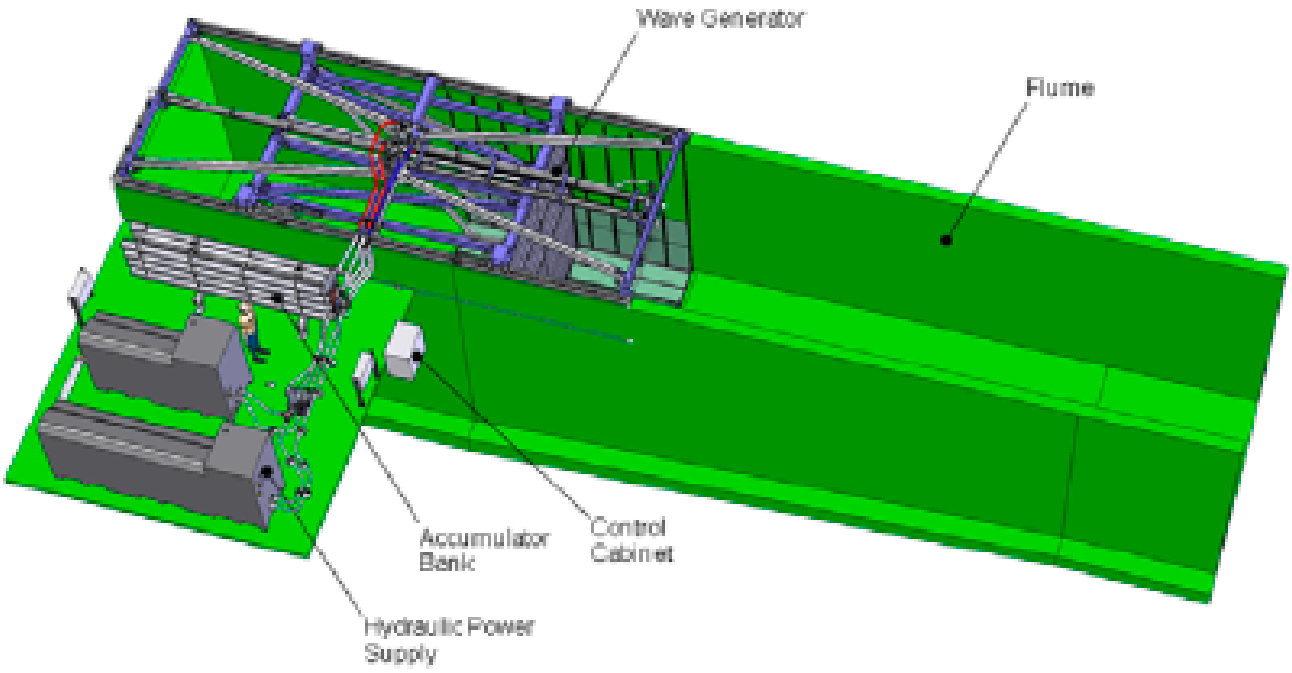

Figure 8. Conceptual rendering of the new piston wave maker installed in the Large Wave Flume. (Image courtesy of MTS Corporation).

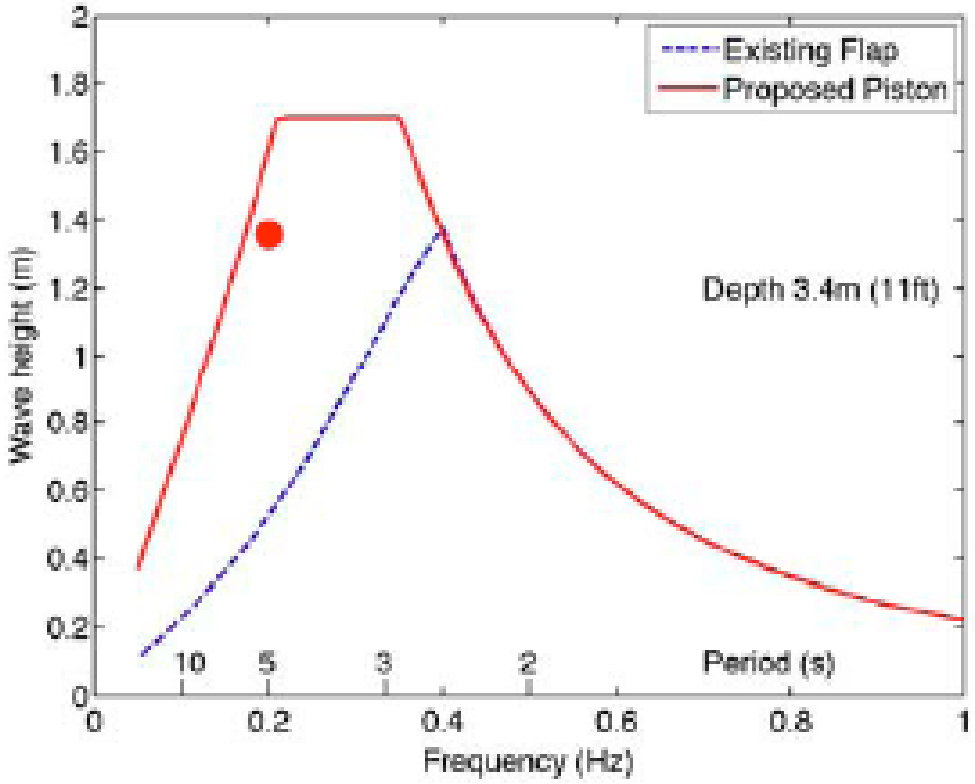

Figure 9. Theoretical performance curve comparing existing (dashed, blue) and proposed (solid, red) wave makers at design water depth d = 3.3 m. Figure shows increased maximum wave heights for lower frequencies (larger wave periods) and the ability to simulate large-scale coastal models under tsunami and hurricane wave conditions (red dot).

5. COMPUTATIONAL SUPPORT

Hydrodynamic models of storm and tsunami waves define the boundary conditions at the coastline for numerical models geared toward detailed analysis of fluid-structure interaction. The environmental loads on a structure include hydrostatic pressure, fluid impingement, form and viscous drag, and impact due to waterborne debris, some of which may induce large structural deformation, yielding, fracture, and collapse or dislodgement. Accurate modeling of coupled fluid-structure interaction is a very challenging problem. Traditionally, the study of coastal waves and structures belong to two separate disciplines and their analysis and numerical techniques usually cannot be coupled. Since the inception of the TWB construction project in FY2000, researchers at OSU have been developing computational fluid-structure interaction software suitable for use by both environmental and structural engineers (Yuk *et al*., 2006). Selected on-going developments related to this goal are briefly summarized here.

The software package LS-DYNA, which contains modules for very large strain deformation, nonlinear materials, fracture, shearing detachment, contact and impact, appears to be a suitable computational structural dynamic (CSD) code for structural analysis needs. It also contains a fluid module based on the Navier-Stokes equations used to model wave impact as well as surface piercing and re-submergence of multiple flexible bodies. Recently, a finite-element based formulation to model the fluid domain called the particle finite element method (PFEM) (Del Pin, 2003) shows promising signs of unifying the simulation of fully coupled fluid-structure interaction. In the PFEM formulation, the continuity and momentum balance equations in the fluid domain are modeled using a Lagrangian formulation and discretized using particle finite-elements. The boundaries at the free surface and at the interface between the fluid and the structure can be modeled exactly with a moving FE grid that is remeshed at every time step.

A combination using the CSD and computational fluid dynamics (CFD) codes from industry with proven robustness and nonlinear capabilities for the analysis of structural behavior, and the PFEM formulation for modeling fluid motions in arbitrary Lagrangian-Eulerian (ALE) form, may provide the best solution for the development of a robust code for simulation of storm waves, tsunami basin experiments and prototype events. This choice allows a unified ALE formulation and computation for both fluid and structural domains. More importantly, it allows for exact means of tracking the fluid-structure interface that determines: (1) the energy input to the wave field by the wave generator; (2) the wave forces on the coastal structures and floating debris; and (3) energy dissipation at the bottom boundary and the beach that may contain porous media and/or movable sediments.

LS-DYNA is also capable of modeling a complex system by first modeling the components of the system as individual modules and then assembling them together to form the system. With this capability, we are able to model an experiment to be conducted at the OSU TRF as follows. We first model the wave basin including wave paddles and water as a single module, and separately an instrumented cylinder including its components as another module, and then insert the cylinder module inside the tsunami wave basin module to form the experimental model. Once the system is in place, we can simulate a test run and compute the strains inside the cylinder. This procedure was used to generate the numerical prediction of wave impact on a cylinder presented in a previous section shown above.

An issue with using a complex code like LS-DYNA is computational resources. To model the fluid-structural interaction experiment at the TWB shown above using 1cm3 elements would lead to the number of fluid and structural elements on the order of 3 x 109. Using a 20-node solid element with 3 degrees of freedom (d.o.f.) at each node would lead to approximately 4 x 1010 d.o.f. An explicit computation of the numerical model for a typical transient experimental test of approximately 20 seconds would exceed the capability of many existing parallel computer clusters. The use of state-of-the-science high-end high-performance parallel computers is necessary.

5. CONCLUSION

Research underway at the NEES Tsunami Research Facility at Oregon State University reflects the NEES mission to further earthquake engineering research, with the ultimate goal to save lives and preserve property. Recommendations by the National Tsunami Research Plan suggest a research roadmap to further scientific understanding of tsunami processes and effects on human lives. The

recommended research includes areas in (1) hazard assessment, (2) warning guidance and (3) response and outreach. It is shown that the research projects at the OSU TRF are not only furthering the NEES mission, but also aligned with the recommended areas of research in the roadmap report. The simultaneous development of numerical modeling tool at the TRF has shown promising results in assisting with the design of wave-basin experiments. These numerical models, both 2-D and 3-D, when matured, are anticipated to become integral parts of technical tools for future experiments at the facility.

ACKNOWLEDGEMENTS

Part of this work is supported by the George E. Brown, Jr. Network for Earthquake Engineering Simulation (NEES) Program of the National Science Foundation under Award Number CMS-0402490. The authors would like to thank NEESR researchers, Hermann Fritz, Yin Lu Young, Philip Liu, Patrick Lynett, Ronald Riggs and John van de Lindt for permission to describe their projects and for providing information and images for this paper. The authors would also like to thank the O.H. Hinsdale Wave Research Laboratory staff for their efforts in assisting researchers to achieve their experimental goals. The first author also wish to acknowledge the financial support from the Office of Naval Research (N00014-04-10008, N0014-07-10207, and N0014-07-10326) for the numerical model development.

REFERENCES

Bernard, E.N., Dengler, L.A. and Yim, S.C. (2006). "National Tsunami Research Plan: Report of a Workshop Sponsored by NSF/NOAA," *NOAA technical Memorandum OAR PMEL-133*.

Del Pin, F., "The Meshless Finite Element Method Applied to a Lagrangian Formulation of Fluid Flows," Ph.D. Thesis, Universidad Nacional del Litoral, 2003.

Lynett P, Liu, P., Mercado, A., Teng, M., and von Hillebrandt-Andrade, C. (2006). "NEESR-SG: TSUNAMOS: A Validated, Multi-Scale Tsunami Model for Hybrid Numerical-Experimental Simulation," NSF award abstract #0619083.

National Science and Technology Council. (2005). "Tsunami Risk Reduction for the United States: A Framework for Action," A Joint Report of the Subcommittee on Disaster Reduction and the United States Group on Earth Observations.

Yuk, D., Yim, S.C., and Liu, P.L-F. (2006). "Numerical Modeling of Submarine Mass-Movement Generated Waves Using RANS Model," *Computers and Geosciences*, Vol.32, pp.681-689.

VULNERABILITY ASSESSMENT OF CAR NICOBAR TO TSUNAMI HAZARD USING NUMERICAL MODEL

Tune Usha[1], M V Ramana Murthy[1], N T Reddy[1], T S Murty[2]

ICMAM-PD, Ministry of Earth Sciences, Govt. of India, NIOT Campus, Pallikaranai, Chennai 600 100., Fax : 044-22460657, Phone : 044-22460991, email :usha@icmam.gov.in

* - University of Ottawa, Ottawa, Canada, Phone : +1-6137395445, Fax : +1-613 562 5173 e-mail:smurty@hotmail.com

ABSTRACT

The December 26, 2004 Sumatra earthquake's epicenter was 163 kms away from Great Nicobar, the southern most island from the archipelago and hence it was strongly felt in the entire Andaman & Nicobar group of islands including Car Nicobar. 3400 people have lost their lives and most of the vital infrastructure were completely destroyed. The presents study aims to understand the vulnerability of the Car Nicobar coast to tsunami hazard from varied sources by using numerical model of tsunami propagation and run-up and compare it with the field data on inundation collected immediately after the tsunami using real time kinematic GPS. A tsunami vulnerability database has been builtup by modelling the past earth quakes recorded in this region. Elevation data collected using Airborne Laser Terrain Mapper (ALTM) was used to generate the inundation scenarios. A GIS database on the tsunami vulnerability of Car Nicobar to tsunami hazard is generated which would be immense use in mitigation and planning.

Science of Tsunami Hazards, Vol. 28, No. 1, page 15 (2009)

1.0 INTRODUCTION

The idyllic island of Car Nicobar, which bore the full fury of the tsunami in December 2004, lies in the heart of the Andaman and Nicobar islands archipelago in the Indian Ocean. It is the northernmost of the Nicobar Islands, which in turn are the southern part of the Indian Union territory of the Andaman and Nicobar islands. It lies at 9º10'N 92º45'E and has an area of 127 km² and is a very small Island, in comparison to the Middle Andaman or South Andaman. The climate of Car Nicobar Island is tropical, as it is just 9 degree from the equator, with an annual rainfall of 400 mm.

The 26th December, 2004 earthquake was followed by high tsunami tidal waves which caused extensive damages in parts of Andaman and Nicobar such as Port Blair harbour, Jetties at Aberdeen, Phoenix Bay, Junglighat and Haddo which were flooded by high tidal waters. However, the extent of damage, loss of life and property in Car Nicobar was unprecedented due to the combined action of high waves and subsidence of land to an extent of 1.3m due to the earthquake. The side of the islands facing the epicenter was the most vulnerable. The Nicobarese villages of Malacca and Kakana on the southeastern side of the island suffered heavy casualities while on the northeastern side, people in the villages of Sawai, Arong, Teatop moved deeper into the forest and formed new settlements. The Malacca jetty was totally destroyed.

2.0 TSUNAMI VULNERABILITY OF THE ANDAMAN AND NICOBAR ISLANDS

India's vulnerability to tsunami-caused destruction was estimated as very low, if not non-existent until the 2004 tsunami event. As a result, not only was there no effort to set up an advance warning and international networking system, but tsunami-vulnerability was not one of the factors taken into account in the determination of the location of our nuclear and space launching establishments and in designing their safety features. Similarly, this vulnerability was not taken into consideration while determining the location of our military establishments in the Andaman and Nicobar Islands and their safety features. However, Andaman and Nicobar islands have not been totally immune to tsunamis, because at least five historical earthquakes have been known to have triggered a tsunami that hit the islands of Andaman and Nicobar (Fig.1).

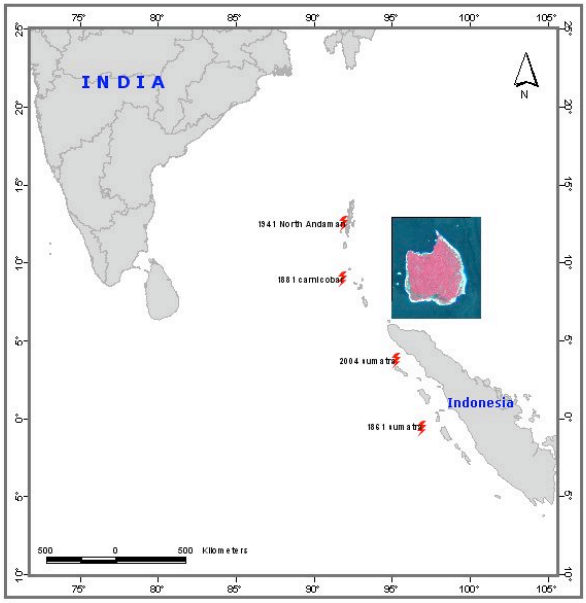

Fig. 1. Tsunamigenic sources that threaten Car Nicobar

2.1 Car Nicobar, India, 1847

The first of the three large historical earthquakes in the Andaman/Nicobar region for which information is available occurred on 31st, October, 1847, however no original account of the 1847 earthquake survived.

2.2 Car Nicobar, India, 1881

The second recorded earthquake was on 31st December 1881 at Car Nicobar. Data for the study of this earthquake were compiled by Oldham (1884) who, on the basis of astronomical clock recordings in Madras (Chennai) and Calcutta (Kolkatta), believed the earthquake occurred on the locus of these two cities beneath the Bay of Bengal (400 km west of the Andaman Islands). Seismographs had yet to be invented but tide gauges at eight harbors surrounding the Bay of Bengal recorded the largest surface waves and the resulting tsunami, and these data provide a powerful constraint on timing and rupture parameters. The earthquake with magnitude Mw-7.9 is calculated to have occurred near and west of Car Nicobar with two reverse slip ruptures.

2.3 Andaman, India, 1941

The most recent of the major earthquakes in the Andaman islands preceding the recent rupture of 2004 occurred in 1941, a year before Japanese occupation of the islands. However, the earthquake was described only after the Second World War [Krishnan, 1953; Jhingran, 1953] Although the tsunami generated by the 1941 earthquake is stated to have caused much loss of life

along the east coast of India [Murty and Rafiq, 1991] no official (or unofficial) account of the impact of the remote tsunami has been discovered. Jhingran describes the loss of low-lying western-facing forest cover on the Andamans, presumably by a tsunami but mentions no loss of life. Eyewitness reports published informally by the Society of Andaman and Nicobar Ecology (SANE) following the 2004 earthquake add further details to the official 1941 accounts. The central watch-tower of the cellular jail in Port Blair collapsed along with a hospital and other masonry structures. Eyewitnesses speak of subsidence of Ross Island (as in the recent earthquake), requiring its abandonment in favor of the current mainland capital, Port Blair.

2.4 Sumatra, Indonesia, 2004

The worst tsunami disaster in living history was caused by an earthquake in the Indian Ocean off the island of Sumatra measuring 9.3Mw. More than 300 000 people were killed in eight Asiatic countries (in particular Indonesia/Sumatra, Sri Lanka, India, Thailand, Myanmar, Maldives, Malaysia and Bangladesh). The flood wave even reached coastlines several thousand kilometres away, like East and Southeast Africa. There were also casualties in Somalia, Tanzania, Kenya, Madagascar and the Seychelles.

2.5 Sumatra , Indonesia, 1861

Based on past historical records and the tsunami of the recent past, an attempt has been made to study the vulnerability of the islands of Andaman and Nicobar to tsunamis. Car Nicobar by virtue of its proximity to the earthquake source and low land elevation was severely damaged and hence was extensively surveyed for extent of inundation and runup immediately after the tsunami. The field data collected was used to validate the numerical models used to calculate the vulnerability of the island due to tsunami hazard. the A GIS based risk atlas is developed using Numerical models to study the extent of inundation and run-up for various historic earthquake scenarios. Inundation scenarios have been generated for four past earthquake scenarios. In order to assess the maximum extent of inundation and run-up that could occur in future, a hypothetical earthquake scenario was also generated by loading the Sumatra 2004 earthquake seismic parameters on the Car Nicobar source.

3.0 METHODOLOGY

The main objective of this work is to provide an estimate of wave height and extent of inundation in the event of a tsunami. Given the time constraints of computing the three stages of tsunami modeling, namely, wave generation, propagation and inundation in real time, the work is expedited by generating a database of pre-computed scenarios, which is found to be an useful tool in tsunami mitigation. The pre-computed database contains information about tsunami propagation in the open ocean from a multitude of potential sources. When a tsunami event occurs, an initial source is selected from the pre-computed database. In the initial stages of the tsunami, this selection is based only on the available seismic information for the earthquake event, similar to one of the pre-computed scenario. For the identified earthquake scenario, the large scale inundation map is selected from the database.

Inundation studies can be conducted taking a probabilistic approach in which multiple tsunami scenarios are considered, and an assessment of the vulnerability of the coast to tsunami hazard is evaluated, or they may focus on the effect of a particular 'worst case scenario" and assess the impact of such a particularly high impact event on the areas under investigation. The results of a tsunami inundation study should include information about the maximum wave height and maximum inundation line. This information can be used by emergency managers and urban planners primarily to establish evacuation routes and location of vital infrastructure. On the basis of the model prediction, vulnerability maps will be prepared which will be useful in disaster management and mitigation activities. These maps help in defining the limits of construction of new essential facilities and special occupancy structures in tsunami flooding zones

An inundation modeling study attempts to recreate the tsunami generation in deep waters, wave propagation to the impact zone and inundation along the study area. To reproduce the correct wave dynamics during the inundation computations high resolution bathymetric and topographic grids are required. The high quality bathymetric and topographic data sets needed for development of inundation maps require maintenance and upgrades as better data becomes available and coastal changes occur. In the present study elevation datasets have been collected using Airborne Laser Terrain Mapper (ALTM) for a distance of 2km from the coast all around the island. ALTM datasets were corrected for the mean sea level and the vertical error was found to be about 0.35m. For higher altitudes inland, 1:25000 toposheet was used to derive the elevation data. On the sea side, bathymetry data was obtained from C-Map and NHO charts. The General

bathymetric chart of the oceans (GEBCO) was used to populate the deep sea regions. The datasets were so built so as to have very precise data for the near coastal regions both on the land and sea side which plays the dominant part for inundation studies and the offshore datasets were populated using global bathymetry datasets (Fig.2).

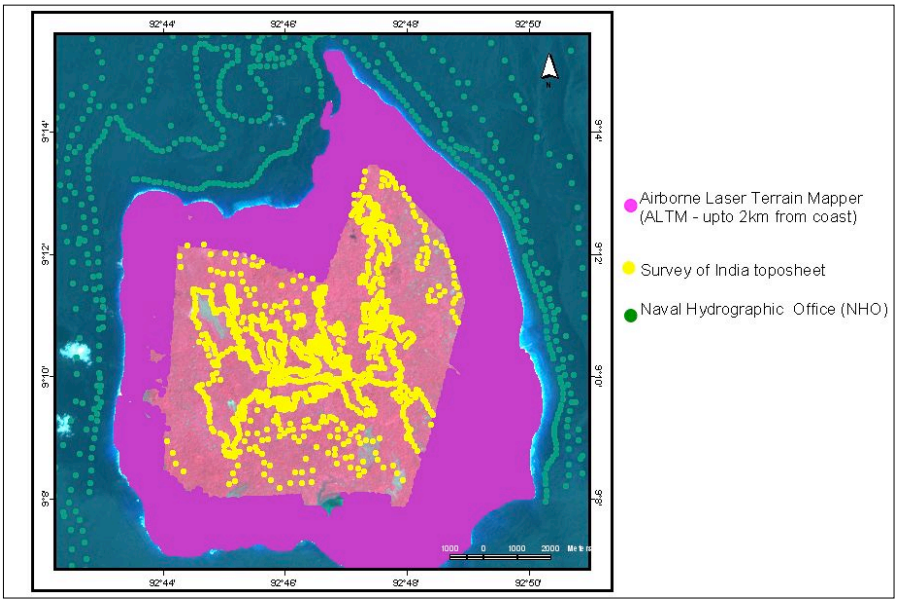

Fig 2. Data used to populate the near coastal regions

4.0 **NUMERICAL MODEL FOR TSUNAMI INUNDATION**

The use of numerical modeling to determine the potential run-ups and inundation from a local or distant Tsunami is recognized as useful and important tool, since data from past tsunamis are usually insufficient to plan future disaster mitigation and management plans. Sufficiently accurate modeling techniques have been developed in the recent years, and these models require proper inputs on detailed bathymetry and topographic data for the area being modeled. In the present study a finite difference code of TUNAMI N2 (Imamura, 1996) was employed to predict the inundation. The parameters used for computataion of the sea surface deformation at source for various historical earthquakes are given in Table 1.

Table 1. Parameters used for computation of sea surface deformation at source

Parameters	2004 Sumatra	1941 Andaman	1881 Car Nicobar	1861 Sumatra	Worst-case
Source	Sumatra	North Andaman	Car Nicobar	Sumatra	Car Nicobar
Longitude	95.85^0 E	92.5^0 E	92.43^0	97.5^0	92.43^0
Latitude	3.32^0 N	12.1^0 N	8.52^0	-1.00	8.52^0
Magnitude	9.3 Mw	7.7 Mw	7.9 Mw	8.5 Mw	9.3 Mw
Slip	15 m	5 m	5 m	4 m	15 m
Fault Length	500 km	200 km	200 km	305 Km	500 km
Fault Width	150 km	80 km	80 km	101 Km	150 km
Strike Angle	345^0	20^0	350^0	320^0	345^0
Dip Angle	15^0	20^0	25^0	12^0	15^0
Rake Angle	90^0	90^0	90^0	90^0	90^0
Focal Depth	20 km	30 km	15 km	30 km	20 km

These seismic parameters are provided as input to construct dislocation for determination of the static Tsunami source (initial wave) in the domain. The predictions of the models are directly related to the quality of the data used to create the bathymetry and topography of the model area. Considerable time, resource and effort are necessary to collect high resolution bathymetry and elevation data of the coastal areas. The model results obtained using the high resolution bathymetry and elevation data are calibrated and validated using field observations. The model once validated can be used for creating different scenarios of extreme inundation and run-up by varying the source parameters that actually the trigger the tsunami.

4.1 Generation of computational grids

To create the computational grids for tsunami model, ALTM data and 1:25000 Survey of India toposheet and NHO charts was used along with GEBCO and SRTM datasets. As a nested grid system was used to run the model, the inner most study area grid was constructed using highly accurate altm dataset and NHO chart values.

4.2 Field measurements

Immediately after the tsunami, field measurements on inundation and runup were made along the Car Nicobar coast specially along the Indian Airforce Base at Malacca. Run-up measurements at different sites along the coasts were made using Realtime Kinematic Global Positioning System (RTKGPS). In Car Nicobar a maximum runup of about 7m and an inundation of 1km was observed near Malaca (Table 2).

Table 2. Field Measurements at Car Nicobar on Inundation and Run-up

Id	Latitude	Longitude	Elevation (m)	Inundation (m)
1	9.173491884	92.82259519	2.4813	695
2	9.157835800	92.82230271	8.0579	900
3	9.161034506	92.82278315	8.3134	893
4	9.164605948	92.82333409	7.1946	870
5	9.164617939	92.82330192	7.2213	874
6	9.164629949	92.82326922	7.1634	876
7	9.164664574	92.82317327	7.0282	880
8	9.164688440	92.82310983	6.9155	876
9	9.164699524	92.82307782	6.8499	895
10	9.164722952	92.82301324	6.7947	882
11	9.164735309	92.82298218	6.7301	910
12	9.165120533	92.82363841	6.6481	842
13	9.166610636	92.82404471	5.8565	790

4.3 Validation of model results

The model results were validated using the field data on inundation collected immediately after the tsunami (Table 3, Fig.3 and Fig.4).

Table 3. Observed and Predicted Inundation for 2004 Sumatra earthquake source

Id	Latitude	Longitude	Observed (m)	Predicted (m)
1	9.173491884	92.82259519	695	700
2	9.157835800	92.82230271	876	600
3	9.161034506	92.82278315	893	870
4	9.164605948	92.82333409	870	880
5	9.164617939	92.82330192	874	850
6	9.164629949	92.82326922	876	950
7	9.164664574	92.82317327	880	947
8	9.164688440	92.82310983	876	945
9	9.164699524	92.82307782	895	950
10	9.164722952	92.82301324	882	980

11	9.164735309	92.82298218	910	990
12	9.165120533	92.82363841	842	844
13	9.166610636	92.82404471	790	789

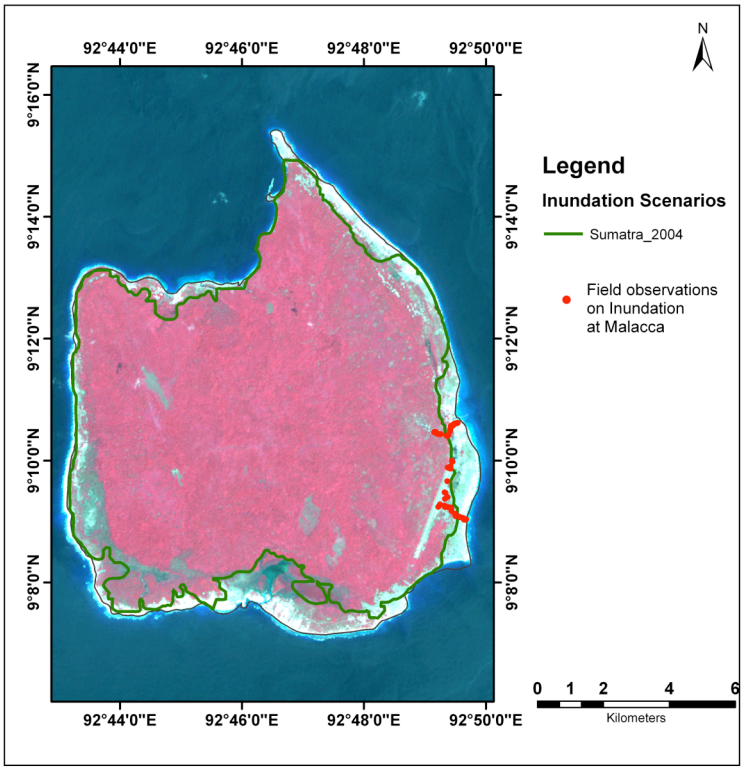

Fig. 3. Validation of model results using field data

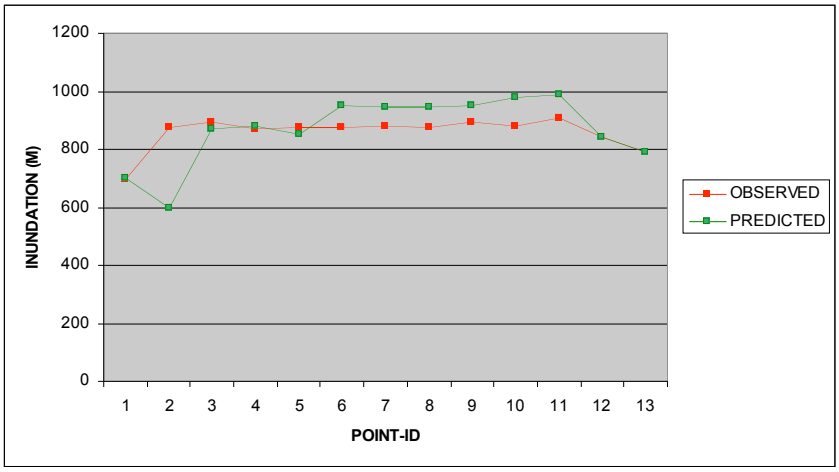

Fig. 4. Comparison between observed and predicted inundation

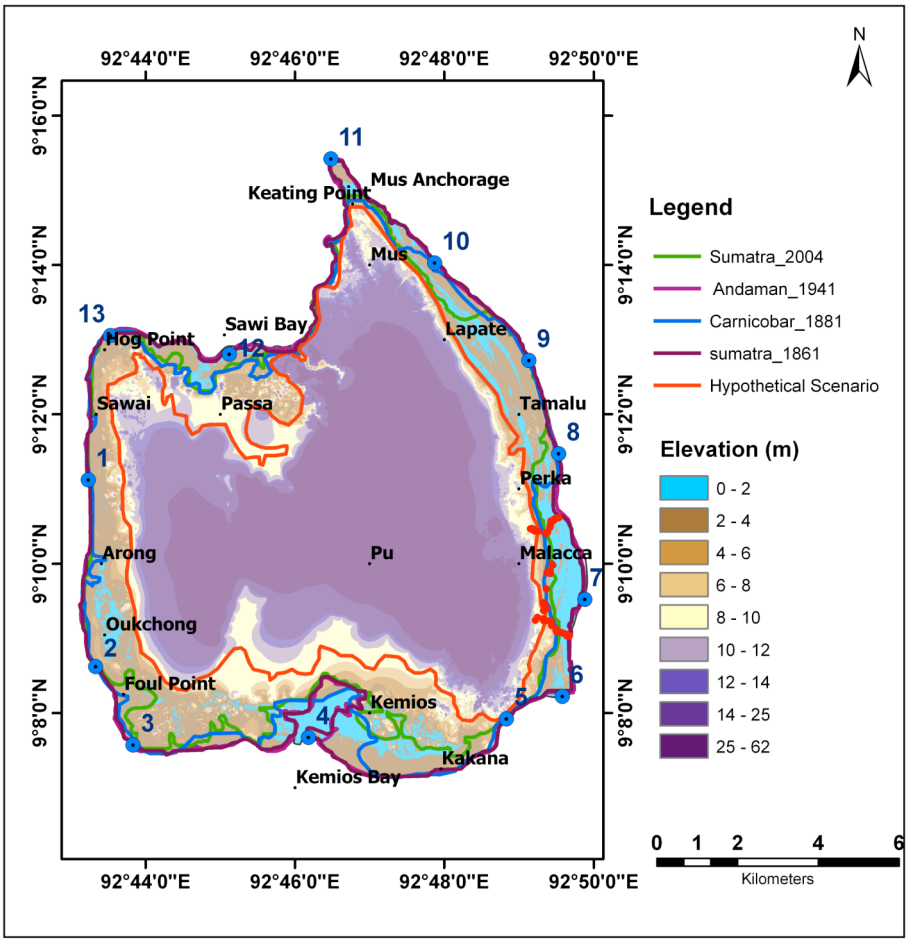

Fig. 5. Extent of Inundation for Various earthquake scenarios

5.0 OBSERVATIONS AND DISCUSSION

The extent of inundation due to four historical earth quakes and one hypothetical worst case scenario is given in Fig.5. The inundation and runup predicted along the selected points along the shore are tabulated below(Table 4 and 5).

Table 4. Predicted Inundation at Car Nicobar due to the various Tsunamigenic sources

Inundation in meters.

Id	Longitude	Latitude	Sumatra 2004	Car Nicobar 1881	Andaman 1941	Sumatra 1861	Hypothetical Scenario
1	92.720520	9.185373	120	-	-	-	921
2	92.722187	9.143707	106	-	-	-	1290
3	92.730520	9.126207	340	141	-	-	1886
4	92.769687	9.127873	1630	971	1557	1570	2302
5	92.813853	9.132040	82	66	-	-	130
6	92.826353	9.137040	768	727	160	157	1215
7	92.831353	9.158707	808	940	110	141	1386
8	92.825520	9.191207	388	97	-	-	1205
9	92.818853	9.212040	117	-	-	-	1413
10	92.798020	9.234540	526	102	-	-	643
11	92.774687	9.257040	1183	1267	-	-	1375
12	92.752050	9.215474	532	607	138	184	2896
13	92.725520	9.218707	121	133	-	-	1231

Table 5. Predicted Run-up at Car Nicobar due to the various Tsunamigenic sources

Runup in meters.

Id	Longitude	Latitude	Sumatra 2004	Car Nicobar 1881	Andaman 1941	Sumatra 1861	Hypothetical Scenario
1	92.72052	9.185373	2.34	2.65	0.24	0.36	6.96
2	92.72219	9.143707	2.75	2.75	0.28	0.58	6.60
3	92.73052	9.126207	2.66	2.40	0.31	0.59	7.69
4	92.76969	9.127873	3.44	3.68	0.64	1.02	8.49
5	92.81385	9.13204	5.14	3.63	0.81	1.08	7.34
6	92.82635	9.13704	3.77	3.31	0.33	0.71	5.26
7	92.83135	9.158707	2.07	3.48	0.18	0.49	6.10
8	92.82552	9.191207	1.97	2.50	0.14	0.37	5.04
9	92.81885	9.21204	2.06	2.81	0.13	0.32	5.31
10	92.79802	9.23454	3.67	2.67	0.20	0.40	4.48
11	92.77469	9.25704	2.59	2.24	0.27	0.41	3.41
12	92.75205	9.215474	2.92	3.53	0.44	0.65	10.40
13	92.72552	9.218707	1.75	2.10	0.23	0.50	5.61

5.1 Inundation and run-up due to Sumatra, Indonesia, December 26, 2004 earthquake

Inundation and Water level at Car nicobar due 2004 Sumatra Tsunami caused by an earth quake of 9.3 Mw and at a distance of 750km, SE of Car Nicobar is shown in Fig. 6.The maximum inundation at the coast from the shore was 720m in Malaca (Point 6) whereas the water entered further inland through creeks (Pt.4 and Pt.11). The maximum run-up was 5.1m. . Along the coast there are significant spatial gradients in tsunami run up signatures, which are attributed to topographic profiles along the coastline. The tsunami surge penetrates along the shore up to berm level along straight coast and penetrated inland large distances inland wherever low lands/ creeks connected to sea. Along the coast the run up heights varied between 2.0m to 5.1 m and the run up distances from 100 to 800m.

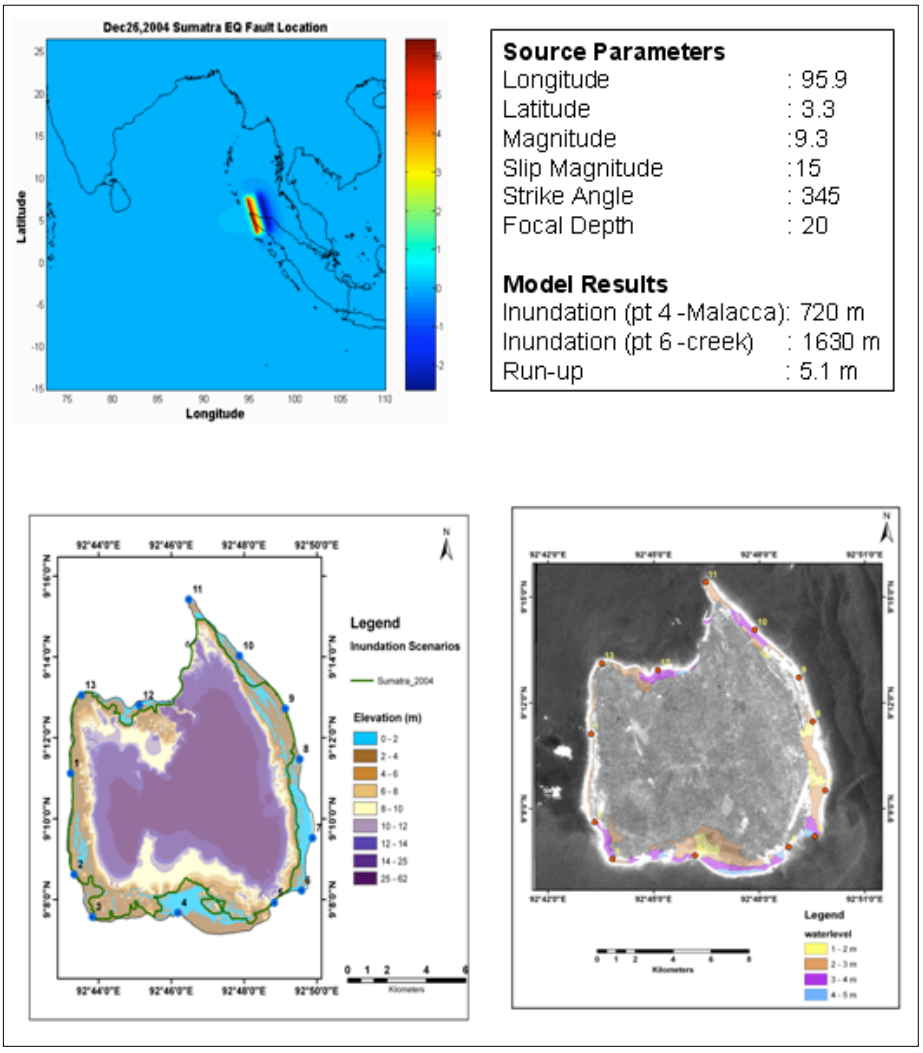

Fig.6 Inundation and Water level at Car Nicobar for 2004 Sumatra Tsunami – Earth quake of 9.3 Mw and at a distance of 750km, SE of Car Nicobar

5.2 Inundation and run-up due to Car Nicobar, India, December 31, 1881 earthquake

Inundation and Water level at Car Nicobar due 1881 Car Nicobar Tsunami caused by an earth quake of 7.9 Mw and at a distance of 75km, SW of Car Nicobar is shown in Fig.7. The maximum inundation at the coast from the shore was 900m (Point 7) whereas, the water entered further inland through creeks (Pt.4 and Pt.11). The maximum run-up was 3.5m. Along the coast the run up heights varied between 2.0m to 3.5 m and the run up distances from 100 to 900m.

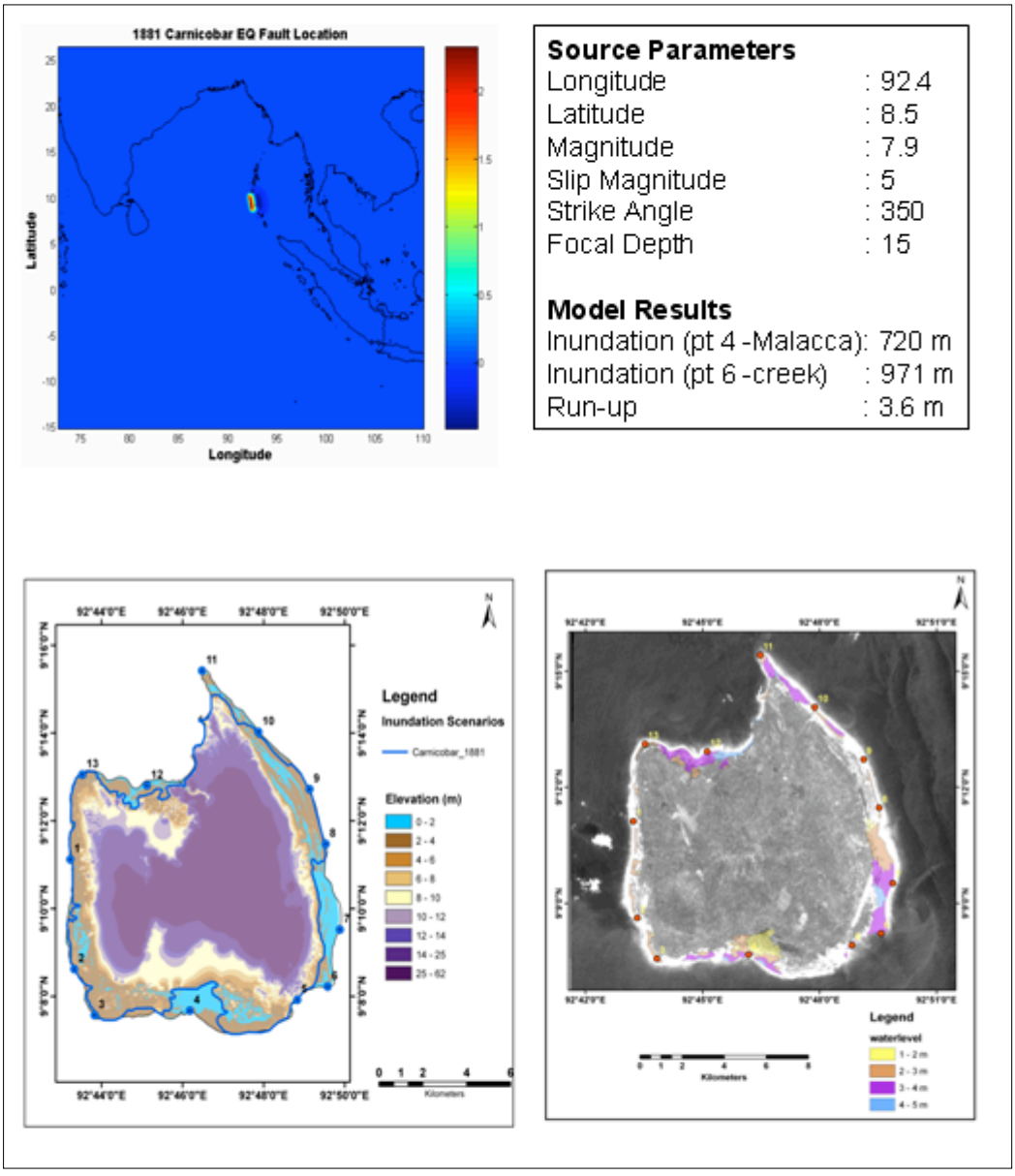

Fig.7. Inundation and Water level at Car Nicobar for 1881 Car Nicobar Tsunami – Earth quake of 7.9 Mw and at a distance of 75km, SW of Car Nicobar

5.3 Inundation and run-up due to Andaman 26 June 1941 earthquake

Inundation and Water level at Car Nicobar due 1941 Andaman tsunami caused by an earth quake of 7.7 Mw and at a distance of 330km, North of Car Nicobar is shown in Fig.8. Though there was an observed rise in water level it was very mimimal and the inundation inland was also not very significant. However water entered inland through creeks upto a distance of 1.5km.

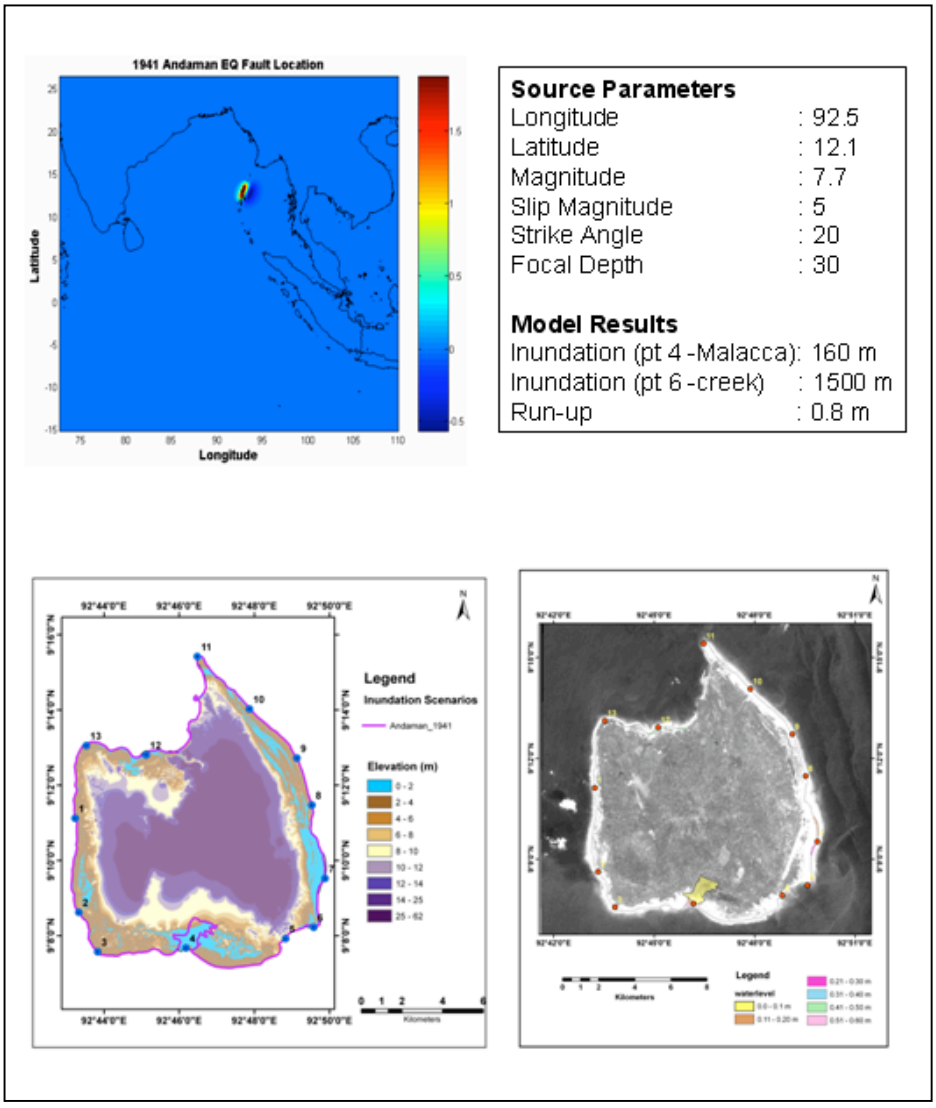

Fig.8. Inundation and Water level at Car Nicobar for 1941 Andaman Tsunami – Earth quake of 7.7 Mw and at a distance of 330km, North of Car Nicobar

5.4 Inundation and run-up due to Sumatra 1861 earthquake

Inundation and Water level at Car Nicobar due 1861 Sumatra tsunami caused by an earth quake of 8.5 Mw and at a distance of 810km, NE of Car Nicobar is shown in Fig. 9. Though there was an observed rise in water level it was very mimimal and the inundation inland was also not very significant. However water entered inland through creeks upto a distance of 1.5km.

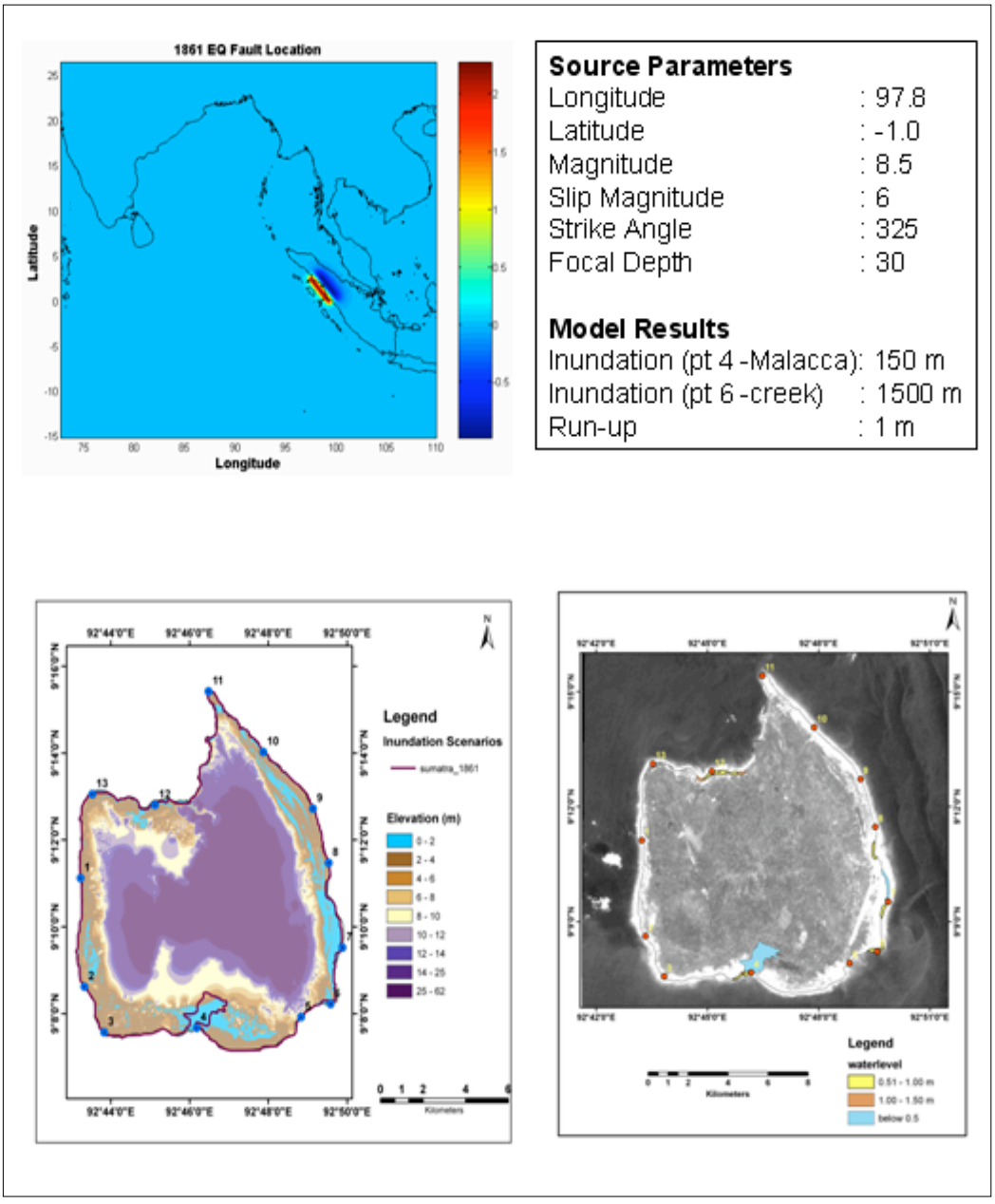

Fig. 9 Inundation and Water level at Car Nicobar for 1861 Sumatra Tsunami – Earth quake of 8.5 Mw and at a distance of 810 km, NE of Car Nicobar

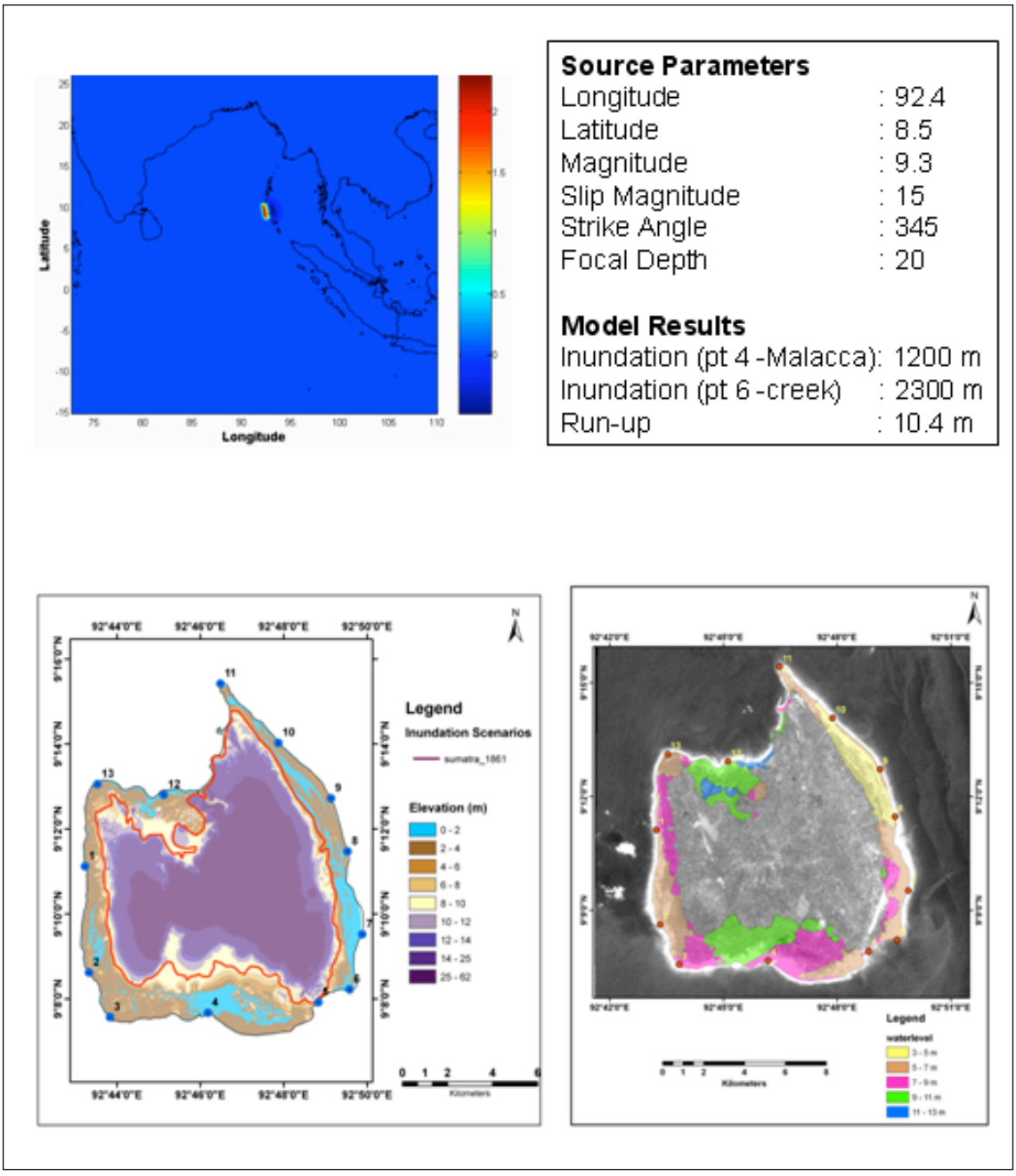

Fig. 10 Inundation and Water level at Car Nicobar for worst case scenario Tsunami – Earth quake of 9.3 Mw and at a distance of 75 km, SW of Car Nicobar

5.5 Inundation and run-up due to a hypothetical worst case scenario

A worst case scenario was developed by forcing the Sumatra 2004 earth parameters on the 1881 Car Nicobar earthquake location. Since this location was only at a distance of 75km SW of Car Nicobar large scale inundation and run-up heights were predicted by the model. The maximum inundation was about 3km (point 12) while the maximum run-up as10.40 m.The maximum inundation and run-up at Car Nicobar for historical earthquake scenarios and one hypothetical worst case scenario is listed below (Table 6).

Table 6 . Maximum inundation and run-up calculated along Car Nicobar coast

Location	Source Distance	Magnitude	Land inundation	Inundation-creeks	Max.up Runup
Sumatra-2004	750	9.3	720	1630	5.1
Andaman-1941	330	7.7	160	1597	0.8
Car Nicobar 1881	75	7.9	720	971	3.6
Sumatra-1861	810		150	1570	1
Worstcase scenario	75	9.3	1200	2300	10.4

6.0 **HIGH WATER LEVELS**

High Water Levels of Tsunami Persisted for Several days in A & N Islands and Media reports as well as scientific observations suggested that, even though the 26 December 2004 tsunami lasted only a few hours in A & N Islands, high waters persisted for several days. The results of the numerical model for 2004 Sumatra tsunami also indicate high water levels along the Car Nicobar coast. The question then is what physical processes is responsible for these high water levels. A brief explanation is provided below in terms of the so called Oscillations of the First Class (OFC) and Oscillations of the Second Class (OSC) in the oceans. The OFC are essentially gravity modes while the OSC are called rotational modes or elastoidal-elastoid intertia oscillations. The OFC would exist with or without earth's rotation but their frequency is modified due to earth's rotation, whereas the OSC owe their existence to earth's rotation.

The frequency range of OFC and OSC is separated by the so called pendulum day defined below;

$$2T_p = \frac{2\pi}{\omega \cdot \sin\theta}$$

Tp = period of revolution of a Foucault Pendulum;
θ = latitude; ω = angular velocity of earth's rotation
ω = Angular velocity of Earth's rotation

As can be seen from the above equation, the pendulum day, which is defined as the time taken by a Foucalt Pendulum to complete one rotation, depends on the latitude. It is generally understood that once the long gravity wave energy from a tsunami (or a storm surge) gets trapped on the shelf around an island system, it will take at least one pendulum day (in reality it takes several pendulum days) for the energy to be gradually dissipated.

The pendulum day is estimated below for the southern extreme of the Nicobar Islands and northern extreme of the Andaman Islands.

Southern extreme = 6° N latitude
Length of pendulum day = 231 hours
Northern extreme = 14° N latitude
Length of pendulum day = 100 hours

The Andaman and Nicobar islands stretch from 6 degrees to 14 degrees North and pendulum days varies from 231 to 100 hours. Car Nicobar lies at 9 degree latitude and thus, one can speculate that the water levels stayed high in the Car Nicobar island due to trapping of the tsunami energy on the shelf.

7.0 CONCLUSIONS

The vulnerability of the Car Nicobar coast to tsunami hazard was studied using numerical models. High accuracy elevation data collected using ALTM survey was an invaluable for the coastal inundation modelling carried out on Car Nicobar coast for various past earthquake scenarios. The island seems to be most vulnerable along the Eastern and the southern side compared to the western side. Moreover the persistence of high water level around the island for many days after the tsunami is due to the length of the pendulum day in the Andaman and Nicobar islands which varies from 231 to 100 hours.

ACKNOWLEDGEMENTS

We thank Dr. B R. Subramanian, Adviser and Sci-G, Ministry of Earth Sciences, ICMAM-PD, Government of India for the guidance and support extended to us during the entire course of this work.

REFERENCES

Aida, I. (1977) Tsunamis accompanied by Land slides, Kaiyo-Kagaku. Monthly Journal of Marine Sciences, Japan, 9, 103-110.

Ammon, J. Charles, and J. Chen (2005) Rupture Process of the 2004 Sumatra-Andaman Earthquake. Science, 308, 1133-1139.

Bilham, R. (2005) A Flying Start, Then a Slow Slip. Science, 308, 1126-1127.

Goto, C. and N. Shuto Effects of Large Obstacles on Tsunami Inundations. pp. 521-525. In K. Iida and T. Iwasaki (eds.) Tsunamis: Their Science and Engineering, Terra Scientific, Tokyo/Reidel, 1983.

Houston, J.R. and H.L. Butler (1979) A numerical model for tsunami inundation, Final Report, US Army Corps of Engineers, Hydraulic Laboratory, Waterways Experiment Station, Viksburg, MS, Technical Report. HL-79-2.

Imamura, F. Review of Tsunami Simulation with a Finite-Difference Method. pp. 25-42. In H. Yeh, P. Liu, and C. Synolakis (eds.) Long-Wave Runup Models, World Scientific, Singapore, 1996.

Ioualaen, M., Asavanant, J., Kaewbanjak, N., Grilli, S.T., Kirby, J.T., and Watts, P (2007) Modelling the 26 December 2004 Indian Ocean tsunami: Case study of impact in Thailand, J. Geophys. Res., 112, C07024

Iwan, D.W. Earthquake Spectra, The professional journal of the earthquake engineering research institute, UNESCO and EERI, Special issue III, UNESCO, France, 2006.

Kajiura, K. (1963) The Leading Wave of a Tsunami, Bulletin Earthquake Research Institute, 41(3), 535-571.

Mansinha, L. and D.E. Smylie (1971) The Displacement Fields of Inclined faults, Bulletin on Seismological Society of America, 61, 1400-1433.

Okada, Y. (1985) Surface Deformation due to Shear and Tensile Faults in a Half-Space. Bulletin of Seismological Society of America, 75 (4), 1135-1154.

Satake, K. Tsunamis. pp. 437-451. In W.K. Lee, H. Kanamori, P.C. Jennings, and C. Kisslinger (eds.) International Handbook of Earthquake and Engineering Seismology, 2002.

Shuto, N. and C. Goto (1978) Numerical Simulation of Tsunami Run-up. Coastal Engineering in Japan, 21, 13-20.

Shuto, N., C. Goto, and F. Imamura (1990) Numerical simulation as a means of warning for near field tsunamis. Journal of Coastal Engineering in Japan, 33(2), 173-193.

Shuto, N (1991) Numerical Simulation of Tsunamis- Its Present and Near Future, Natural Hazards, 4, 171-191.

Stein, S. and E. Okal (2005) Speed and size of Sumatra earthquake. Nature, 434, 581-582.

Synolakis, C.E. Tsunami and Seiche. pp. 9.1-9.79. In W.F. Chen and C. Scawthorn (eds.) Earthquake Engineering Handbook, CRC Press, Washington D.C., 2004.

Takeda, H. (1984) Numerical Simulation of Run–up by Variable Transformation. Oceanographical Journal of Japan, 40, 271-278.

Titov, V. and F. Gonzalez (1997) Implementation and testing of the method of splitting tsunami (MOST) model, NOAA Technical Memorandum ERL PMEL-112.

Titov, V.V. and C.E. Synolakis (1997) Extreme Inundation Flows during the Hokkaido-Nansei-Oki Tsunami. Geophysics Research Letter, 24 (11), 1315-1318.

Uda, T. (1988) Numerical simulation and experiment on tsunami run-up. Coastal Engineering In Japan, 31, 87-104.

ASSESSMENT OF POTENTIAL TSUNAMI GENERATION IN CHINA'S BOHAI SEA FROM DIRECT GEOTECTONIC AND COLLATERAL SOURCE MECHANISMS

George Pararas Carayannis

Tsunami Society

Honolulu, Hawaii 96815, USA.

Email: drgeorgepc@yahoo.com

ABSTRACT

The Bohai Sea borders northeastern China's most populous and highest economic value coastal areas where several megacities are located. Critical infrastructure facilities exist or are under construction, including a nuclear power plant and super port facilities. Large reserves of oil have been discovered and a number of offshore oil platforms have been built. The extent of development along coastal areas requires a better assessment of potential tsunami risks. Although tsunamis do not pose as much of a threat as earthquakes in this region, locally destructive tsunamis have been generated in the past and future events could have significant impacts on coastal populations and China's economy, particularly because most of the development has taken place in low-lying regions, including river deltas. The present study examines the geotectonics of the Bohai basin region, the impact of past historical events, and the potential for local tsunami generation from a variety of direct and collateral source mechanisms triggered by intra plate earthquakes. More specifically, the present study examines: a)major active faults bounding the Bohai Basin; b) the resulting crustal deformation patterns of tectonic structures that have resulted in catastrophic earthquakes in recent years; c) the basin-wide extension - with local inversion - extending into the Bohai Sea that generated tsunamigenic earthquakes in 1888 and 1969; and d) deformational future seismic events with the potential to generate local tsunamis directly or by collateral mechanisms of folding, en-echelon bookshelf failures, or from destabilization/dissociation of structural accumulations of gas hydrate deposits within the basin's thick sedimentary stratigraphic layers.

1. INTRODUCTION

The Bohai Sea (also referred to as the Bohai Gulf or Bay, or just the Bo Hai) is a semienclosed coastal, shallow sea on the northeastern coast of China. The gulf is formed by the Liaodong Peninsula to the northeast and the Shandong Peninsula to the south (Fig. 1). It has a mean depth of about 20 m and a maximum depth of about 70 m near the northern coast of the Bohai Strait where it connects with the Yellow Sea (Fig. 2). Bo Hai consists of three bays: Laizhou Bay to the south, Liaodong Bay to the north, and Bohai Bay to the west. Major rivers, the Huang He, the Liao He, and the Hai He empty into Bo Hai. The Bohai Sea borders northeastern China's most populous and highest economic value coastal areas where several megacities are located in developed regions of Shandong, Hebei, Liaoning and Tianjin Province. Dalian, on the the eastern shore of Liaodong Peninsula of Liaoning Province, is an example of such a developing coastal megacity.

Figure 1. Bohai Sea, NE China.

Critical infastructure facilities exist or are under construction throughout the region. Currently, China has nine nuclear generators in commercial operation along its eastern coasts. The first nuclear power plant in the northeast - the Hongyanhe Nuclear Power Plant - is being constructed at the Donggang Town of Wafangdian City, in Liaoning. Furthermore, large reserves

of oil have been discovered and a number of offshore oil platforms have been built or are under construction. The extent of development along the coastal areas of the Bohai Sea requires a better assessment of potential tsunami risks. Although tsunamis do not pose as much of a threat as earthquakes in this region, locally destructive tsunamis could be generated in the future that could have significant impacts on the coastal populations and the economy of China, particularly because most of the development has taken place in low-lying regions, including river deltas. The present study examines the geotectonics of the Bohai Basin region, the impact of past historical events and evaluates the potential for local tsunami generation from a variety of direct and collateral source mechanisms triggered by earthquake, landslides or other collateral occurrences.

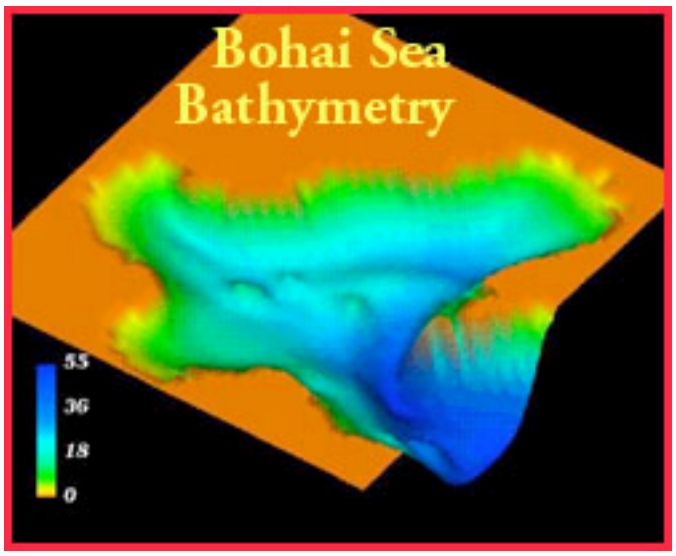

Fig. 2. Bathymetry of the Bohai Sea

2. SEISMOTECTONIC SETTING OF THE BOHAI BASIN AND SEA.

The collision of India with the Asian mainland during the earliest Eocene (~50 Ma) has resulted in the growth of the world's largest orogenic belt - the Himalayas and the associated Tibetan plateau. The seismicity of the entire region is the result of extension caused in part by crustal extrusion of Southeastern Asia (Tapponnier and Molnar, 1977; Peltzer and Tapponnier, 1988; Pararas-Carayannis, 2008d). China's seimotectonic evolution is characterized by the merger of several microcontinents throughout the entire Phanerozoic (Zhang et al., 1984; Hendrix and Davis, 2001; Yin and Nie, 1996). The collision and associated convergence and extension have

created 64 major tectonic zones in China, which can be subdivided into a smaller number of tectonic "regions" (Davies et al. 2001; Zhang et al.,1984).

The seismotectonic setting of eastern China is complex. Most of the large earthquakes in the region are associated with a mechanism of eastward extension that results in shallow crustal mass transfer. The extension process was initiated by early Tethyan Torsion and subsequent Sinian Torsion which continued during the Cenozoic (Fig. 3).

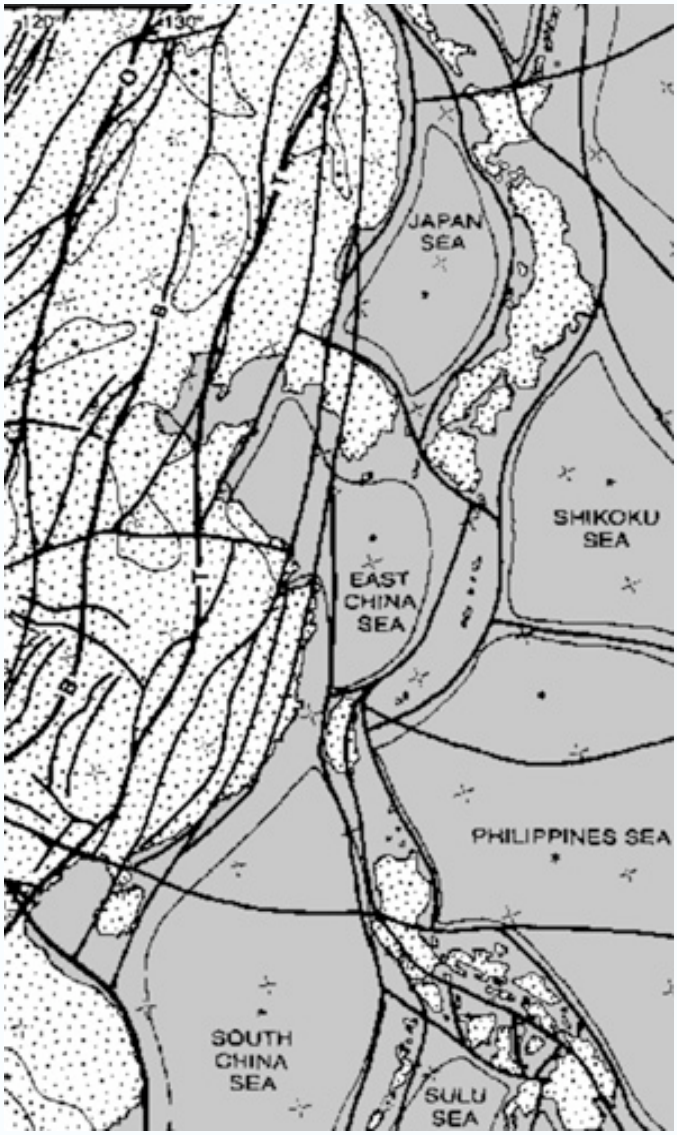

Fig. 3. Tethyan Structure of Eastern China and Adjacent Seas

The Bohai Basin was formed during the Late Quaternary to the east of the Cenozoic rift basin of North China and underwent compound and complex tectonic events during its formation and development (Ye, et al., 1985; Hellinger et al, 1985). The Basin is an apparent collage of island arcs and possible microcontinental blocks on the Mongolian accretionary fold belt and has a complex seismotectonic setting (Davis et al., 2001). It covers an area of about 200,000 km2. Two different deformational mechanisms have been proposed for its Cenozoic formation (Castellanos & Mann, 2005).

The first mechanism postulates a two-stage extension consisting of Paleogene rifting in a WNW-ESE direction followed by Neogene thermal subsidence. The two-stage rifting mechanism is attributed to the combined rollback of the subducted Pacific plate beneath the Asian continent, lithospheric extension of the overriding continental plate, and to thermally-driven, regional subsidence (Ye et al., 1985). The second postulated mechanism pertains to a more localized Cenozoic pull-apart basin - formed at a right-step in a right-lateral shear system parallel to the Asian continental margin (Allen et al., 1997). Either of the postulated evolutionary mechanisms of pull-apart rifting or subduction/rollback could account for the extensive deformation that has taken place in the Bohai Basin and has created the recent predominent strike-slip faulting and the right-stepping pull-apart control on a younger sag section. Either mechanism can account for the significant and evolving structural changes and the formation of dense seismic zones in the Bohai Basin, that can generate tsunamis.

Most of the numerous strike-slip and normal faults on land in the Liaoning, Beijing, Tianjin, Hebei and Shandong Provinces are active structures responsible for a number of major destructive earthquakes in the past. The earthquakes have occurred along numerous active faults that bound the Basin. The Bohai Sea is part of this inner-land sea basin. Similarly, the geotectonics of the Bohai Sea are complex. Regional compressive stresses have formed a series of active tectonic zones and a group of conjugated shear fracturing systems on land which extend into the sea.

Since the Oligocene period, there has been active subsidence in the middle part of the Bohai Sea, forming an extensive depression known as "Bozhong" (Yu et al., 1995). This is the area that is rich in oil. The extensive subsidence has been caused by the superimposition of local tensional stresses produced by the left-lateral strike-slip on the Beijing-Penglai seismogenic zone, the right

lateral strike-slip on the Yingkou-Weifang fault zone and the activity of the pull-apart structural system in the eastern basin, as well as by the uplift of the deep mantle (Xu et al, 2004). The major part of this depression in the northwest quadrant is bounded by the north-west trending Beijing-Penglai fault zone and the north-north-east trending Tan-Lu fault zone (Xu et al, 2004) (Fig. 4, Fig.5).

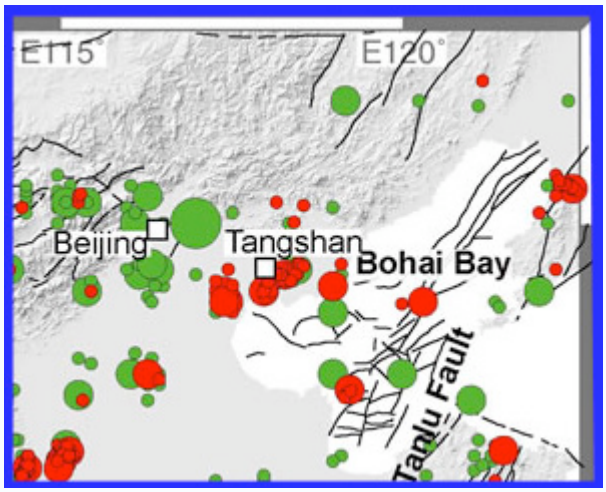

Fig. 4. Bohai Sea Faults - Recent (red circles) and Historical (green circles) Earthquakes (Modified Missouri University Graphic)

3. SEISMICITY OF THE BOHAI BASIN AND SEA

The long-term crustal deformation patterns in the Bohai Basin and Sea - as determined from GPS measurements (Chen et al., 2007) - exhibit a relatively complete left-lateral strike-slip movement along the active fault zone, although there is also some evidence of reverse type of faulting movement that could be significant for tsunami generation. Most of the recent small and large earthquakes in the Bohai Basin had ruptures with prominent NE orientation, although, further north, there is also a seismic dense zone that has a NW direction (Fig. 5). However, studies of crustal deformation by stages (Chen et al., 2007) also indicate that a series of NE-trending large-scale, anomalous gradient zones have appeared along the Zhangjiakou-Bohai Sea fault zone. The seismicity of the basin is stronger south of the 39th parallel - and this is the area where most of the larger earthquakes have occurred in the past. Almost all of the dense seismic zones that can produce strong earthquakes are concentrated in this southern part of the Bohai Sea (Wang, 2007).

As the historic record indicates such shallow seismic activity near densely populated areas as Haicheng or Tangshan can be extremely damaging. Also, such earthquakes can generate local tsunamis. According to historical records there have been 6 great earthquakes of Ms 8 and 16 major earthquakes of Ms 7 in the area, in the past 2000 years (Gu, 1983; Ma, 1988, Pararas-Carayannis. 2007). Generally, these large earthquakes have occurred along the major active faults that bound the Bohai Basin. Numerous strike-slip and normal faults on land in the Liaoning and Hebei Provinces are the predominant active structures where very destructive earthquakes occurred more recently.

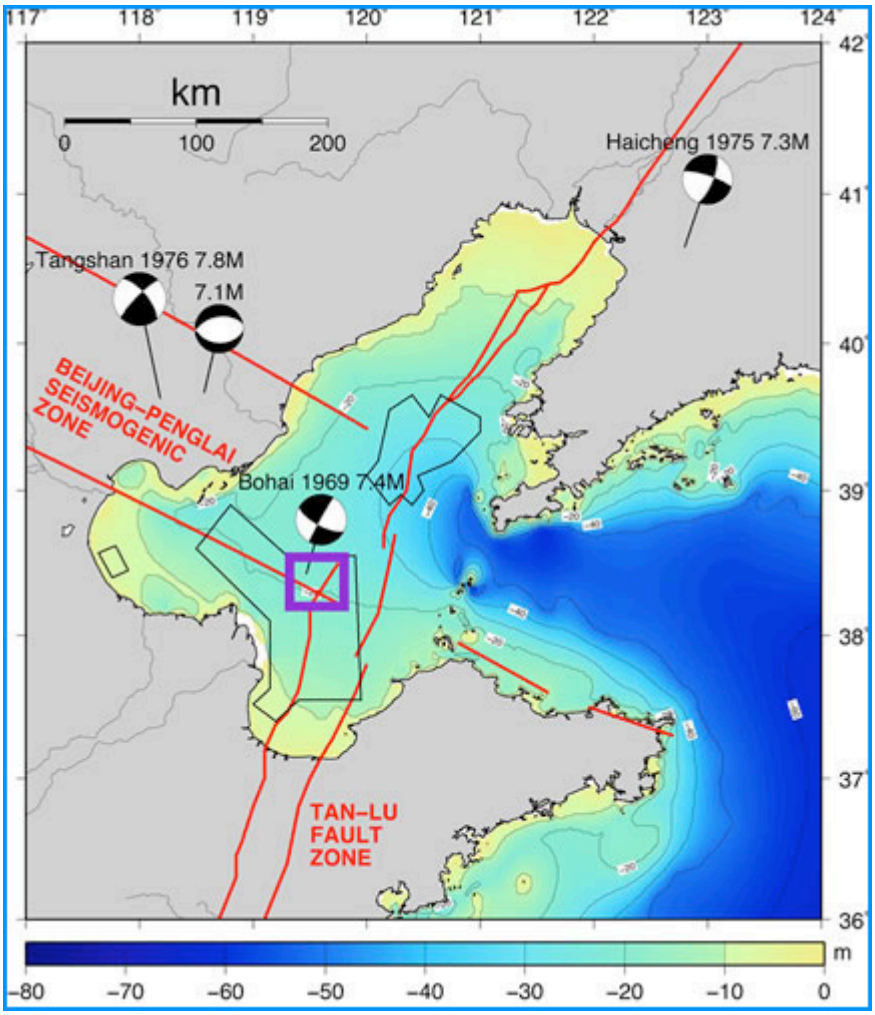

Fig. 5. Major seismotectonic and seismogenic fault zones in the Bohai Basin and Sea. Earthquake epicenters and focal mechanisms of recent earthquakes. Bathymetry based on GEBCO digital data base (modified graphic, after Yang & Xu, 2004 and Xu et al,. 2004).

As previously indicated, the fault-plane solutions of earthquakes in the area usually show right-lateral strike-slips with prominent NE orientation, although some had NW orientation with a normal dip-slip component. Reccurrence frequencies also vary. Although earthquake recurrence intervals along any individual fault in the Bohai Basin is relatively long (usually in the range of several thousand years), the composite recurrence interval for the whole region is in the order of a few decades (Ma et al., 1989). Five earthquakes with Ms > 7 have occurred in this region between 1966 and 1976. These earthquakes resulted in hundreds of thousands of casualties and in significant economic damage. Worse of all was the July 28, 1976 Tangshan earthquake in the Hebei Province.

The complex intraplate earthquakes in North China are presently being studied by US institutions funded by the National Science Foundation's PIRE (Partnerships for International Research and Education) in close collaboration with numerous Chinese institutions. The studies include integration of seismic imaging of earth structure, geodetic measurement of crustal deformation, paleoseismic reconstruction of earthquake histories, and geodynamic computer simulations. Such studies are expected to provide a better understanding as to the causes of large earthquakes in Northeast China, such as the 1976 Tangshan event that leveled the city and caused the greatest death toll in recent history.

3A. Historical Bohai Basin Earthquakes and Tsunamis.

A review of recent and historic earthquakes is relevant in assessing the potential for tsunami generation in the Bohai Sea. As stated, six earthquakes of Ms 8 and sixteen earthquakes of Ms 7 occurred in the past 2,000 years - some of which were tsunamigenic (Wang J., 2007; Pararas-Carayannis, 2007). The records are not clear, particularly for the older events. According to these records, tsunamigenic earthquakes occurred in 1548 and in 1888 (Fig. 6). Other possible tsunamis may have been generated by earthquakes in 173 and in 1597, although the latter is doubted as being a strong event (Wang, 2007) - thus the reported tsunami may have been generated by a collateral mechanism. Many more tsunami must have occurred but have remained undocumented.

The September 22, 1548 earthquake had an estimated magnitude M 7.0 and epicenter at about 121.0 E. Its latitude is not known but it is believed that it occurred at sea. The earthquake of

October 6, 1597 had an estimated magnitude of M 7.0 and epicenter at about 38.5 N. 120.0 E. The most significant tsunamigenic earthquakes occurred in 1888 and in 1969. The tsunamigenic earthquake of June 13, 1888 had an estimated magnitude M 7.5 and epicenter at about 38.5 N, 119.0 E. (Wu and Zang, 1989). The most recent tsunamigenic earthquakes in the Bohai Sea occurred on July 18, 1969.

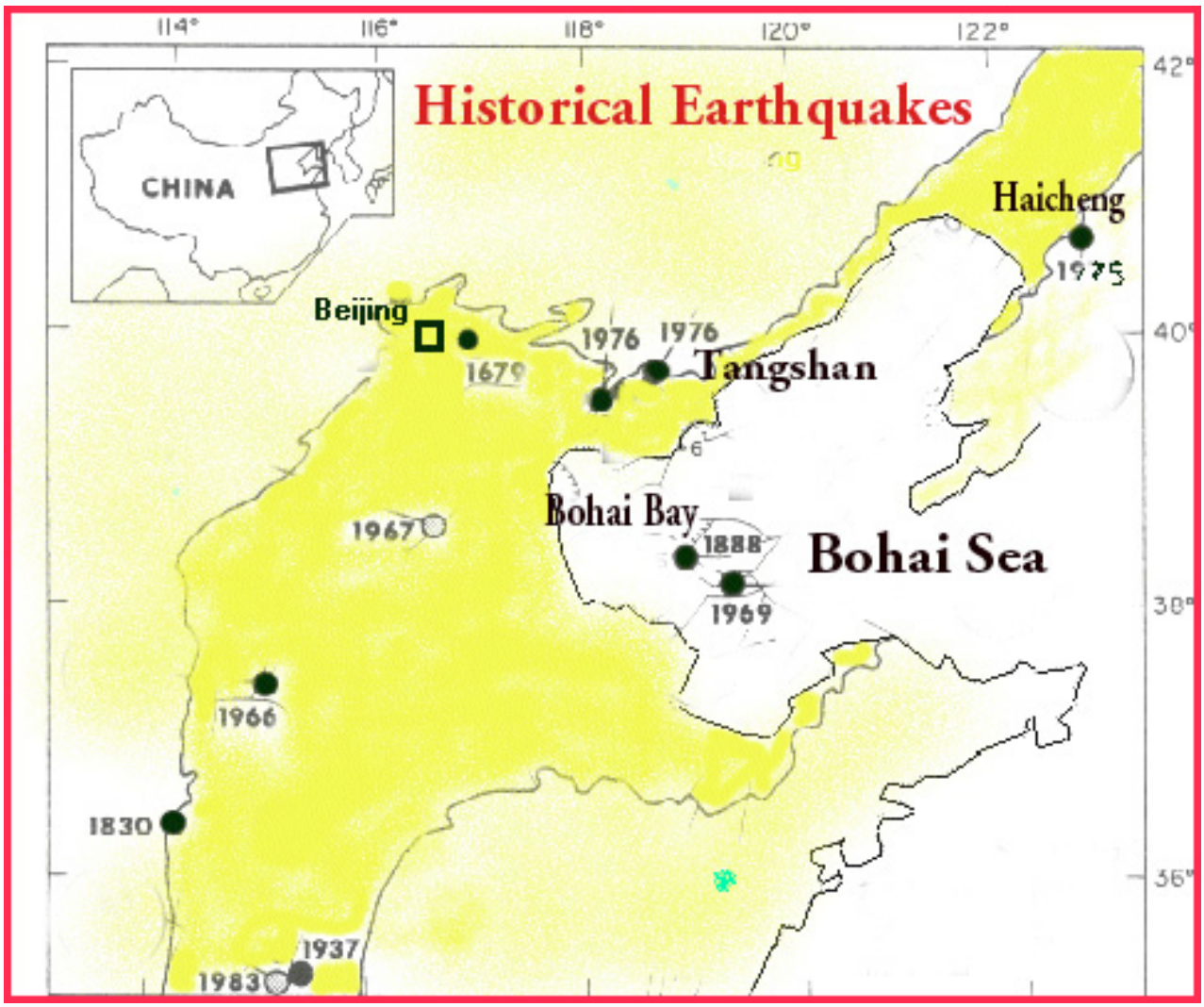

Fig. 6. Historical earthquakes in the Bohai Sea and in Northeast China.

On February 4, 1975, and on July 28, 1976, there were major earthquakes in the Bohai Basin. The 1975 Haicheng and the 1976 Tangshan earthquakes were extremely destructive. The two 1976 Tangshan earthquakes in Hebei Province resulted in the greatest death toll in recent history. Their

impact on land around Tangshan has been described adequately in the literature but there has been no information on whether a tsunami was generated. However, the seismic intensities, the aftershock distribution and the observed crustal movements of the Tangshan quake,s indicate that the coastal region of Bohai Bay was impacted, and therefore a local tsunami must have been generated but not reported. Apparently, the degree of earthquake destruction on land shrouded the damaging effects and impact from a tsunami.

The Earthquake and Tsunami of July 18, 1969

The shallow tsunamigenic earthquake of July 18, 1969 in the Bohai Sea had an estimated Richter magnitude of M 7.4 and epicenter at 38.2 N, 119.4 E. Its strike was f=195°, its dip angle was d=85 degrees and its slip angle l=65 degrees. The seismic moment was M o=0.9x10^{19}, its rupture length was L=59.9km and the rupture propagation speed was estimated at Vr=3.5km/s; The angle from the strike to the propagation direction were n wL R =160 (Wu & Zang, 1989, 1992) (Fig. 7). The quake generated a small tsunami with a height ranging from 1~2 m. above normal tide level. The tsunami was responsible for losses in the coastal region near Tangshan in the Hebei Province, but no details are available. Also, no details are available as to the height of the tide at the time of the earthquake and whether the 1 to 2 meter reported tsunami occurred at high or low tide (Pararas-Carayannis, 2008a).

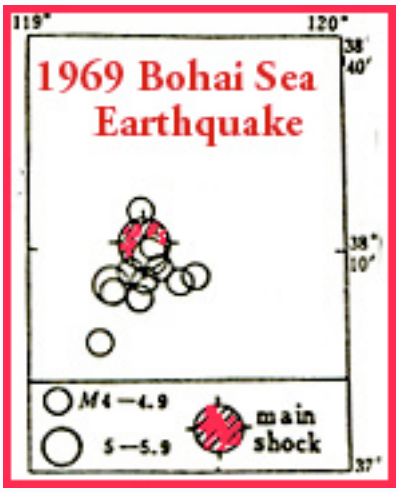

Fig. 7. Epicenter and major aftershoks of the Earthquake of July 18, 1969 in the Bohai Sea.

The Haicheng Earthquake of February 4, 1975 in the Liaoning Province

The Haicheng earthquake of February 4, 1975 had magnitude M=7.3 and epicenter at 40.6 N, 122.8 E (Chen Y. et al. 1976, Zhu and Wu, 1982; Wang et al., 2006; Pararas-Carayannis, 2008b). The region where it occurred is characterized by an active structural system which extends, not only in the Haicheng-Yingkou region but, also along the entire South Liaoning Province. The seismic activity on this structural system is mostly concentrated along a belt bounded by the Liao River depression and the Liaodong Peninsula uplift (Earthquake Administration of Liaoning Province). The activity of the tectonic structure is oriented in NW direction and has formed a series of active faults as well as new folds. Active faults in the region with a NE orientation include the Niuju-Youyangou, the Jinshanling, the Shuangtaizihe-Zhaojiabaozi fault and the Jinzhou. Other faults in the area include the Dayanghe, the Ximuhe, the Zhuanghe and the Yalujiang (Earthquake Administration of Liaoning Province).

The epicenter of the Haicheng earthquake was located in the region where faults with the NE and NW directions converge, but do not intersect. Stress along the Dayanghe fault - which has a NW orientation - was apparently released by this earthquake (Figure 8). Although far from the sea

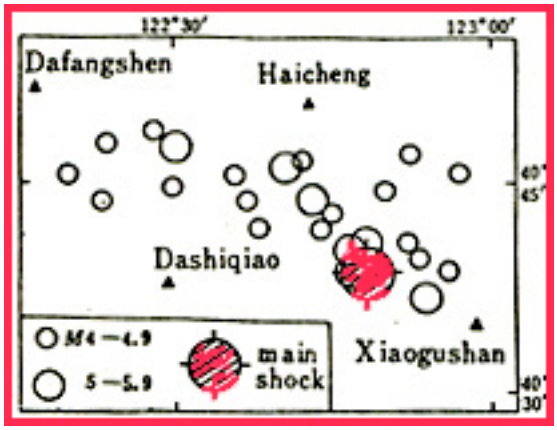

Fig. 8. Epicenter, major aftershocks of the Earthquake of February 4, 1975 near Haicheng, Liaoning Province.

and thus did not generate a tsunami, the same seismic zone extends into the Bohai Sea, so there is the potential for future tsunami generation if an earthquake occurs closer to the coast of Liaodong Bay or on the Yellow Sea coast of Liaoning Province. As indicated, the coseismal intensity lines, the aftershock distribution as shown in Figure 8 and subsequent surveys of crustal displacement

patterns indicate that the main rupture plane of this event involved a left-lateral strike slip with a NWW orientation (strike = 288°, dip = 78° N, rake = 342°). Subsequent studies of the seismic waves estimated the seismic moment to be 3 x 10^{26} dyne-cm and the source duration 7 sec. Since the fault length of this earthquake was about 22 km, the observed P waves supported a rupture velocity estimate of about 3.2 km/sec. The average dislocation was computed to be 2.8 m and the stress drop about 53 bars (Cipar, 1979).

The July 28, 1976 Tangshan Earthquakes in Hebei Province

Two earthquakes on July 28, 1976 in the Hebei Province of northeastern China struck and totally destroyed the city of Tangshan (Pararas-Carayannis, 2008c). The main quake had magnitude of M 7.8 (later revised to Mw 7.6) and epicenter at 39.4 N. 118.0 E. (Fig. 9).

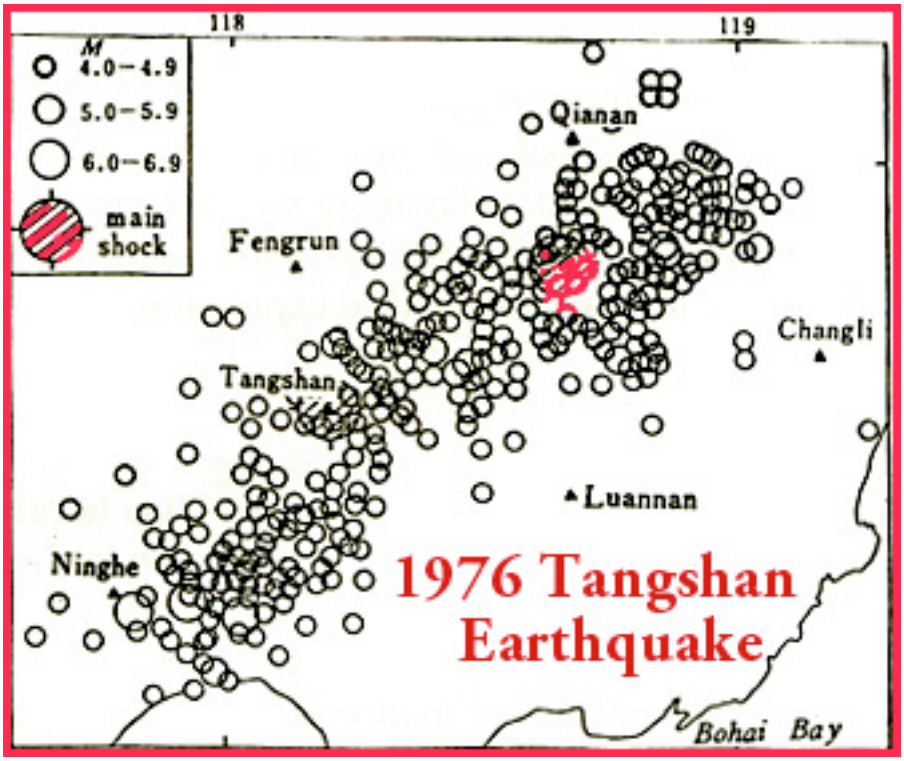

Fig. 9. Epicenter, major aftershocks of the Earthquake of July 28, 1976 near Tangshan, Hebei Province

Many sources listed it as 8.2 on the Richter scale, but Chinese government's official sources revised it to 7.8. It was followed by a major 7.1 magnitude destructive aftershock, some 15 hours

later, that had a magnitude of M 7.1 and epicenter at 39.7 N., 118.5 E. (Mei, 1982; Pararas-Carayannis, 2008c). Both events were shallow (15 km) and occurred near the coast of Bohai Bay. Many strong aftershocks followed the main earthquake, two of which had magnitudes of 6.0 or more. In the following days, there were many more aftershocks ranging in magnitude from 5 to 5.5. Several months later, on Nov 15, 1976, a magnitude 6.0 earthquake struck again the same region (Pararas-Carayannis, 2008c).

The intensities of the 1976 earthquake's ground motions were extensively surveyed and reported (Figure 10). In the epicentral area the intensity was estimated at XI (State Seismological Bureau). The region with intensity X was reported as being elliptical in shape and covering a total area of about 370 km^2.

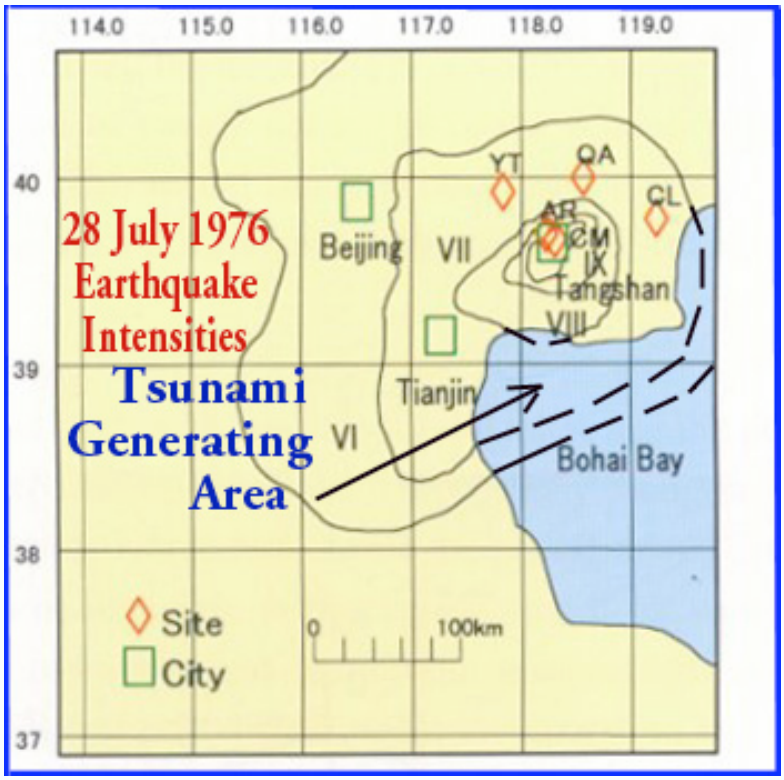

Fig. 10. Intensities of Ground Motions of the Tangshan Earthquake (after Wang Fang 1976, State Seismological Bureau of China). Postulated Tsunami Generating Area.

The region of intensity of IX was reported as being rhombic in shape, also trending in a northeast direction and covering an area of about 1,800 km^2. The region of intensity VIII extended

in a southeastward direction and covered an area of about 7,300 km^2. The region of intensity VII was reported to cover an area of about 33,000 km^2. The zone of maximum destruction was estimated to be about 47 square kilometers. It included the city of Tangshan and the southern suburb along the Beijing-Shanhaiguan railway. Over a four-by-five mile area the devastation of the city was nearly total. About ninety-three percent of residential buildings and seventy-eight percent of commercial and industrial buildings in Tangshan were destroyed.

The actual death toll from this earthquake may never been known with certainty. According to official government accounts the earthquake killed 242,769 people and severely injured another 169,851. However, based on the density of the population and the extent of destruction, these figures have been disputed. At the time Tangshan had 1.6 million inhabitants. Since the earthquake destroyed ninety three percent of all residential buildings, the death toll was estimated to be three times greater than what was reported - ranging from 655,000 to 779,000 people. The extremely high death toll makes the 1976 Tangshan event the second worse earthquake disaster in recorded history. The most destructive earthquake ever, occurred four centuries earlier in 1556 in Shaanxi, China. It is estimated that the 1556 earthquake killed 830,000 people. Another earthquake in the Gansu region in 1920 had killed about 200,000. Intensities of Ground Motions of the Tangshan Earthquake (after Wang Fang 1976, State Seismological Bureau of China)

The 1976 earthquake ruptured a five-mile (8 km) section of a 25-mile strike-slip fault with a north-northeast orientation that passes through the city Tangshan. The fault is part of an extensive strike-slip fault system, known as Tancheng-Ljiang, or Tan-Lu. This system extends in a north-northeast direction for more than 3,200 miles from the north bank of the Yangtze River in eastern China to the west across the Russian border. Specifically, the earthquake occurred at the junction of the YanShan fold-fault zone and the Cangdong fault zone. The YanShan fold-fault zone runs in an east-west direction and lies north of the Tangshan region. To the south, there are several sub parallel northeast-trending fault zones known as the Shanxi fault depression structural belt, the Taihang piedmont fault zone, the Cangdong fault zone, and the Tangcheng-Lijiang fault zone. According to the scientific literature, each of these zones has produced several earthquakes. Several episodes of uplift and other anomalous variations along different segments of the fault zones that comprise the Yan Shan Seismic Belt have been reported. There were substantial ground movements along the segment of the fault that ruptured. Along the west side the ground moved

laterally for about five feet in a north/northeast direction, sub parallel to the major axis of the meizoseismic zone. However, in some areas, horizontal ground displacements of up to 7 meters were subsequently measured. On the eastern side of the rupture, the ground block tipped upward near the south end and downward at the northern end. The quake's intensities, the aftershock distribution, the crustal displacements and the downward tilting at the southern end must have included a good portion of Bohai Bay, thus a local tsunami must have been generated.

4. POTENTIAL FOR FUTURE TSUNAMI GENERATION IN THE BOHAI SEA

Tsunamigenic earthquakes have been generated in the past along active tectonic structures that crisscross the Bohai Sea. In spite of predominantly lateral strike-slip components that characterize most earthquakes in this region, destructive local tsunamis may be generated by a combination of direct and collateral mechanisms that could involve upward and downward crustal block movements, folding of thick sedimentary layers, landslides, destabilization of gas hydrates deposits and mass sediment flows.

4A. Potential for Tsunami Generation from Geotectonic Mechanisms

Analysis of relations between structures and stratigraphic units along cross sections in the Bohai Basin using broadband instrumentation (Zhao & Zheng, 2005), infers the occurrence of past, multiple, deformational seismic events and confirms the basin-wide extension with local inversion which extends extensively into the Bohai Sea. Furthermore, from studies of recent earthquakes in China (Pararas-Carayannis, 2007, 2008) and additional review of the literature on the evolution of Bohai Basin, it has become apparent that the principal regional compressive stresses from crustal extension in this region have a NEE-SWW orientation in the central part of the Bohai, in line with the Beijing-Penglai seismogenic zone but a NE orientation further offshore, in line with the Tan-Lu Fault (Fig. 4, Fig. 5). Counter clockwise drag is responsible for the apparent dextral torsion in this eastern region. Stresses from the crustal extension have formed a series of active tectonic zones and conjugated shear fracturing systems on land, as well as in the Sea. According to recent literature (Chen et al., 2007), the Zhangjiakou-Bohai Sea seismotectonic zone controls the present-day strong earthquake activities in the region. Other major active tectonic zones include the northern section of the northeast trending Yingkou-Weifang and the

Miaoxibei-Huanghekou-Linyi fault zones, and the northwest striking Beijing-Penglai fault zone, which intersect at the center of the Bohai Sea basin - as partly illustrated in Figures 4 and 5.

These tectonic zones subdivide the Bohai Sea area into four secondary neotectonic areas, which are subject to a dominant horizontal, or nearly horizontal, compressive stress field in the direction NE60–90 degrees, while the tensional stress is in a NW30 degree direction (Chen et al., 2007). The long-term crustal deformation patterns in this region exhibit a relatively complete left-lateral strike-slip movement, but there is also some evidence of reverse type of faulting movement (Wang, T., 1988). Although poorly mapped, reverse faults, normal faults and strike-slip faults reach far into the Bohai Sea. Sea floor movements from earthquakes occurring along reverse and normal faults have the potential to generate tsunamis.

Fortunately, most of the earthquakes in this eastern region of the basin have relatively short ruptures, thus sea foor displacements would tend to be limited and tsunamis would be localized. For example, the 1976 Tangshan earthquake ruptured only a five miles (8 kms) along a 25-mile section of a strike-slip fault. Obviously, the multi-directional orientations of the highly fractured faults in this region create asperities which limit rupture length. However, the ground motions of the Tangshan earthquake, the distribution of intensities extending into the Bohai Bay and the observed upward movement of the ground block near the south end of the rupture, as well as the downward movemeny of the crustal block at the northern end, infer that anomalous disturbances of the sea floor can occur along coastal areas of Bohai Bay near Tangshan, as well as in areas further offshore. There were apparent gravity anomalies before and after the earthquake (Chen Y. et al. 1976). Similar ground movement anomalies have been associated also with other historical tsunamigenic earthquakes along faults bordering coastal areas of the Yellow and South China Seas.

Similarly, the 1974 Haicheng earthquake had a short rupture with a NW orientation along the Dayanghe fault. Its epicenter was located in the region where faults with the NE and NW directions converge, but do not intersect. Although far from the sea and could not have generated a tsunami, the quake was along a fault in the same seismic zone which extends into the Bohai Sea.

Thus, there is potential for future tsunami generation if an earthquake occurs closer to the coast of Liaodong Bay.

In brief, local destructive tsunamis can be generated by earthquakes along shear fractures in the Bohai Sea, but particularly along the NE-trending and more active tectonic zones south of the 39th parallel.

4B. Potential for Tsunami Generation from Collateral Mechanisms - Sedimentary folding and En-echelon structural failures.

As indicated, most of the earthquakes in the Bohai Sea involve primarily crustal movements with lateral, strike-slips which usually do not generate large tsunamis. However, the Bohai is loaded with sediments carried by major rivers such as Huang He, Luan He, Liao and Alu Jiang (Fig. 11, 12). The excessive sedimentation may be a significant factor for tsunami generation.

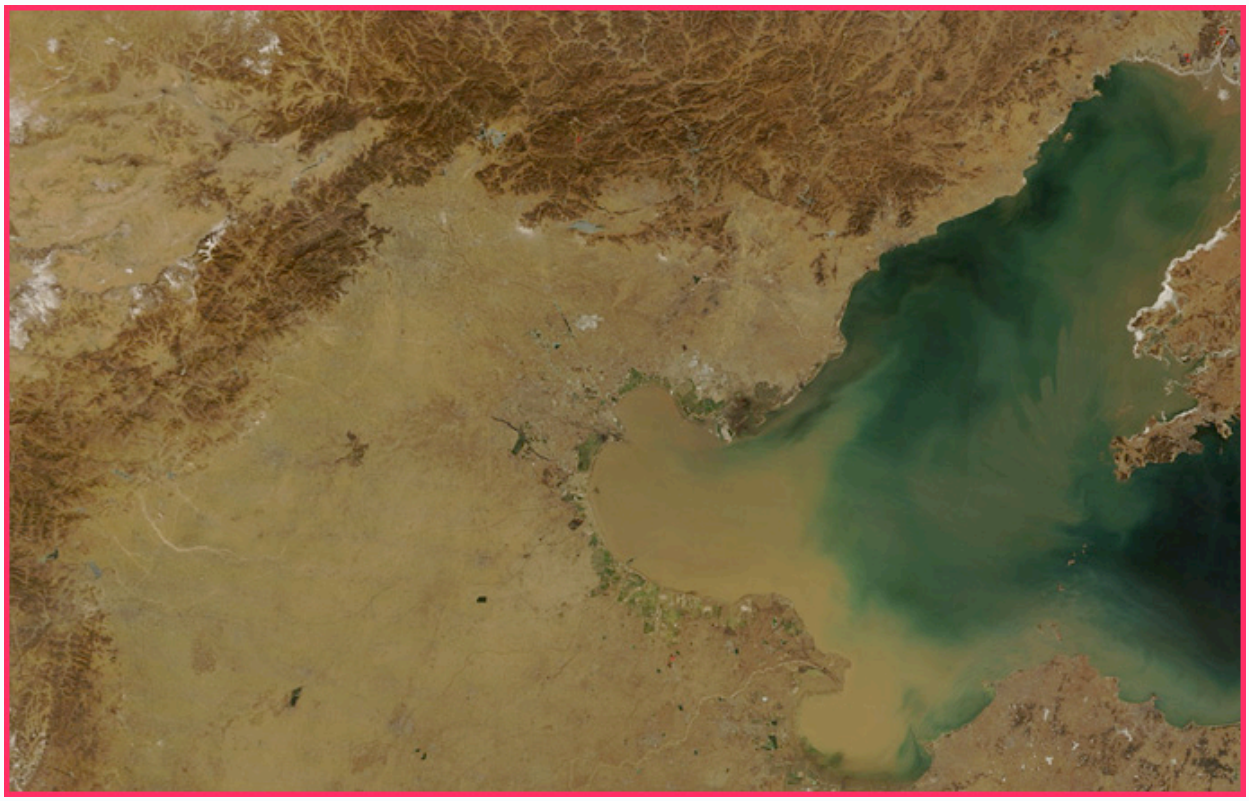

Fig. 11. Satellite photo showing the heavy load of sediments from major rivers flowing into the Bohai Sea.

Deformational seismic events - which apparently occur frequently - have the potential to generate local tsunamis directly or by collateral mechanisms of stratigraphic folding and/or by en-echelon bookshelf failures of the thick sedimentary layers, or by the triggering of submarine landslides. To assess such potential tsunami mechanisms, the structural and tectonic evolution of the Bohai Basin must be re-examined and evaluated. Major rivers deposit large loads of sediments in the the Bohai and Yellow Seas and have created unstable slopes on the shelf that could become potential sources of landlside-generated tsunamis.

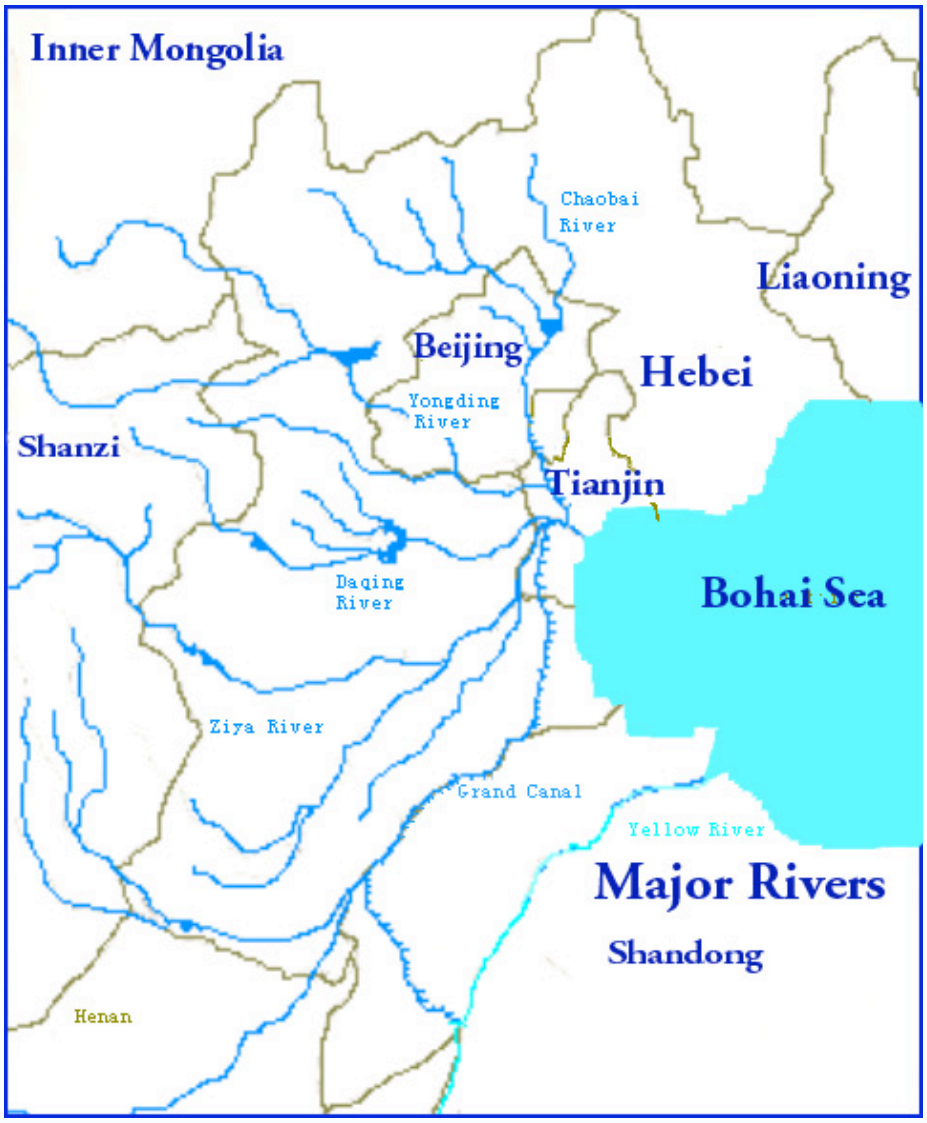

Fig. 12 Major rivers deposit large loads of sediments in the the Bohai and Yellow Seas and have created unstable slopes on the shelf that could become potential sources of landlside-generated tsunamis.

Apparently, geological structure played an important role in the development of palaeochannels in the North China Plain and in the offshore areas. Mountain uplift, subsidence of the plain, and tectonic movement of the basement since the Cenozoic, have interacted with the flashy fluvial regime involving high sediment loads and frequent channel changes (Xu et al, 1996). Over eons of time, the numerous rivers traversing the Bohai Basin have deposited great quantitities of sediments which have filled out full grabens or half grabens - bounded by conjugated shear fracturing systems - which extend into the sea. Thus, the tectonics of the region have influenced changes of the ancient river systems and channels - although now these channels are buried by sediments. Processes of channel development from present tectonic activity continue.

Although the Bohai Sea is not a region near a zone of subduction, the predominent lateral compressive forces of earthquakes along faults that bound the buried grabens, can result in folding and/or in oblique-to-the-rupture bookshelf-types of failures within the thick layers of the loose surficial and the compacted, deeper sediments. The deeper sedimentary layers are probably well consolidated but still prone to folding or en-echelon failure from the tectonic compressive forces, which could generate tsunamis in the manner illustrated by Figure 13. Subjected to similar forces, the surficial sedimentary layers would be more susceptible to slumping and landslides. Slumping or folding could generate local tsunamis. However, the potential for tsunami generation from submarine landslides would tend to be limited and localized, since the Bohai is a relatively shallow sea and the slopes are relatively gentle.

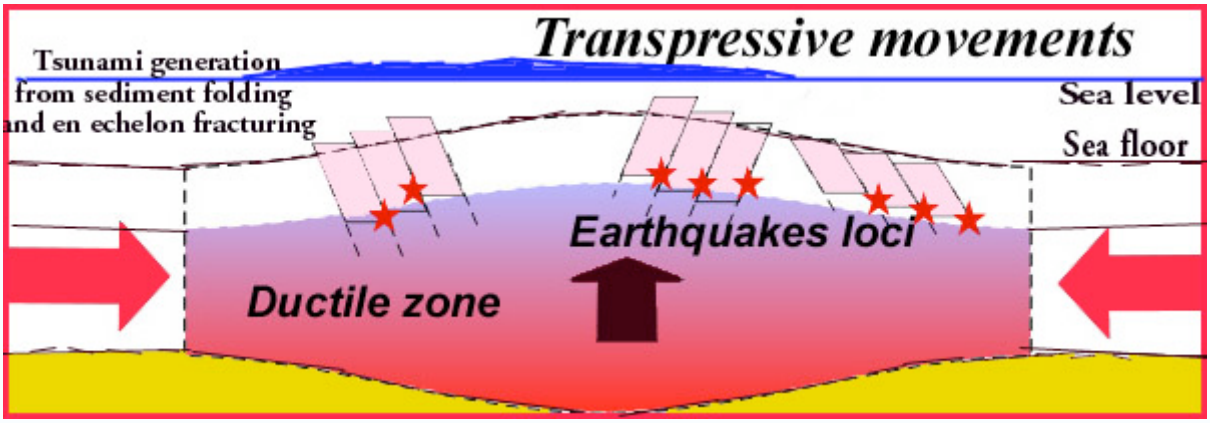

Fig. 13. Tsunami Generation by Compressive Folding of Deeper Sedimentary Layers in the Ductile Zone and En-Echelon and Bookshelf Faulting of Surficial Layers.

In brief, future tectonic movements associated with larger earthquakes in this region - and the compressive forces they generate - could interact with the now submerged fluvial regimes that contain high sediment loads and thus could generate massive sediment movements - even on relatively gentle bathymetric slopes. Such movements could contribute to local tsunami generation. Folding and en-echelon bookshelf type of failures of the deeper consolidated sediment layers could become collateral mechanisms for greater tsunami generation. Such collateral mechanisms can contribute significantly to the generation of destructive local tsunamis anywhere in the Bohai Sea, but particularly south of the 39th parallel, where the denser seismic zones are concentrated, the seismicity is stronger, and greater sedimentation from the Huang He river (Yellow River) has occurred.

4C. En-Echelon Structural Failure Within Consolidated Sedimentary Layers - Mechanism of Tsunami Generation.

As indicated, stress and tectonic displacements caused by an earthquake along a fault - whether strike-slip, normal, or inverse - in a multi-layered sedimentary environment such as that of the Bohai Sea, can induce structural failures that may be oblique to the overall fault orientation and thus result in collateral displacements, en-echelon structural failures, and bookshelf faulting of the seafloor that could enhance tsunami generation. Shear cracks along a fault may be vertical and planar but may result in splits into two or more interacting sections at a stratigraphic interface with different density and stress drop - depending on rigidity contrasts between the adjoining media.

The deeper sediments along such faults in the Bohai Sea may be characterized by different elastic parameters, depending on the degree of hydration, particle size distribution, and compaction densities. Structural inhomogeneities within these deeper better-consolidated layers may result in a series of bookshelf type of structural failures, which will be oblique in orientation to the overall faulting trend. Oblique, en-echelon type of failures could result in multiple ruptures that could also affect the sediments of the upper layers - thus changing the spatial geometry and characteristics of the source area and the mechanism of tsunami generation. Slower rupture rates with different azimuthal orientation can be expected within these layers. Furthermore, net sea floor displacements can be expected to vary and the tsunami's directivity to be different from what may be inferred from fault orientation or focal plane solutions.

For example, the simplified mechanical/geometrical effects left by a model earthquake within a transform fault plane at the sedimentary discontinuity interphase have been extensively investigated by employing the "displacement discontinuity method" (Bonafede & Neri, 2000). Figure 14 illustrates a simple case of such stress-induced displacement discontinuity and the potential changes in the geometry and characteristics of the tsunami source. Additional investigations have dealt with the two-dimensional dynamics of shallow reverse type of faulting upon discontinuity interphases (Madariaga, ?).

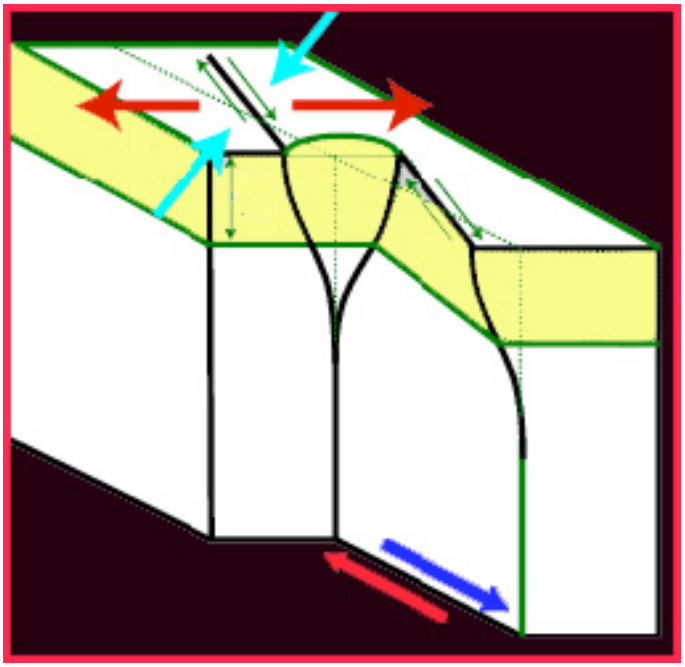

Fig. 14. Stress concentration induced by strike-slip faulting across layer interfaces. (Modified Graphic http://hraun.vedur.is/ja/prenlab2final/img114.gif)

However, in an actual multi-layered sedimentary environment such as that which exists in the Bohai Sea, the geometrical complexities and stress drop values can be expected to vary along planar strike-slip or reverse faults. Faulting in such an environment cannot remain planar. Strike-slip faulting at depth may be accompanied by en-echelon surface breaks in a shallow sedimentary layer - where the stress drop may be lower at the discontinuity interphase, while ductile

deformation at depth may be accommodated by antithetic faulting in the upper brittle layer - enhanced with lower rigidity but higher stress - thus resulting in bookshelf faulting that can augment tsunami generation and alter tsunami directivity (Fig. 14). Such bookshelf failure of sedimentary layers are believed to have resulted in the augmentation and apparent directivity from the north (rather than from the west) when the tsunami of December 26, 2004 struck Aceh, in Sumatra. It is believed that similar bookshelf and en-echelon failures within subducted sediments were associated with the September 2, 1992 earthquake off the coast of Nicaragua and enhanced the tsunami runup (Pararas-Carayannis, 1992).

Indeed, studies of aftershock distribution of earthquakes around the world indicate extensive concentration of their focal depths along sedimentary bedding planes - which would also support that such failure mechanisms contribute to tsunami enhancement and differences in azimuthal tsunami source parameters (Figures 13, 14). Similarly, en-echelon failures with elevated and depressed portions of ramp could alter the sea floor and contribute to tsunami generation (Fig. 15).

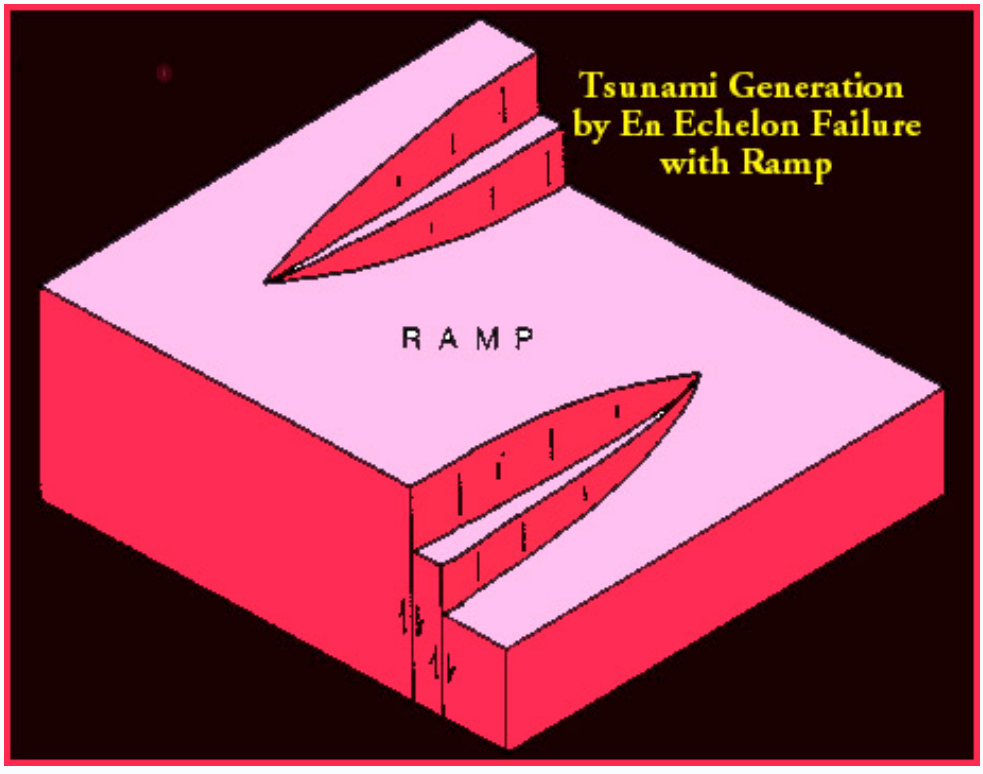

Fig. 15. Tsunami Generation by En Echelon Step Fault Displacement and by Sea Floor Changes with Elevated and Depressed Ramp Structure.

Therefore, we may conclude that such distribution of aftershocks - localized along sedimentary discontinuity layers - not only would indicate the asymmetric interactions between the original fault plane of an earthquake and the shalower sedimentary layers, but would also indicate that significant residual, compressive or tensile stresses can remain over the shallower portion of the fault surface, after the major shock and fault rupture. Thus, strong aftershocks of major or great earthquakes in such sedimentary environments could be significant in tsunami generation and could trigger, at a later time, collateral submarine landslides or other sea floor collapses and structural failures.

In brief, the potential for tsunami generationt in the Bohai Sea is exacerbated by the thick accumulation of sediments (in different states of consolidation) and the multi-layered stratigraphic distribution of sediments with different shear strengths, densities and rigiditites. Folowing an earthquake, en-echelon, bookshelf type of failures with oblique directivity to the general strike orientation could impart greater tsunami energy and alter tsunami directivity. Thus, any mathematical modeling study must consider such complexities of source inputs for such environments of extreme sedimentation.

4D. Potential for tsunami generation from destabilization of Gas Hydrate deposits and mass sediment flows.

As indicated, the Bohai Sea is a region rich in oil and natural gas. Great offshore oil fields, such as the Shengli, the Dagang the Jidong, the Suizhong and the Chengbei, were discovered in recent years and are now being exploited. Numerous oil platforms, scattered in the Bohai, pump huge quantities of natural gas and oil which supply China's increasing energy needs. Apparently, there are also huge structural accumulations of natural gas hydrates (primarily methane hydrate) near known fault systems (Watson et al.,1987). Such gas hydrates must exist in different configurations below the sea floor and include massive thick solid zones, continuous layers, nodules, and widely disseminated interstitial material in the different sedimentary layers. Each of these types of hydrate accumulations may affect differently the seafloor stability. Such natural gas hydrate deposits may be transitionally unstable in shallow (first meters below seafloor) sediments in areas where seafloor temperature or pressure changes over time. Repetitive gas hydrate formation and decomposition are known to cause sediment deformation, slumps, gas blowout

craters, and increase the rate of gas and oil venting to the water column (Milkov, 2002). Since collapse of hydrate-bearing sediments is accompanied by the generation of excess pore pressureand the release of amounts of methane gases, it is likely to cause a breakdown of offshore structures and slope failures. Furthermore, gas hydrate accumulations, if destabilized and dissociated by an earthquake's ground motions and the associated changes in pressure, could cause mass sediment flows - and thus generate local tsunamis (Max, 2002). Dissociation of gas hydrate in surficial sediments, as illustrated by Figures 16 and 17, could reduce substantially the shear strength of distinct layers and result in the formation of a thixotropic mass which could act as a slip surface for subsequent structural failure and downslope mass sediment flows.

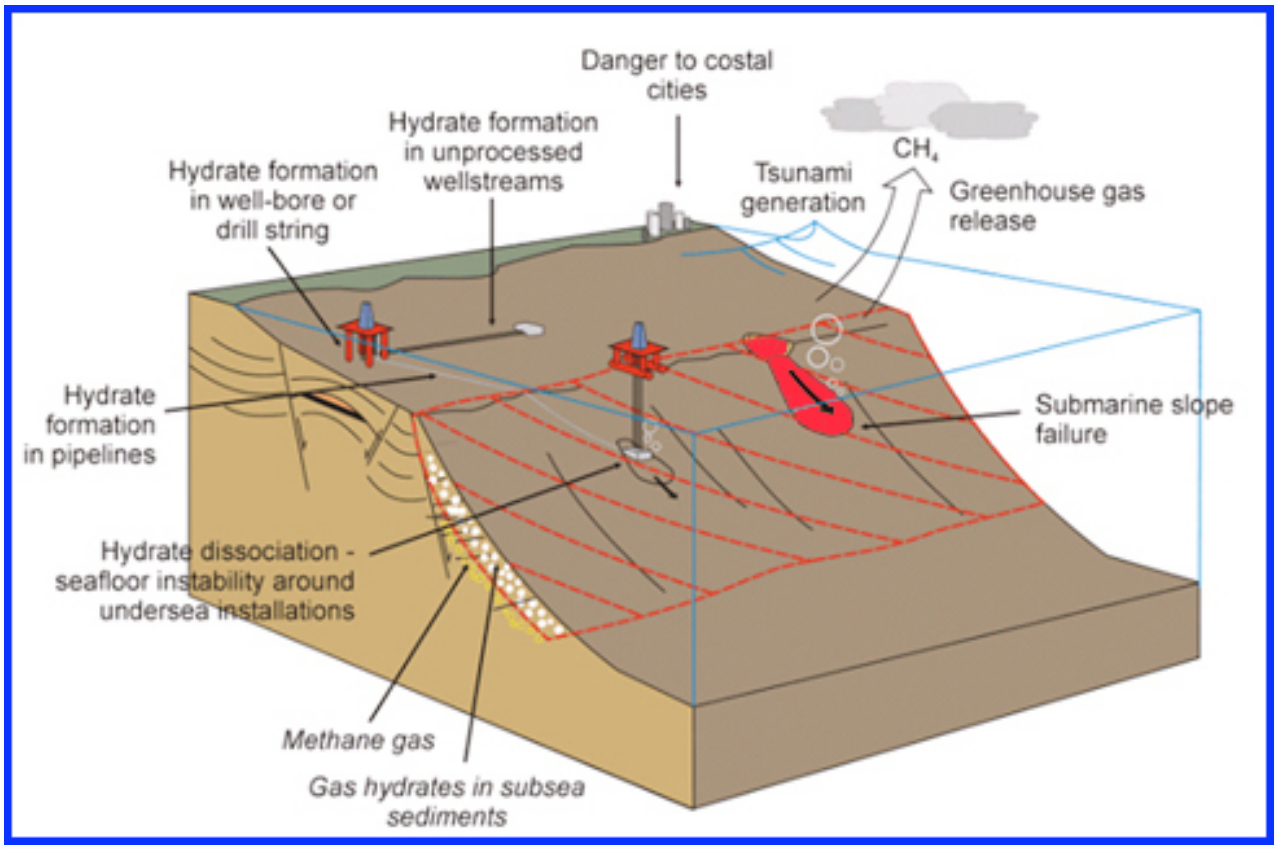

Fig. 16. Tsunami generation by the destabilization and collapse of gas hydrate deposits in sedimenatry environments (modified graphic of Center for Gas Hydrate Research http://geosystems.kaist.ac.kr/ERG-1.html

In brief, hydrate-bearing sediments in the Bohai Sea may destabilize spontaneously by an earthquake's ground motions or slowly on their own without a triggering mechaniss. Often the

mere pumping of oil or natural gas could result in destabilization. Often, gas production methods include depressurization, inhibitor injection, thermal stimulation, and their combinations, or intentional gas extraction from the hydrate itself. The dissociation of the gas hydrate deposits by earthquake ground motions, particularly near offshore oil platforms, could result in large scale slip and sediment mass flows and be a collateral mechanism for tsunami wave generation or enhancemnt. Combined with extensive surface ice during the winter months, local tsunami waves could possibly cause damage to oil rigs operating in the Bohai Sea, as well as to nearby coastal facilities, by the transport and impact of large pieces of floating ice. Given this scenario extensive damage could occur, even with tsunami waves of moderate height amplitude.

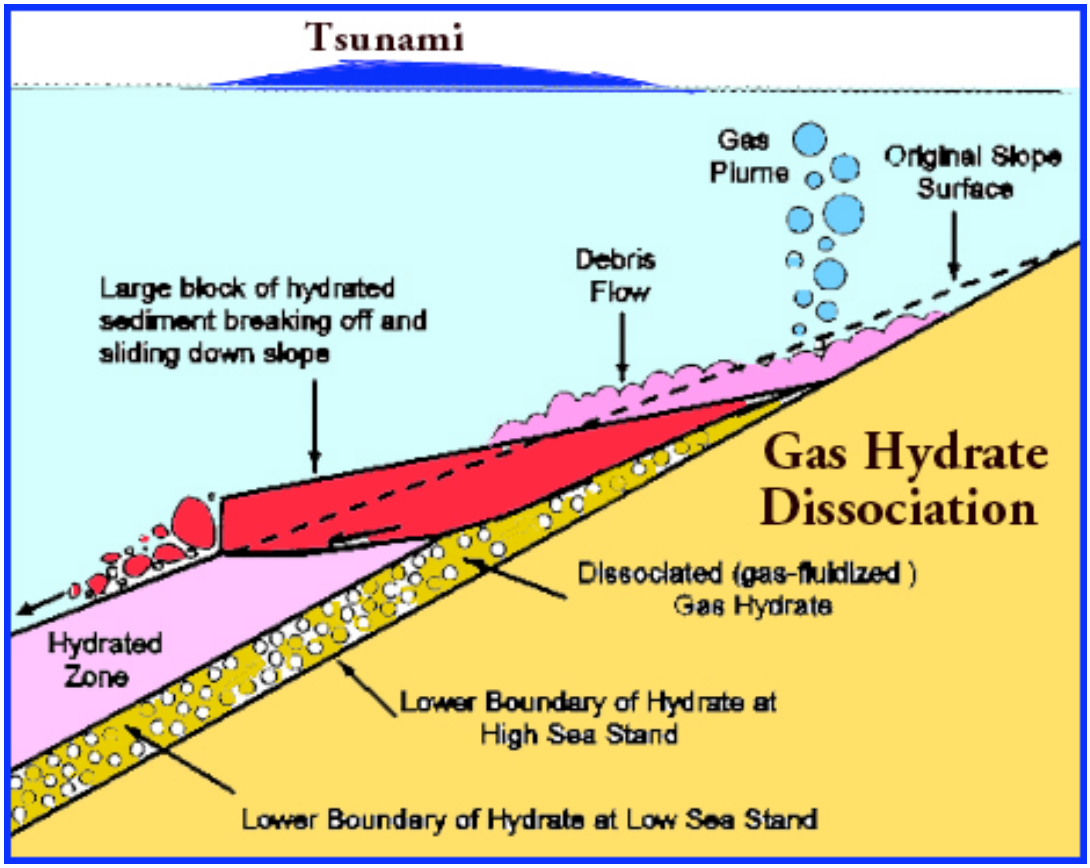

Fig. 17. Structural slope failure and potential tsunami generation from the dissociation of gas hydrates (Modified graphic of the National Energy Technology Laboratory, U.S. Department of Energy (DOE)).

4E. Effects of Astronomical Tides and Ice on Potential Tsunami Destructiveness in the Bohai Sea.

The tides in the Bohai Sea are relatively high (Fig. 18). The tides are primarily dominated by semidiurnal (M2 and S2) and diurnal (K1 and O1) motions (Xu et al 1996). The range of tide heights varies significantly from a minimum of about 2 meters along the shores of Laizhou Bay, to 4.6 meters along the eastern coasts of the Liaoning Province on the Korea Bay, as much as 7 meters along the western coast of North Korea, and even as much as 9 meters further south along the coast bordering the Yellow Sea.

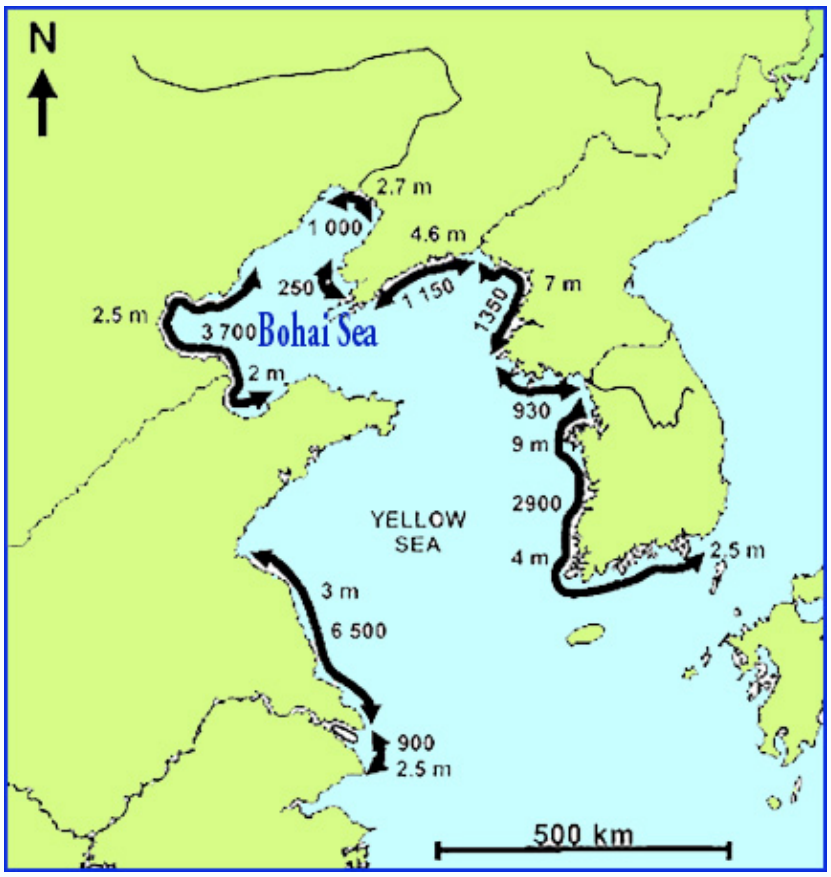

Fig. 18. Extent of astronomical tide height variation along coastal areas of the Bohai and Yellow Seas (Modified after Xu et al. 1996).

The large extent of the astronomical tide variation could have a signifincant effect if a tsunamigenic earthquake occurs at high or near high tide. For example, if a tsunami was generated

at high tide, the eastern shore of Liaodong Peninsula of the Liaoning Province could experience waves that could be 4.6 meters higher than those generated at low tide. Thus, events occurring at high tide could be significantly more destructive. For example, the site where the cooling system of the Hongyanhe Nuclear Power Plant is located could be impacted by tsunami waves that could be 2.7 meters higher than waves generated at low tide. Similarly, the numerous offshore oil platforms that are scattered throughout the Bohai Sea may be susceptible to potential damage if a tsunami is generated in the region. As indicated, given the relatively shallow water depths and the abundant ice-infested waters of the region during the winter months, large pieces of ice carried by the tsunami waves could have a destructive impact. Although ice-induced forces on oil platfom structures and vibrations have been studied in the past (Zhang and Wang, 2008), the dynamic forces from ice carried by tsunami wave action have not been evaluated. The severity of the potential impact would depend on the design of the platform structures. Being more rigid, caisson-built oil platform structures would be expected to fare better than the more common, jacket-built type of oil platform structures which are lighter and weaker.

5. CONCLUSIONS

The Bohai Sea surrounds one of China's most populous and highest economic value regions. Recent earthquakes on land have had great impact. Tunamis do not pose as much of a threat, but locally destructive tsunamis could be generated in the future which can be expected to have more significant impact since most of the recent development has taken place along low-lying coastal areas where several megacities are located and infrastructure facilities exist or are under construction. In spite of predominantly lateral strike-slip components that characterize most earthquakes in this region, there is also evidence of reverse type of faulting movements. Although poorly mapped, reverse faults, normal faults and strike-slip faults reach into the Bohai Sea and earthquakes occurring along such faults can generate tsunamis.

Destructive local tsunamis may be generated by earthquakes along shear fractures in the Bohai Sea, but particularly along the NE-trending and more active tectonic zones south of the 39th parallel. Local tsunamis may be also generated by a combination of collateral mechanisms that could involve folding of thick sedimentary layers, landslides, destabilization/dissociation of gas hydrates deposits and mass sediment flows. Future tectonic movements associated with larger earthquakes in this region could interact with the now submerged fluvial regimes that contain high

sediment loads and thus could generate massive sediment movements. Folding and en-echelon bookshelf type of failures of the deeper consolidated sediment layers could become collateral mechanisms for greater tsunami generation, particularly in areas where denser seismic zones are concentrated, the seismicity is stronger, and greater sedimentation has occurred. Thus the potential for tsunami generation in the Bohai Sea is exacerbated by the thick accumulation of sediments and the multi-layered stereographic distribution of sediments with different shear strengths, densities and rigidities. Following an earthquake, en-echelon, bookshelf type of failures with oblique directivity to the general strike orientation could impart greater tsunami energy and alter expected tsunami directivity.

Finally, dissociation of the abundant gas hydrate deposits by an earthquake ground motions, particularly near offshore oil platforms, could result in large scale slip and sediment mass flows. Combined with extensive surface ice during the winter months, local tsunami waves could possibly cause damage to oil rigs operating in the Bohai Sea, as well as to nearby coastal facilities, by the transport and impact of large pieces of floating ice.

6. REFERENCES

Bonafede, M.; Neri, A., 2000. Effects induced by an earthquake on its fault plane:a boundary element study. Geophysical Journal International, Volume 141, Issue 1, pp. 43-56, 2000.

Castellanos, Hugo and Paul Mann, 2005. Pull-Apart vs. Subduction Rollback Mechanisms For The Cenozoic Formation Of Bohai Basin, Eastern China AGU Fall Meeting, San Francisco, CA. 2005.

Chen, Yun-Tai; Gu, Hao-Ding; Lu, Zao-Xun, 1976. "Variations of gravity before and after the Haicheng earthquake, 1975 and the Tangshan earthquake, 1976", Physics of the Earth and Planetary Interiors, Volume 18, Issue 4, p. 330-338.

Chen Guo-guang, Xu Jie, Ma Zong-jin1, Deng Qi-dong, Zhang Jin and Zhao Jun-meng, 2007. Recent tectonic stress field and major earthquakes of the Bohai sea basin, Acta Seismologica Sinica, Volume 17, Number 4 / July, 2004, pp.438-446, Published by Springer in Earth and Environmental Science, 2007.

Cipar John 1979, "Source processes of the Haicheng, China earthquake from observations of P and S waves", Bulletin of the Seismological Society of America; December 1979; v. 69; no. 6; p. 1903-1916.

Davis, G. A., Zheng, Y., Wang, C., Darby, B. J., Zhang, C., and Gehrels, G., 2001, Mesozoic tectonic evolution of the Yanshan fold and thrust belt, with emphasis on Hebei and Lianoning provinces, northern China: Memoir - Geological Society of America, v. 194, p. 171-197.

Earthquake Administration of Liaoning Province, Quan Yingdao, "An Earthquake of MS7.3 in Haicheng, Liaoning Province on February 4, 1975", World Data Center for Seismology, Beijing.

Hellinger, S.J., Shedlock, K.M., Sclater, J.G. and H. Ye, 1985. The Cenozoic evolution of the north China basin, Tectonics 4 (1985) 343–358.

Hendrix, M.S., and Davis, G.A., 2001, Paleozoic and Mesozoic tectonic evolution of central Asia: from continental assembly to intracontinental deformation: Boulder, Colo., Geological Society of America, vi, 447 p.

Keilis-Borok, V. I. and Soloviev, A., (Edis.), 2003. Nonlinear Dynamics of the Lithosphere and Earthquake Prediction. Springer-Verlag, Berlin-Heidelberg.

Ma, L. and Gao, X., 1996. The state of intensive monitoring and prediction at the Metropolitan Area before Asian Game in 1990. He, Y. N. (Ed.), The Selected Papers of Earthquake Prediction in China, Dedicated to the 30 th International Geological Congress, Seismological Press, Beijing, 255-259.

Madariaga, Raul, 2008?. Dynamics of shallow reverse faulting in 2D Max, Michael D. 2002, Mass Flow in Marine Sediment: Physical Causes and Possible Examples from the Geological Record, Tsunami Society Symposium, Honolulu, Hawaii 2002.

Mei, S. R. (Ed.), 1982. Tangshan Earthquake in 1976. Seismological Press, Beijing (in Chinese, reviewed abstract in English). Milkov, Alexei V. 2002, Global Distribution and Significance of Natural Gas Hydrate. Tsunami Society Symposium, Honolulu, Hawaii 2002.

Pararas-Carayannis, G., 1992. The Earthquake and Tsunami of 2 September 1992 in Nicaragua. Wepage Article: http://www.drgeorgepc.com/Tsunami1992Nicaragua.html

Pararas-Carayannis, G., 2007. Historical Earthquakes in China. Webpage Article: http://www.drgeorgepc.com/EarthquakesChina.html

Pararas-Carayannis, G., 2008a, The Earthquake and Tsunami of July 18, 1969 in the Bohai Sea, China. Webpage Article: http://drgeorgepc.com/Earthquake1969ChinaBohai.html

Pararas-Carayannis, G., 2008b. The Earthquake of February 4, 1975 in Haicheng, China. Webpage Article:http://drgeorgepc.com/Earthquake1975ChinaHaicheng.html

Pararas-Carayannis, G., 2008c. The Tangshan Earthquake of July 28,1976 in China. Webpage Article: http://drgeorgepc.com/Earthquake1976ChinaTangshan.html

Pararas-Carayannis, G. 2008d. The Earthquake of May 12, 2008 in the Sichuan Province of China. Website: http://www.drgeorgepc.com/Earthquake2008ChinaSichuan.html

Shou, Zhonghao 1999. "The Haicheng Earthquake and Its Prediction", Science and Utopya 65, page 34, November 1999" (in Turkish; Reviewed English abstract)

Ye, H., Shedlock, K.M., Hellinger, S.J. and J.G. Sclater, 1985. The north china basin: an example of a Cenozoic rifted intraplate basin, Tectonics 4 (1985) 153– 169.

Yin, X. C., Wang, Y. C., Peng, K. Y. and Bai, Y. L., 2000. Development of a new approach to earthquake prediction: Load/Unload Response Ratio (LURR) theory. Pure Appl. Geophys. 157, 2365-2383.

Yin, A., and Nie, S., 1996, A Phanerozoic palinspastic reconstruction of China and its neighboring regions, in Yin, A., and Harrison, T. M., eds., The Tectonic evolution of Asia: Cambridge [England] ; New York, Cambridge University Press, p. 442-485.

Yu Jianguo, Li Sanzhong, Wang Jinduo, Timothy M. Kusky ; Wang Xinhong ; Lu Shengqiang, 1995. Relationship between salt diapirism and faulting in the central structural belt of the Dongying sag, Bohai Gulf basin, ChinaQuaternary International Volume 25, 1995, Pages 13-17.

Wu Zhongliang and Shaoxian Zang, 1989. Source parameters of bohai earthquake, July 18, 1969 and yongshan earthquake, May 11, 1974 determined by synthetic seismograms of teleseismic P waves. Acta Seismologica Sinica. Seismological Society of China. Volume 5, Number 1 / February, 1992, pp. 1993-1344 (Online Issue)

Zhang, Z.M., Liou, J.G., and Coleman, R.G., 1984, An outline of the plate tectonics of China: Geological Society of America Bulletin, v. 95, p. 295-312. Zhang, G. M. and Ma, L. (Eds.), 1993. Study on the Datong-Yonggao Earthquake. Seismological Press, Beijing (in Chinese; reviwed English Abstract).

Zhang, Y. X., Liu, G. P., Chen, Q. F., Ma, L. and Yang, W. Z., 1998. The feature of anomaly evolution before Shunyi M S 4.0 earthquake and estimation for the tendency of the quake by LURR. Earthquake 18(1), 49-56 (in Chinese).

Zhang, Y. X. and Liu, G. P., 2000. Study on characteristics of anomalies near by epicenter of Zhangbei M S 6.2 earthquake and their spatial and temporal evolution. Earthquake 20(1), 53-58. Zhu, F. M. and Wu, G., 1982. The Haicheng Earthquake in 1975. Seismological Press, Beijing (in Chinese - English abstract).

Wang, K., Chen,Q.-F., Sun, S. and A. Wang, 2006, Predicting the 1975 Haicheng Earthquake, Bulletin of the Seismological Society of America, June 1, 2006; 96(3): 757 - 795.

Wang Jian, 2007. Historical earthquakes and a tsunami in Bohai Sea. Journal Acta Seismologica Sinica. Publisher Seismological Society of China ISSN 1000-9116 (Print) 1993-1344 (Online), Volume 20, Number 5 / September, 2007.

Wang, T.H., 1988. Genetic types of thrust faults in Eastern China petroliferous regions, Earth Sci. 13 (1988) 627– 634.

Watson, M.P., Hayward, A.B., Parkinson, D.N. and Z. Zhang, 1987. Plate tectonic evolution, basin development and petroleum source rock deposition onshore China, Mar. Pet. Geol. 4 (1987) 205–225.

Xu Qinghai, Wu Chen, Yang Xiaolan and Zhang Ningjia, 1996. Palaeochannels on the North China Plain: relationships between their development and tectonics. Studies of the Palaeochannels on the North China Plain, Geomorphology, Volume 18, Issue 1, December 1996, Pages 27-35.

Zhang D., and S. Wang, 2008, Failure modes analyses of ice-resist jacket platforms in Bohai Sea. Dalian University of Technology, Dalian 116024, China (Abstract seen)

Zhao Liang and Tianyu Zheng, 2005, Seismic structure of the Bohai Bay Basin, northern China: Implications for basin evolution. Earth and Planetary Science Letters 231, Issues 1-2 (Feb. 2005) Pages 9– 22.

Zhongliang Wu and Shaoxian Zang, 1992, Seismological Society of China (Acta Seismological Sinica Publisher), ISSN 1000-9116 (Print) 1993-1344 (Online) Issue Volume 5, Number 1 / February, 1992.

GEOMORPHOLOGICAL AND SEDIMENTOLOGICAL CHANGES DURING AND AFTER THE DECEMBER-2004 INDIAN OCEAN TSUNAMI NEAR THE VELLAR RIVER AND THE M.G.R. ISLAND AREA OF THE CENTRAL TAMIL NADU COAST, INDIA

S.R. Singarasubramanian[1], M.V. Mukesh[1], K. Manoharan[1], P. Seralathan[2], K.Sujatha[1], and D. Bakkiaraj[1]

1. Department of Earth Sciences, Annamalai University, Annamalainagar, Tamilnadu, India. 608002. laksrs@yahoo.com

2. Department of Marine Geology and Geophysics, Cochin University of Science and Technology, Cochin, Kerala, India 682016

ABSTRACT

The present study reviews geomorphic changes and sediment characteristics in the Vellar river and the M.G.R. island in the Cuddalore District, of Tamilnadu, India, caused by the 26th December, 2004 Indian Ocean Tsunami. The island has an area of about 12,000 m^2 and it is separated from the mainland by a channel. It is bounded to the east by the Vellar River and to the north and south by the Muzhukkuthurai lagoon. A vegetated coastal dune with a length of about 1.5 km protected the island. Tsunami waves ranging in height from 4 to 6 meters breached the dunes, caused erosion and carried debris of destroyed coastal buildings westward to more than 50 m inland. The tsunami run up was up to 1.3 m. Very fine sand with a thickness of one meter filled the Muzhukkuthurai lagoon in the west. Heavy erosion resulted in a steep beach gradient. Sediments transported from the SE and the SSE direction resulted in greater accretion along the intertidal region. The sediment layer exhibited trampled and load structures, indicating deposition by the flooding and receding motion of the water, moving at high velocity. The sediments ranged from fine to medium in size and were well sorted.

Key Words: *2004 Indian Ocean Tsunami, breaching, sedimentation, trampled and load structures.*

Science of Tsunami Hazards, Vol. 28, No. 1, page 67 (2009)

1. INTRODUCTION

Tamilnadu has a coastline of about 1026 kms in length. The coastal zone is one of the most fragile, complex and productive ecosystems. The various geomorphic landforms developed during the Quaternary period register the imprints of past geological processes. A widely varying nature of landforms and their disposition along the beaches and inland represents the successive phases of transgression and regression of sea level. In India, coastal geomorphologic studies have been given new impetus only in the early 1980s, since the advent of aerial photos and remote sensing. In the study area, Loveson and Rajamanickam (1998) have observed an emergence along the Southern Tamilnadu coast. Anbarasu (1994) has given a broad spectrum of evolution of coastal landforms of Northern Tamilnadu. Karikalan (1996) and Karikalan, et. al. (2001a) have studied the heavy mineral assemblages of different quaternary landforms. Coastal geomorphic features of Porto Novo region, Tamilnadu was studied by Karikalan et. al (2001b).

On 26th December 2004, a massive, shallow-focus (10 km) earthquake (epicenter 3° 7'N, 95° 7'E, origin time 6.29 IST) occurred in the seismically active zone along the Sunda Trench, near NW of Sumatra at a depth of about 1300 meters. The earthquake-triggered tsunami waves that begun striking the Tamilnadu coast of India at about 8.45 IST. The waves ranged from 3 to 10m in height.

Most of the geomorphic or sedimentologic studies that have been carried out in the past were on the tsunami sediment deposition along coasts. The majority of the research has been conducted along the coasts of the Pacific Ocean, particularly along the North American coast (e.g. Clague, 1997; Atwater and Moore, 1992; Nichol et. al. 2002). The 26th December 2004, Indian Ocean tsunami inundation and its sediment deposits were studied by Chandrasekaran (2005); Narayan, et. al., (2005); Narayana et. al (2005); Raval (2005); Singarasubramnaian, et. al (2005 & 2006), and others.

The present study describes some of the changes to coastal geomorphic features, such as sand dunes and channels, caused by the destructive tsunami waves. The observed impact included erosion but also inland deposition of new sediments and re-deposition of eroded sediments.

2. STUDY AREA

The study area forms part of Vellar river basin in central Tamilnadu, on the east coast of India. The major land area is called “M.G.R. Tittu” and is bounded by the Bay of Bengal to the east, Vellar to the north and the Muzhukkuthurai lagoon in the south and west. The aerial extent of the island is about 12,000 m^2. The study area is depicted in the Survey of India topo-sheet 58 M/10, which covers the area extending from 79º 45’ to 79º 50’ E, and from 11º 30’ to 11º 27’30” N. (g.1).

3. GEOMORPHOLOGY

The landforms in the study area are primarily of depositional nature, such as deltaic alluvial plains, chenniers, palaeo-lagoonal plains, beach ridges, sand dunes, beaches, palaeo-barriers, palaeo-tidal flats, river mouth bars and natural levees. The Vellar River is ephemeral in nature and flows south easterly at the lower reaches.

4. METHODOLOGY

The coastal geomorphic features were studied by a field survey and use of the topographic maps. The extent of tsunami inundation was determined from high water marks and debris deposits. Trenching, at intervals of 5cm from the top collected sediment samples. Standard sediment size analysis was carried out and statistical parameters were calculated (Folk and Ward, 1957) to deduce the depositional environment.

5. RESULTS AND DISCUSSION

The coastal area between the Vellar estuary and Muzhukkuthurai has prominent, stable sand dunes and ridges 4 to 6 m in height and with a lot of vegetation. The M.G.R. Island, between Vellar and Muzhukkuthurai, is relatively small in size and sustained greater destruction by the tsunami. About 175 people, mostly fishermen, lived in about 80 houses constructed over the crest of the stable palaeo dunes. A long sand dune of about 3m in height protected the island community. There were several more major and stable dunes with vegetation on the island as well as a major coconut tree plantation.

5.1 Post Tsunami changes

A series of three waves from a SE direction begun to strike the coast at about 8.50 IST. The waves devastated the entire island and the adjoining regions. The maximum tsunami run-up height at M.G.R. Island was more than 3m. The waves completely inundated the island, destroyed all homes and killed about 80 people. The Muzhukkuthurai lagoon and Vellar River apparently reduced the extent of tsunami inundation and the intensity of the waves in other banks further inland. At Muzhukkuthurai the extent of flooding ranged from 1,000 to 1,200 meters inland and the maximum tsunami run-up was 1.2 m. Most of the breached or eroded sediments were deposited along the shores of the Muzhukkuthurai lagoon and the Vellar River.

The fore dunes offered coastal protection by reducing tsunami wave velocities and by refracting wave paths. However, they were completely eroded. The waves not only altered the geomorphic features of the island and of the adjoining areas but also brought voluminous sediments from the shelf and the coast. Also the stable palaeo dunes were breached by the waves. Three months after the tsunami sand bars developed in the south with orientation perpendicularly to the coast. This is evidence of changes in local coastal morphology and wave direction caused by the tsunami. Small-elevated land surfaces could also be seen near the mouth of the Vellar River immediately after tsunami (Plate-I), but slowly these became flatter and merged. Complete closure of both the Vellar estuary and the Muzhukkuthurai lagoon inlet were evidence of post tsunami sedimentation. Also, reworked dune sediments were deposited in the Muzhukkuthrai lagoon west of the M.G.R. Island. In the canal, the thickness of the tsunami deposit was about one meter. These changes were evidence of the ferocity of tsunami waves. Near the coast, the thickness of the tsunami deposits varied from 5 to 15 cm. The erosional features were more prominent in the small island. Tsunami waves had eroded the profile of the beaches to a depth of about 120 cm. Tsunami deposits had a buff coloration and could be easily differentiated from normal tidal dune sediments. Trampled structures were prominent over the planar beds (Plate-I). This was indicative that the

sediments were deposited under conditions of high water velocity and turbulence. Their size varied from fine to medium with the phi mean size ranging from 1.567 to 2.3 and the standard deviation from 0.277 to 0.422. This indicates that the sediments were composed mainly of medium, well-sorted sand. Nearly positively skewed sediments were dominant with platykurtic to leptokurtic nature.

As shown in the core (Fig.1), medium sands were dominant over the fine sands at certain depths. The presence of the fine sands indicates deposition from suspension. Tsunami deposits were well to very well sorted in character. Sands which are normally deposited on portions of beaches within the breaking wave zone, wash continuously thin sheets of sediments which invariably lack admixtures of fine-grained sediments (Friedman and Sanders, 1978). The shelf region normally contains well-sorted river sediments deposited by rivers during the ice age, when the coastal areas emerged. Though the wave action is considered to be responsible for sorting the sediments on the beaches, the dominance of well-sorted sediments is attributed to improvement of uniformity in grain size by the removal of both coarser and finer fractions by strong wave energy. Well to very well sorted sediments in the study region indicated sudden winnowing or back and forth motion by the depositing agent.

Friedman (1961) has attributed that such winnowing action is the reason for positive skewness of beach sands and that such action removes the fine grained particles leading to a back of tail of fine-grained material. Also, predominant positive skewness in size of sediments indicates unidirectional transport (channel flow) or deposition in sheltered, low energy environment (Brambati, 1969). The sediment characteristics in the study area indicated scouring which changed the local bathymetry from 20 to 30 m, i.e. the low energy marine environment where waves cannot interact with seabed sediments. The leptokurtic nature of sediments indicated fluctuation in energy conditions of the depositing medium.

6. CONCLUSIONS

The 26th December, 2004 tsunami event along the Tamilnadu coast brought lot of geomorphic and sedimentological changes. In the study area the tsunami resulted in the breaching of sand dunes, the filling of lagoon, erosion and the loss of numerous lives. It can be concluded from the study that stabilized dunes with vegetation offer some protection to the coast from natural marine disasters like cyclone surges, tsunamis or extreme storm waves. Also that the Vellar river and the Muzhukkuthurai lagoon reduced tsunami inundation and extent of destruction in the inland region. Thus, the coastal morphologies played an important role in protecting the coast and the coastal communities. The particle size analysis in the study area indicates that the sediments that were deposited by the waves of the tsunami inland ranged from fine to medium, well-sorted sands. These deposits showed typical color and textural variations from the normal tidal sediments. Near the estuary they were superimposed over the pre-existing dark carbonaceous estuarine clays. Overall, the deposits exhibited trampled structures over the planar beds which indicates that the tsunami deposition of sediments occurred under high wave velocity conditions.

PLATE- I DESTRUCTIONS BY TSUNAMI WAVES: A- SAND BAR DEPOSITION IN VELLAR ESTUARY; B- SAND BAR DEVELOPMENT IN M.G.R. ISLAND; C- AERIAL VIEW AND ERODED SAND DUNE IN M.G.R.ISLAND; D- WATER RUN-UP HEIGHT (1.2m) IN MUZHUKKUTHURAI; E- STABLE DUNE WITH VEGETATION, PARTIALLY BREACHED; F- ERODED DUNE AND UPROOTED TREES; G- 4' EROSION IN THE SETTLEMENT AREA IN M.G.R.ISLAND; H-HANGING HOUSE AFTER EROSION; I- STABLE CONTINUOUS DUNE WITH VEGETATION, BUT PARTIALLY BREACHED; J- LAYERED SEDIMENTS OVER ESTUARINE CLAY BY TSUNAMI; K- LAYERED SEDIEMENTATION OVER CARBONISED CLAY; L- TRAMPLED STRUCTURE OF TSUNAMI SEDIMENTS OVER MASSIVE DEPOSITS.

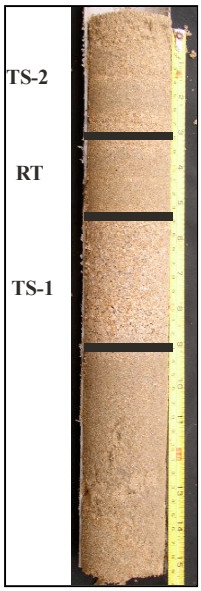

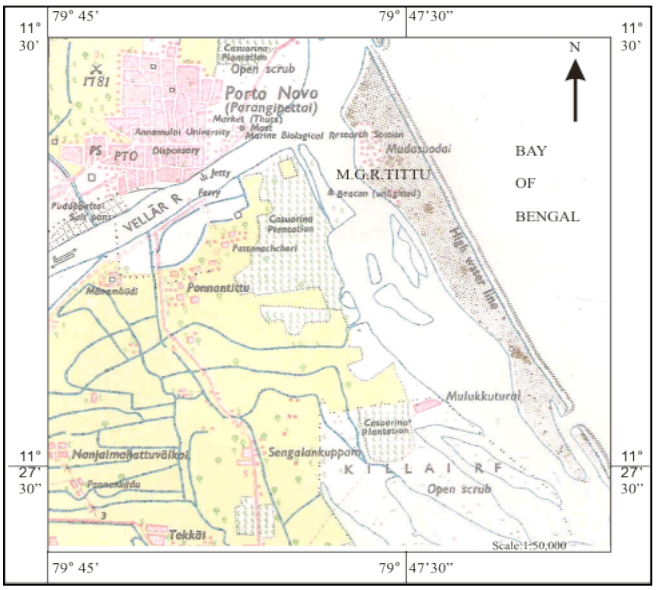

Fig. 1. Core sampled near Vellar

Map 1 Showing study area

TS-1 &2 Tsunamigenic Sediment

RT- Retreating wave deposit.

Acknowledgement

The author expresses thanks to the co-authors for their valuable help during the fieldwork and analysis. He also thanks the university authorities for permitting the execution of this work as part of a degree requirement.

REFERENCES

ANBARASU, K. (1994) Geomorphology of the Northern Tamilnadu coast using Remote sensing Techniques. Unpublished Ph.D. thesis, Bharathidasan University, Tiruchirapalli. P.184.

ATWATER, B.F and MOORE, A.L. (1992) A tsunami about 1000 years ago in Puget Sound, Washington. *Science* 258; Pp.1616-1617.

BRAMBATI, A. (1969): Stratigraphy and sedimentation of Siwaliks of North Eastern India. *Proc. Inter. Sem, Intermontane Basins: Geology and Resources,* Chiang Mai, Thailand. P.427-439.

CHANDRASEKARAN, N (2005) : Tsunami of 26th December 2004: Observation on inundation, sedimentation and geomorphology of Kanyakumari Coast, South India. *22nd IUGG Inter. Tsunami Symp. Chania.* PP 49-56.

CLAGUE, M.L. (1997). Evidence for large earthquakes at the Cascadia subduction zone. *Reviews of Geophysics* 35(4); Pp.439-460.

FRIEDMAN, G.M. (1961) : Distinction between (*sic*) dune, beach and river sands from their textural characteristics: Jour. Sed. Petr., V.31, P. 514-529.

FRIEDMAN. G.M. and SANDERS, E.J : (1978) *Principles of Sedimentology,* John Wiley and Sons, pp. 396 &792

KARIKALAN, R. (1996), A study of sediments from the Quaternary landforms around Parangipettai, South Arcot, Tamilnadu. Unpublished M.Phil., Thesis. Tamil University, Thanjavur. P.136.

KARIKALAN, R., ANGUSAMY, N., MOHAN, P.M. and RAJAMANICKAM, G.V. (2001 a), Distribution of heavy minerals in the Quaternary sediments around Vellar basin, Parangipettai, Tamilnadu. A handbook of placer mineral deposits, *New Academic Publishers*, New Delhi. Pp.158-170.

KARIKALAN, R., ANBARASU, K. and RAJAMANICKAM.G.V. (2001 b) Coastal geomorphology of Portonovo region South Arcot District, Tamilnadu. *Ind. Jour. of Geomorph*. Vol.6 No. 1 &2, Pp. 157-169.

LOVESON, V.J. and RAJAMANICKAM, G.V. (1998) Evidence for phenomena of emergence along Southern Tamilnadu Coast through remote sensing techniques, Tamil Civilisation, Tamil University publication. Vol. 6. Pp.188-199.

NARAYAN, J.P., SHARMA, M.L. and MAHESHWARI, B.K. (2005): Effects of medu and coastal topography on the damage pattern during the recent Indian ocean Tsunami along the coast of Tamilnadu. *Science of Tsunami Hazards*, v. 23 (2), p. 9

NARAYANA, A.C., TATAVARTI, R. and SHAKDWIPE, M. (2005): Tsunami of 26 December, 2004: Observations on Kerala Coast. *Jour. of Geol. Soci. India,* v.65 pp. 239-246.

NICHOL, S.L., LIAN, O.B. and CARTER, C.H. (2002). Sheet gravel evidence for a late Holocene tsunami runup on beach dunes, Great Barrier Island, New Zealand. *Sedimentary Geology* 3073.

RAVAL, U., (2005) : some factors responsible for the Devastation in Nagapattinam Region due to the tsunami of 26th December, 2004. Jour. of the Geol. Society of India. v. 65(5). Pp. 647-649.

SINGARASUBRAMANIAN, S.R., MUKESH, M.V. and MANOHARAN K., (2005) A preliminary report on coastal sediment characteristics after M 9 tsunami event along the central Tamilnadu, East coast of India. Proc. of the special Tsunami Session at APAC, 2005(ed) Byung Ho Choi, Fumihiko Imamuna, 2005, pp.209-221.

SINGARASUBRAMANIAN. S.R., MUKESH, M.V, MANOHARAN, K., MURUGAN, S., BAKKIARAJ, D. JOHN PETER, A. and SERALATHAN, P. (2006): Sediment characteristics of the M 9 tsunami event between Rameswaram and Thoothukudi, Gulf of Mannar, Southeast coast of India. *Int. Jour. Sci. of Tsunami Hazards*, Vol. 25, No.3 pp.160-173.

INUNDATION MAPPING – A HAZARD STUDY BASED ON THE DECEMBER 26, 2004 TSUNAMI ALONG THE KARAIKAL COAST OF INDIA

K. Chittibabu & R. Baskaran*

Department of Geology,
National College,
Trichirapalli-01, India.

Department of Industries and Earth Sciences,
Tamil University,
Thanjavur-10, India.
*e-mail: baskaranrajagopalan@yahoo.com

ABSTRACT

A study of tsunami impact was undertaken along India's Karaikal coast from Poovam in Karaikal to Nagore, Nagapatinam. An integrated approach was adopted for the preparation of thematic maps on land use, land cover and coastal geomorphology using multispectral remote sensing data. RTK GPS instruments were used for the collection of topographic data with contour intervals of 0.5m. The GIS tool was used to incorporate the elevation data, the extent of tsunami inundation and the thematic maps derived from remote sensing data. The present study highlights the most vulnerable areas of tsunami inundation and provides demarcations of suitable sites for rehabilitation.

Science of Tsunami Hazards, Vol. 28, No. 1, page 75 (2009)

1. INTRODUCTION

Along the coast of Tamilnadu, the inland inundation from the December 26, 2004 tsunami varied from 300-900 meters, while run-up heights ranged from 3-7 m. (Kumar et al., 2008). The waves struck the Karaikal coastal region, flooding fishing villages and causing the loss of more than 500 people. The maximum tsunami run up elevation was 5.2m in this region. At the village of Akkaravatam the maximum inland inundation was about 2.1 km and the maximum tsunami height was about 7m. It is believed that the local bathymetry resulted in wave convergence and the observed high amplification of the tsunami at this location – which emphasizes the significance of coastal geomorphology and bathymetry in the variation of run up heights and inundation (Jay et al., 2005).

Based on actual data prior to 1968 (Gonnert et al, 2001), a classification of the coast for storm surges of different heights (A: <2m; 2-5; C:>5m) was made. Along the coastal belt north of latitude 20^{o}N where the cyclones occur more frequently, maximum surges occur in Sunderbans. The southeast coast of Karaikal is designated as "C" category. This is a region of maximum storm surge with amplitude of 0.3m and combined surge plus wind wave amplitude, totaling 1.3m.

There has been considerable research in determining the impact of tsunamis on coastal environments as well as the nature of inundation, run up heights, erosional and depositional effects and destruction along coasts. Alami and Tinti (1991) evaluated the tsunami hazard along the Moroccan coast by comparing tsunami data with the set of available earthquake data. Dawson (1994) suggested that the geomorphologic processes associated with tsunami run-up and backwashes are highly complex. Raval (2005) reported severe destruction along the coast of Nagapatinam, South India, primarily caused by its geographic setting, which enhances inundation. Mohan (2005) concluded that the elevated coastal dunes and the beach ridges along a coastline could act as barriers in minimizing inundation along the northern parts of the Tamilnadu coast. In the present paper, we describe our work on mapping the extent of inundation along the Karaikal coast and in finding a relationship between the extent of tsunami inundation and run-up height, with the help of field measurements, by using RTK-GPS and Leica Total Station and the co-ordinates and elevations of locations where evidence of tsunami was preserved.

2. STUDY AREA

The study area (Fig. 1 & 2), covered 160 sq. km. along the coast of Karaikal, from the village of Poovam to Nagore. The study area is also illustrated with satellite imagery (Fig. 3).

Major parts of the investigated coastal area consist of alluvium, beach dunes, tidal flats and sandy bars. The entire study area is occupied by coastal community settlements. Beach resorts, farmhouses, aquaculture ponds, theme parks, tourist spots, and artificial parks are mainly located on the southeast coast of Karaikal (Fig. 5). Fishing is the main occupation of people living in the suburban coastline, whereas in the urban coastline the inhabitants are also employed by industries and governmental and non-governmental organizations.

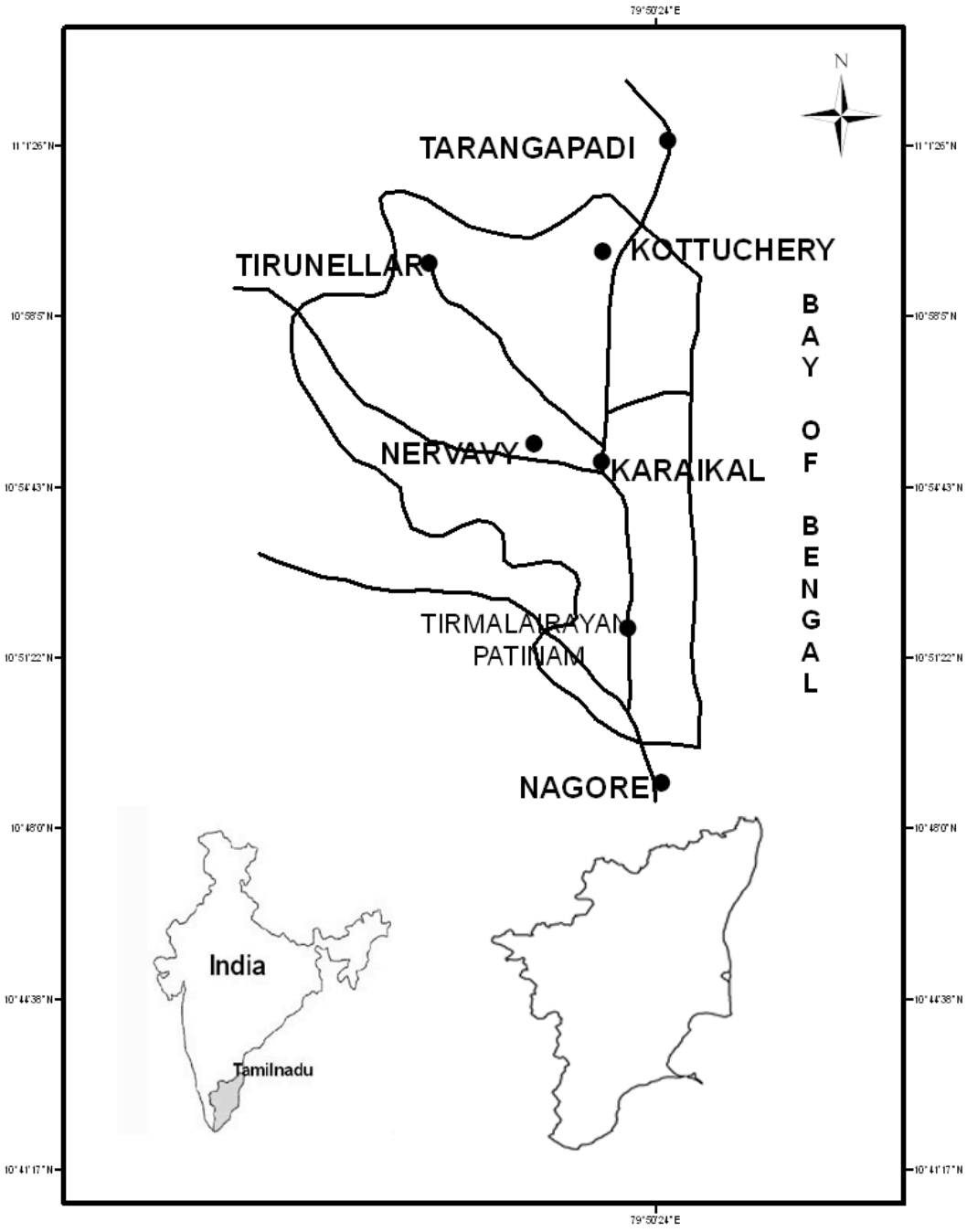

Fig. 1. Index Map of the Study Area.

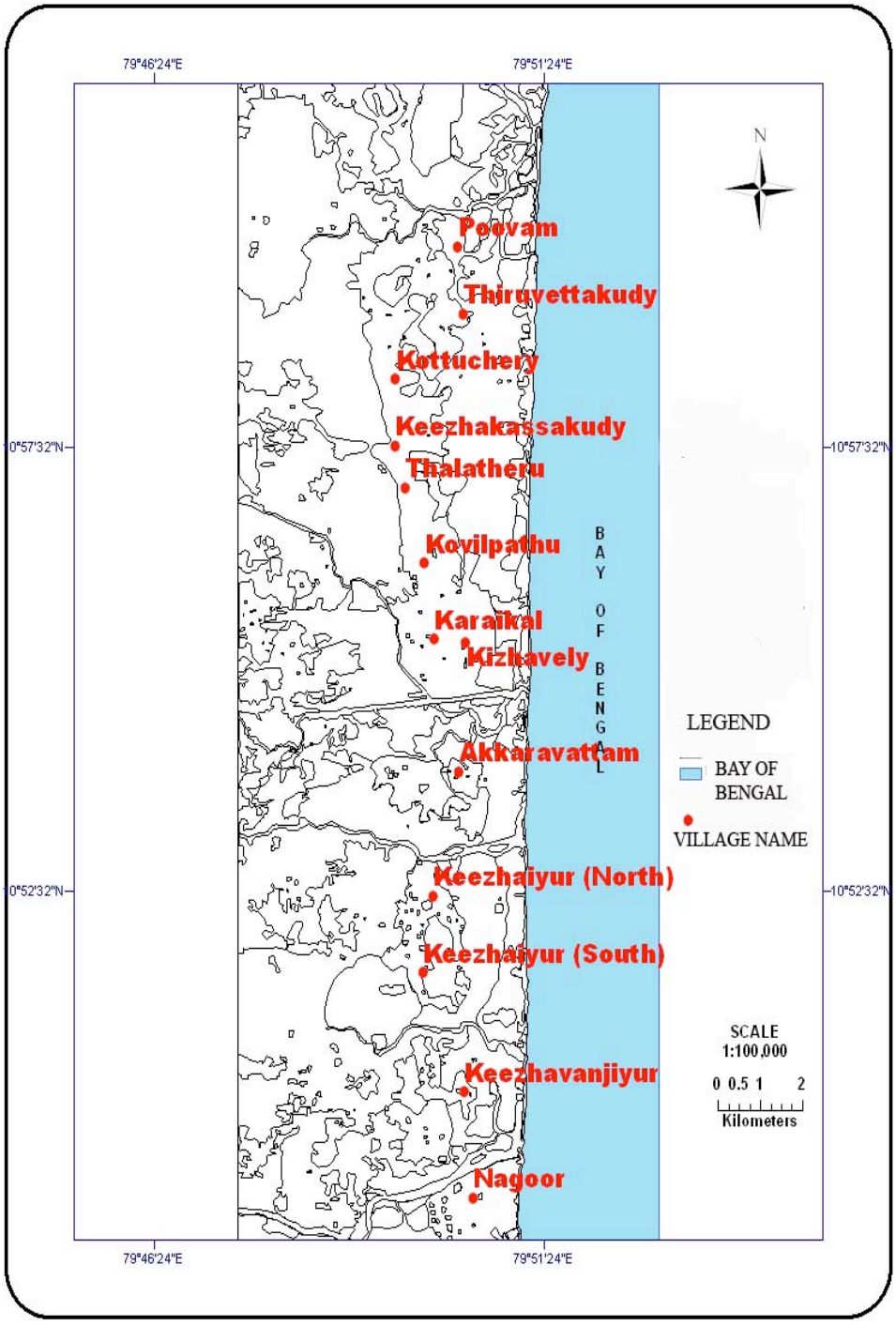

Fig 2. Map of Locations of the Study Area.

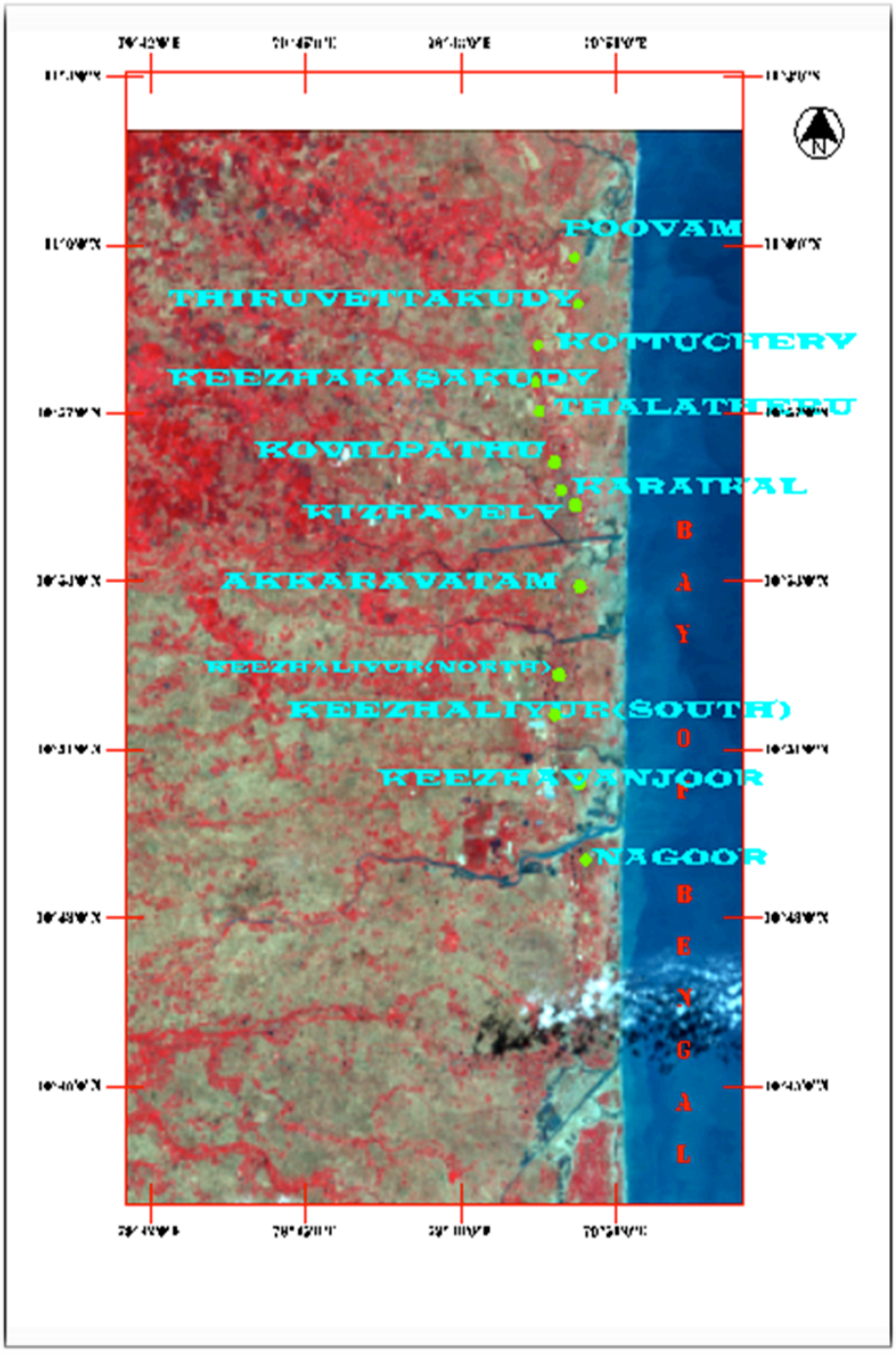

Fig. 3. Satellite Imagery of the Study Area.

3. METHODOLOGY

Inundation maps are depictions of coastal areas that identify regions, populations, and facilities that are at risk from tsunami attack. Emergency planners for disaster response and mitigation could use such maps. These maps require an assessment of local and far-field geologic hazards, and the calculation of potential coastal flooding. Detailed fieldwork was undertaken along the12 km coastal stretch from Poovam to Nagore to assess the extent of inundation (Fig. 4). Co-ordinates of the 10 inundation limits and the shoreline were measured using Magellan hand held GPS with a spatial resolution of 10 m. The inundation limit was identified using field evidence, such as withering of plants sensitive to salinity or presence of organic debris left by the tsunami waves. Watermarks on compound walls were rare and were used wherever available. The direction of propagation of tsunami was noted based on transported blocks of damaged compound brick walls or broken tree trunks. Also, examined was the geomorphologic set up of the region, such as the presence of dune ridges. For the preparation of land use/land cover maps, LISS III satellite data was used. ERDAS Imagine software was used for image processing. Land use/cover categories were mapped using such multi-spectral imagery. Geo-referencing with Ground Control Points (GCP) - such as road intersections - collected with Magellan GPS, refined the images (2005 IRS P6 LISS-III). Baseline maps of villages were scanned and geo-referenced using ARC GIS 9.1 and measuring co-ordinates (Lat/Long; WGS 84) of known survey monuments. Village boundary stones were preferentially used for GCP. At least six GCP readings were taken for each village and thus the RMS error was kept minimum; points that did not correspond properly were deleted. The village maps were overlaid on the satellite image and the correspondence of features present was confirmed. The marginal water bodies and roads depicted on the maps were useful for the accuracy of the recording process. The rectified village maps were digitized using ARC GIS 9.1, GIS package in the Integrated Coastal and Marine Area Management (ICMAM) Project Directorate of the Ministry of Earth Sciences, Government of India, in Chennai. Ground truth information collected during elevation mapping was used to validate these details.

4. LAND USE/COVER MAP (POOVAM TO NAGORE).

1. Tsunami inundation limits and run-up level mapping along the study area;
2. Transfer of inundation points over a geo-referenced satellite imagery;
3. Elevation mapping for the preparation of 0.5 km interval contour data using RTK GPS (Real – Time Kinematic GPS) along the study area at different transects;
4. Post-tsunami remote sensing data (LISS-III) for land use/cover mapping using ERDAS package;
5. Preparation of larger scale (1:50000) action plan maps by incorporating all the above thematic parameters and cadastral maps in a GIS environment.

A tsunami inundation map, representing a source and a community-specific “credible worst case scenario”, is a powerful planning and hazard mitigation tool (Gonzalez et al., 2002).

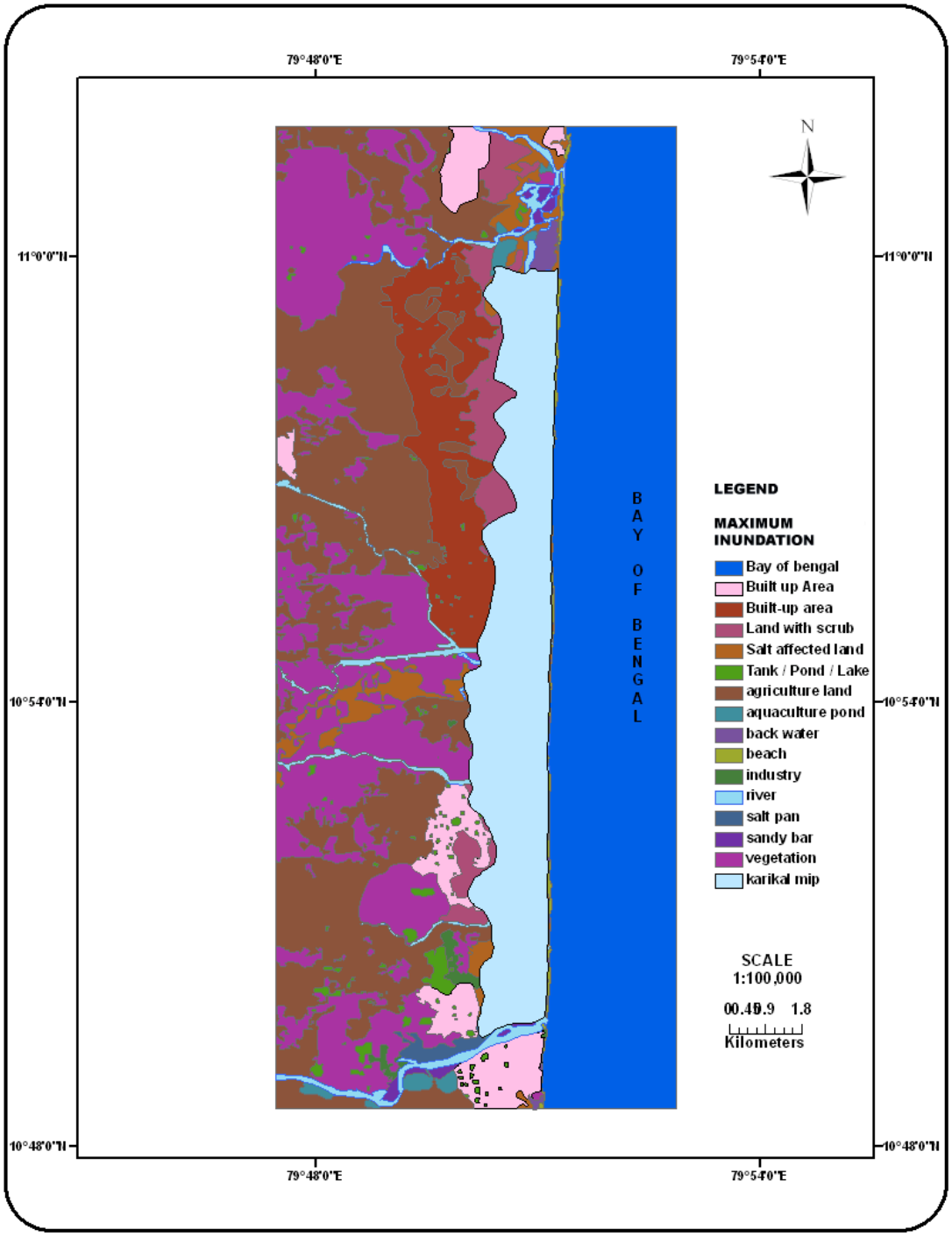

Fig. 4. Inundation Map from Poovam to Nagore.

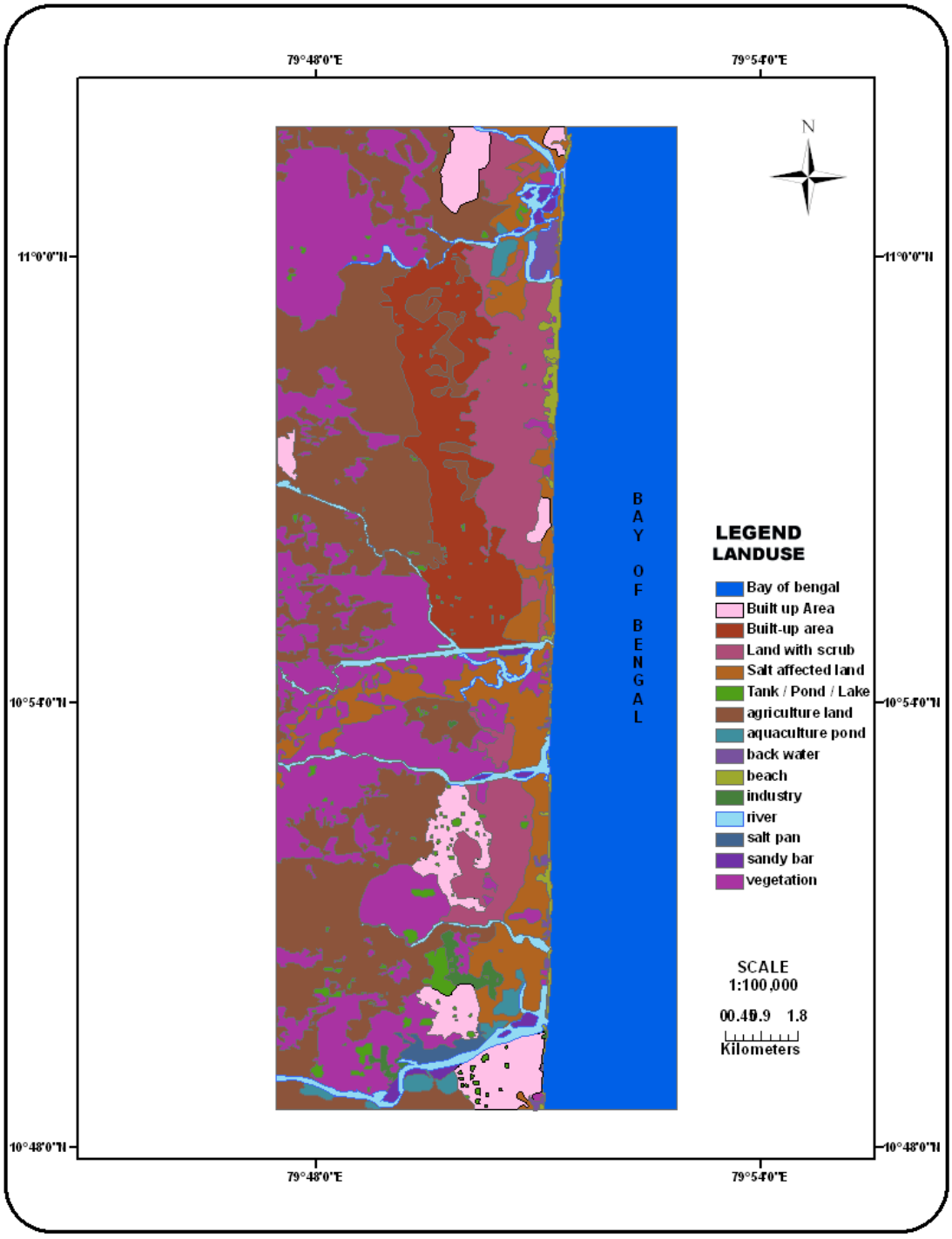

Fig 5. Land Use/Cover Map (Poovam to Nagore).

Such a program of mapping tsunami inundation is of great usefulness to emergency managers. Modeling tsunami inundation is required to properly assess the risk (Groat, 2005). With the growth of population in coastal areas, there is an increased need for better scientific understanding of earthquake and tsunami hazards. Simple maps of expected tsunami paths and travel times, based on crude bathymetry, have been of important operational value in developing a tsunami-warning infrastructure (Mofjeld et al, 2004). Table 1 illustrates the tsunami inundation limits in meters and the coordinates of latitude and longitude of specific locations of the study area, in reference to the high tide datum data provided by the Government of Tamil Nadu. The inundation limits have been plotted on base map top sheets (1:25,000) of the Survey of India (SOI). Figure 3 shows the tsunami inundation limits for a coastal area, which extends from Poovam to Nagore.

Table 1: Tsunami inundation limits and area of submergence. Sl. no, name of the village, maximum inundation limit (in km), minimum inundation (in km).

S.No	**Village Name**	**Max (in Km)**	**Min (in Km)**
1.	Thiruvettakudi	1.50	0.93
2.	Kottucherry	1.48	1.18
3.	Kilakasakudi	1.48	1.05
4.	Thalatheru	1.54	0.88
5.	Kovilpathu	1.70	1.17
6.	Kizhavely	1.75	1.14
7.	Akkaravattam	2.09	----
8.	Keezhaliyur North	1.98	1.27
9.	Keezhaliyur South	1.97	1.29
10.	Vanjoor	1.69	1.34

5. RESULTS AND DISCUSSION

Maximum inundation is shown for the following villages: Akkaravatam (2.09), North Keezhaliyur (1.98m) and South Keezhaliyur (1.97m). In these villages the predominant landform is mud flat with low elevation. Furthermore two rivers and a canal border the village of Akkaravatam. In the northern part of the study area from Keezhalavely to Thiruvettakudi villages, the area is partially covered by beach ridges and plains parallel to the shoreline. Hence inundation was minimum as in Thiruvettakudi village (0.93m) due to the presence of a major ridge parallel to the shoreline.

REFERENCES

Alami, S. O. E., Tinti, S., A (1991) Preliminary evaluation of the tsunami hazards in the Moroccan coasts, Sci. Tsu. Haz., 9(1), 31–38.

Besana, G. M., Ando, M., and Mirabueno, M. H., (2004) The may 17, 1992 event: tsunami and coastal effects in eastern mindanao, Philippines, Sci. Tsu. Haz., 22(2), 61–68.

Chadha, R. K., Latha, G., Yeh, H., Peterson, C., and Katada, T. (2005) : The tsunami of the great Sumatra earthquake of M 9.0 on 26 December, 2004 – impact on the east coast of India, Cur. Sci., 88, 1297–1301.

Dawson, A. G. (1994): Geomorphological effects of tsunami run-up and backwash, Geomorpho., 10(1–4), 83–94.

Gonzalez, F. I., Titov, V., Mofjeld, H., and Venturato, A. (2002): The NTHMP Inundation Mapping Program, Second Tsu.Symp., Hawaii, 15, 52p.

Groat, C. G.: Statement of Charles G. Groat, Director, US Geological Survey US Department of the Interior before the Committee on Science US House of Representatives,.

Gupta, H. K. (2005): A note on the 26th December 2004 Great Sumatra earthquake, J. Geol. Soc. India., 66, 247–248, 2005.

Harinarayana, T. and Hirata, N (2005): Destructive Earth quake and Disastrous Tsunami in the Indian Ocean, What Next?, Gond. Res., 8(2),246–257.

Houston, J. R. (1974): Tsunami predictions for Southern California coastal communities, USA, Proceedings, IUGG Tsunami Symposium, Wellington, New Zealand.

Houston, J. R. and Garcia, A. W. (1974): Type-16 flood insurance study, tsunami predictions for Southern California, Waterways Experiment Station, Technical Report H-7: 3, Vicksburg.

Houston, J. R. (1980): Tsunami elevation predictions for American Samoa, WES Technical Report No. HL-80, 16.

Houston, J. R. and Garcia, A. W. (1978): Type 16 Flood Insurance Study: Tsunami Predictions for the West Coast of the Continental United States: US Army Engineer Waterways Experiment Station, Technical Report H-78, 26.

Imamura, F. (2008): Risk Evaluation and Real Time Information for Tsunami Disaster Mitigation. Proc. Workshop on Wave, Tide www.nat-hazards-earth-syst-sci.net/8/617/2008/ Nat. Hazards Earth Syst. Sci., 8, 617–626.

Janaka j. (2006) Wijetunge Tsunami on 26 december 2004: spatial distribution of tsunami height and the extent of inundation in sri lanka. Sci Tsu Haz Vol. 24, No. 3, page 225.

Mofjeld, H. O., Gonz´alez, F. I., Titov, V. V., Venturato, A. J., and Newman, J. C. (2004): Effects of tides on maximum tsunami wave heights: Probability distributions, Journ. of Atmos. and Ocean. Tech., 24(1), 117.

Mohan, V.: December 26, 2004 tsunami: A field assessment in Tamil Nadu, in: Tsunami: The Indian Context, edited by: Ramasamy,

Murthy, P.G.K.(2002), An in sight into internal waves in the seas around India, proc. ICONS 2002,Int.Conf., on Sonar-sensors and systems, pp.525-532.

Murthy. K. S. R, Subrahmanyam. A. S, Murty. G. P. S, Sarma. K. V. L. N. S, Subrahmanyam. V, Mohana Rao. K, Suneetha Rani. P, Anuradha. A, Adilakshmi. B. and Sri Devi.(2006) T.Factors guiding tsunami surge at the Nagapattinam–Cuddalore shelf, Tamil Nadu, east coast of India current science, vol. 90, no. 11, 10.

Raval, U. (2005): Some factors responsible for the devastation in Nagapattinam region due to tsunami of 26 December 2004, J. Geol. Soc. India., 65(5), 647–649.

Satheesh Kumar,.C, Arul Murugan .P, Krishnamurthy R. R, Prabhu Doss Batvari. B, Ramanamurthy. M. V, Usha. T, and Pari. Y. (2008) Nat. Hazards Earth Syst. Sci., 8, 617–626, www.nat-hazards-earth-syst-sci.net/8/617/2008.

Smith, S. E., Williams, D. G., and Johnson, N. A. (1997): Nurtured by Knowledge: learning to do participatory action-research, The Apex Press, Ottawa, Canada.

Sundar, V. and Sundaravadivelu, R. (2005): Layout of Groin field shoreline changes (Kurumbanai, Vaniyakudi and Simoncolony), Proceedings of Coastal problems and Solutions, IIT Madras, Chennai.

Thakur. N. K. & Pradeep kumar.A. (2007), role of bathymetry in tsunami devastation along the east coast of India.(current science, vol. 92, no. 4.

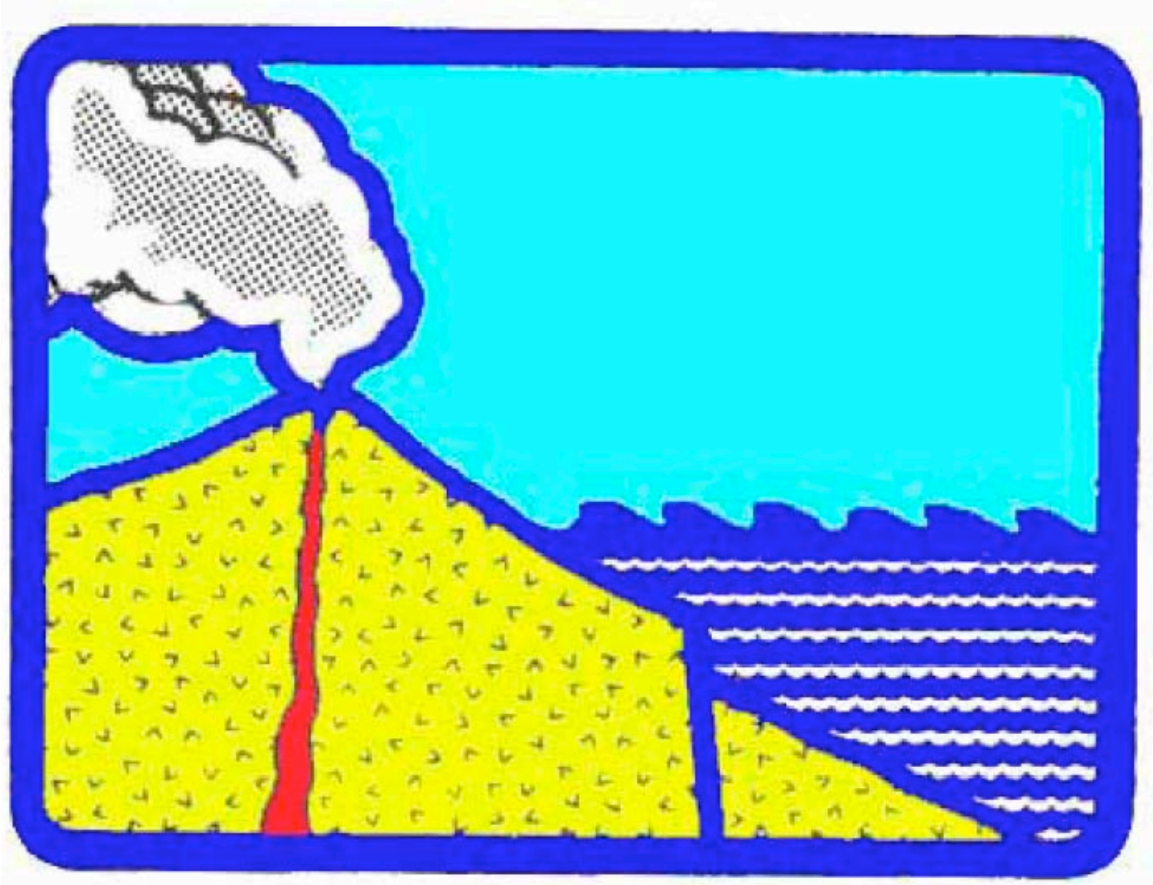

Tsunami Society
1741 Ala Moana Blvd. #70
Honolulu, HI 96815, USA

WWW.TSUNAMISOCIETY.ORG